Assessing the microbial potential for aromatic hydrocarbon degradation in groundwater from the Griftpark, Utrecht and in batch experiments

Emmi Sommer

Student number: 5965519

Marine Sciences

Utrecht, 14 December 2018

Supervisors:

Dr. Jan Gerritse - Deltares (J.Gerritse@deltares.nl)

Dr. Jack Middelburg - Utrecht University (J.B.M.Middelburg@uu.nl)

Deltares
Enabling Delta Life

Universiteit Utrecht
Faculty of Geosciences

Abstract

The groundwater and subsoil of the Griftpark in Utrecht (The Netherlands), a former industrial site, is contaminated with aromatic hydrocarbons into great depths. Currently, the contamination is constrained by a bentonite slurry wall around the park and by extracting groundwater, which is thereafter cost-intensive purified. biogeochemical analyses of the field samples of eight monitoring wells in and around the Griftpark revealed that sulfate-reducing conditions were dominating. Only in the bulk of the contamination, located in the northern part of the Griftpark, methanogenesis occurred. In order to reduce the extraction costs, the potential of the microorganisms community to degrade aromatic hydrocarbons under different conditions was investigated. In light of that batch experiments were performed to test eight scenarios by adding either: Oxygen, oxygen + nutrients, chlorate, nitrate, sulfate, ferrihydrite, nothing or mercury chloride (sterile). The batches were prepared with heavily polluted source water (B22) and mixed with relatively clean water from wells downstream of the Griftpark (BW205 and 60). The contamination in the BW205 and 60 batches was almost completely removed within 14 days in all scenarios. A high potential for aerobic degradation of the contamination in the Griftpark was determined. Adding nutrients or chlorate did not improve the removal of aromatic hydrocarbons, but led to toxic concentrations of nitrite in the groundwater. In the batches with alternative electron acceptors, hypoxic conditions were present, presumably delaying the reduction of nitrate, sulfate, chlorate and ferrihydrite, respectively. Consequently, the incubation of the batches should continue with recontaminating the BW205 and 60 batches.

Statement of originality for the MSc thesis

I declare that:

1. this is an original report, which is entirely my own work,
2. where I have made use of the ideas of other writers, I have acknowledged the source in all instances,
3. where I have used any diagram or visuals I have acknowledged the source in all instances,
4. this report has not and will not be submitted elsewhere for academic assessment in any other academic course.

Student data:

Name: Emmi Elsa Sommer

Registration number: 5965519

Date: 14th of December

Signature:

Acknowledgement

First, I would like to thank my thesis supervisor Dr. Jan Gerritse from the research institute Deltares for his trust and confidence in me to work on this comprehensive project. He constantly supported and guided me in the right direction, but also allowed for this paper to be my own work.

Furthermore, I would like to thank all the experts from Deltares, without their technical support and expertise this research would not have been possible. I would like to give special thanks to Fredericke Hannes for giving me instruction for the DNA analyses and always making time to help me with problems I encountered; to Erik Vilsteren, Rob van Galen and Coen Mulder from the Utrecht Univeristy, for helping me with the Dionex and ICPOES samples and analyses; to Andre Cinje for his help with the fiedwork and preparation; to Marcelle van Waals and Alex van Renesse from TNO for their introduction to and help with the GC-MS; to Johan van Leeuwen for his constant flow of ideas during meetings. Also I would like to give special thanks to my fellow Deltares interns - Alex, Charlotte, Edith, Pim and Derek for all the fun lunch breaks.

I would also like to acknowledge the support of Dr. Jack Middelburg from Utrecht University as the second reader and supervisor of this thesis, and I am grateful for his quick responses to questions which arised during my research.

Moreover, I am very grateful to my family, friends and my partner Becko for encouraging me throughout the year. Thank you all for giving me the strength to pursue my goals.

Contents

List of Figures

List of Tables

1 Introduction

Fossil fuels are naturally formed by the long-time geochemical burial of organic matter in the sediment (Widdel & Rabus, 2001). Depending on the type of sediment, this organic matter can eventually be transformed into coal or oil (Berner, 2003). Among other components, fossil fuels contain volatile aromatics such as benzene, ethylbenzene, toluene, and xylene (collectively known as BETX) as well as polycyclic aromatic hydrocarbons (PAHs). Aromatics are ringed hydrocarbon molecules which represent one of the most often used fractions of petrochemicals in the industrialized world (Hinchee *et al.*, 1995). Through heating in factories, these volatile hydrocarbons are recovered as a gas, which was widely used in the 19th century for lighting, heating and cooking. The various manufacturing processes and transport that coal and petroleum oil undergo often produce waste which ends up in the subsurface due to incorrect disposal and accidental release via fuel spillages or leaking storage tanks at former gas plants (Bergmann *et al.*, 2011), contaminating the site. Once the subsoil is reached, the hemotoxic (Loibner *et al.*, 2004), teratogenic and potentially carcinogenic (Menzie *et al.*, 1992; Lu *et al.*, 2011) substances migrate vertically and have the potential to leach into the groundwater. As groundwater is used for drinking water production, remediation of these former industrial sites is necessary. Hence, the aromatic hydrocarbons have to be removed from the groundwater to eliminate the risk of ingestion. So far, there are two options for this: purification and degradation. Until 1980, treating the groundwater physiochemically has been by far, the most commonly employed remediation strategy (Hinchee *et al.*, 1995). Due to the high expenses of the purification processes, stimulation of biodegradation is considered as a convenient alternative. Hence, research was undertaken to study the ability of subsurface microorganisms to degrade petroleum-derived hydrocarbons (Chapelle, 1999; Ehrlich *et al.*, 1985; Wilson *et al.*, 1986; Heitkamp & Cerniglia, 1988; Fredrickson *et al.*, 1991) since the 1980s.

Microorganisms obtain energy for cell production and maintenance by catalyzing the transfer of electrons from electron donors to electron acceptors. Hence, the growth and metabolism of microorganisms in most natural environments is not only limited by the

availability of electron acceptors but also nutrients. Until the late 1980s, it was widely believed that molecular oxygen was necessary to degrade petroleum hydrocarbons, but hydrocarbon contaminated aquifers usually become anoxic with a redox gradient along the groundwater flow path (Meckenstock *et al.*, 2004). This envoked the question of whether microorganisms can degrade petroleum-derived hydrocarbons anaerobically. This was proven to be possible by laboratory studies showing that degradation occurred under sulfate (Edwards *et al.*, 1992), nitrate (Hutchins, 1991), iron-reducing (Lovley *et al.*, 1989) and methanogenic conditions (Grbić-Galić & Vogel, 1987) and was confirmed in field studies conducted by Cozzareli and colleagues in 1990. Due to the majority of the contamination being present in regions where oxygen is depleted, the research focus has shifted towards anaerobic degradation.

Nitrate-based bioremediation has been proven to be a cost-effective and simple approach for the removal of organic compounds in sediment (Shao *et al.*, 2009) and groundwater. Moreover, nitrate is much more soluble in water than oxygen (Hutchins, 1991). In terms of electron accepting capacity, it can yield free energy almost as much as under aerobic conditions (MacRae & Hall, 1998; Rockne *et al.*, 2000). Therefore, in situ nitrate-based bioremediation has been increasingly applied in the bioremediation of groundwater, soil and sediment contamination (MacRae & Hall, 1998; Uribe-Jongbloed & Bishop, 2007). Since sulfate is typically one of the most abundant anion in natural waters (Miao *et al.*, 2012; Hem, 1985), studies also focused on the potential of sulfate-based degradation of hydrocarbons. Furthermore, Lovley & Lonergan (1990) showed that oil compounds can be degraded using a poorly crystalline Fe(III) oxide as the electron acceptor. Moreover, several studies have been conducted, confirming anaerobic and aerobic degradation of benzene using perchlorate or chlorate as an alternative electron acceptor (Chakraborty *et al.*, 2005). During the degradation of chlorate, oxygen emerges. In theory, this oxygen can be further used for the degradation of aromatic hydrocarbons. Hence, introducing alternative electron acceptors to the system as bioremediation techniques to clean up a petroleum hydrocarbon contaminated sites has been successfully implemented (Chapelle, 1999).

The dangers of groundwater contamination have made the undertaking of remediation projects important in many countries. In the case of The Netherlands, despite it being a relatively progressive country regarding environmental protection (Hinchee *et al.*, 1995), 250,000 sites, in 2015 alone, were found to contain various degrees of soil and groundwater pollution (Statistics Netherlands, 2015).

1.1 Griftpark - Background information

One of the largest soil remediation projects in Dutch history is the Griftpark located in Utrecht. The project started in 1993 and is still ongoing. The Griftpark is a very popular and modern city park in the middle of Utrecht situated between the districts of Vogelenbuurt, Tuinwijk, and Wittevrouwen (see figure 2). The following information was obtained from the Royal HaskoningDHV (2014) report.

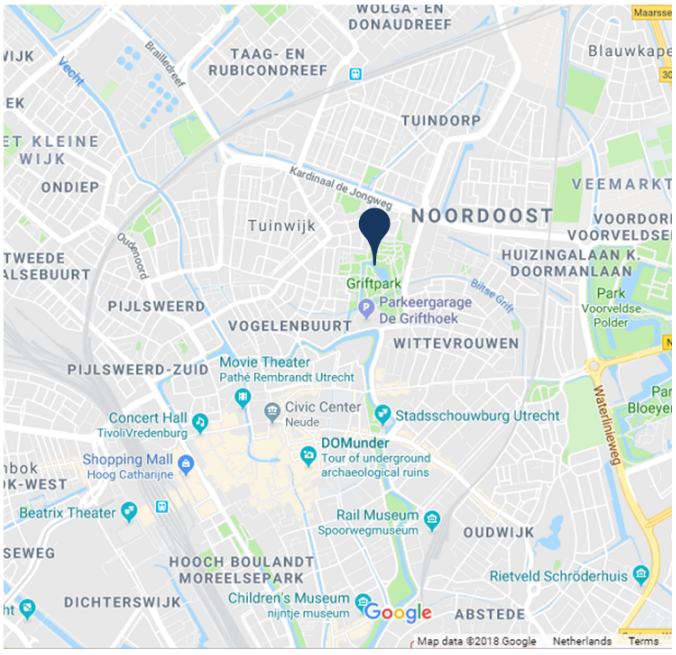

Figure 2: A map of a part of Utrecht. The blue pin shows the location of the Griftpark. The picture was obtained from Google maps, accessed 4th of December 2019)

From 1860 to 1962 several manufactured gas factories and many other industrial activities were located and carried out at the location of today's Griftpark. In 1860, a municipal gas factory was built with three gas tanks and three tar sumps (see figure 3). Here gas

was made from coal, oil and hydrogen and for a short time (1918-1920), briquettes. The dumping of by-products such as tar (Herder & Kolkman, 2000), mono- and polocyclic aromatic hydrocarbons (BTEX and PAH) and inorganic compounds such as cyanide and heavy metals contaminated the site. Since 1860, the gas plant had expanded considerably and soil-threatening activities were present throughout the site. Moreover, from 1899, fertilizer was produced with ammonia as a by-product (Herder & Kolkman, 2000). Furthermore, the printing company, Lumax, brought toluene to the Vaaltterrein for years. Due to the risk of fire, the cleaning officials did not want to transport the toluene in barges to landfills outside the city. As a consequence, the toluene was left on the ground. The map from 1912 and the picture in figure 3 from 1925 and 1937, respectively, show which factories were present and their locations in the Griftpark at this time.

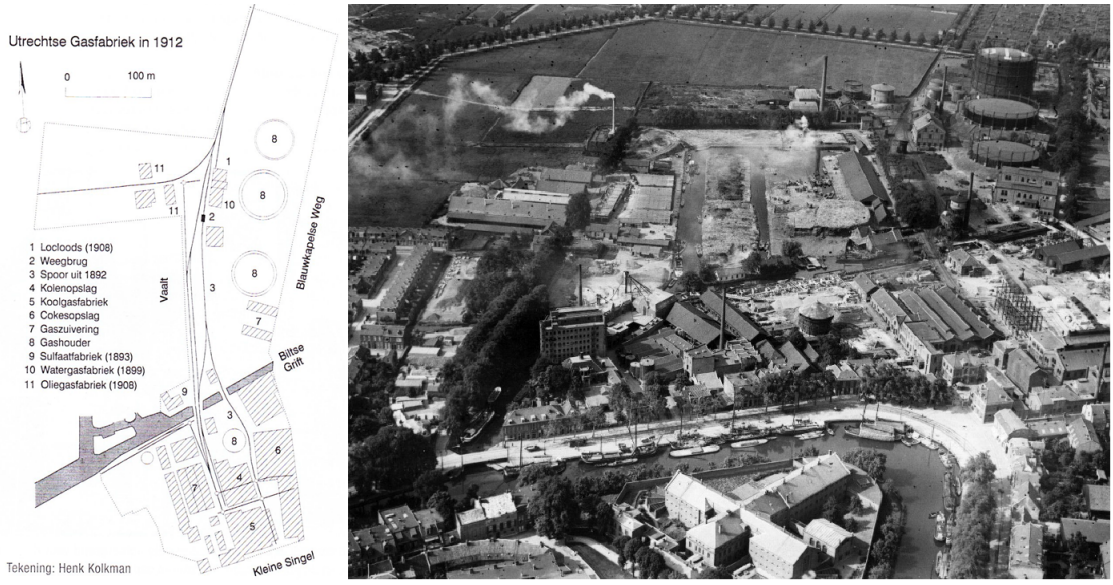

Figure 3: A map (drawn by Henk Kolkman in Herder & Kolkman (2000)) with corresponding picture (taken in 1925, Utrechts Archief 80453) of the factories located in the Griftpark from 1912.

Between 1993 and 2002, the topsoil of the Griftpark was remediated and a park was established. The spreading of mobile pollution is controlled using the IBC method (isoleren = isolating, beheersen = constraining and controleren = monitoring). In 1996, the contamination was isolated and constrained by the construction of bentonite slurry walls around the major fraction of the contamination, and by the extraction of groundwater. The

extracted groundwater is, until today, transported via a pipeline into a nearby wastewater treatment plant and purified. Furthermore, frequent monitoring around and in the isolated area is carried out to check the quality of the groundwater and that the contamination does not enter the environment outside the slurry wall. So far, the contamination has not been fully removed, but the risks have been controlled with this IBC method. Specific focus has to be put on the transition area between Kedichem and Harderwijk formations in the soil which result in the absence of the aquitard (clay layer). Above this so-called hole, the vertical penetration of the pollutants is decelerated by the extraction of the groundwater. The immediate abortion of the extraction of the groundwater would lead to a heavy polluted deeper aquifer within a couple of years. However, as a result of pumping activities of the groundwater, the situation of the contamination has changed to such an extent that the previous examinations carried out are no longer representative (Royal HaskoningDHV, 2014).

In 2018, the project entered a new phase with a new assignment and scope. An important reason for this is the commencement of the Area Plan Regional Groundwater Management Utrecht, further referred to as Area Plan. The Griftpark with its screen wall falls within the contaminated dynamic zone of the established management area according to The Area Plan. The municipality of Utrecht aims to reduce the activities and cost required for groundwater extraction and treatment. An important condition is that this can be done without additional risks for the surrounding area. For this purpose, Utrecht municipality has asked a research consortium of Wageningen University and Research (WUR), Utrecht University (UU) and Deltares to explore possibilities to reduce groundwater extraction and treatment. In the research consortium, UU is responsible for reactive transport modelling of mobile contamination. WUR will focus on stimulating contaminant biodegradation in the subsurface. Deltares will determine the natural biodegradation potential of risk-determining mobile contaminants by microbial populations in the Griftpark. The aim of this master thesis is to make an assessment of the biodegradation potential of microbial communities in the Griftpark for risk-determining contaminants, including benzene and other mobile toxic aromatics.

1.1.1 Contamination in the Griftpark

The Griftpark is contaminated with BTEX and PAHs up to 20 m below the ground-level from 1989 (Heidemij, 1989). During the historical investigation conducted in 2014 (Royal HaskoningDHV, 2014), the area and its contamination state were mapped using archival documents such as old maps, construction files, and company information (see figure 4).

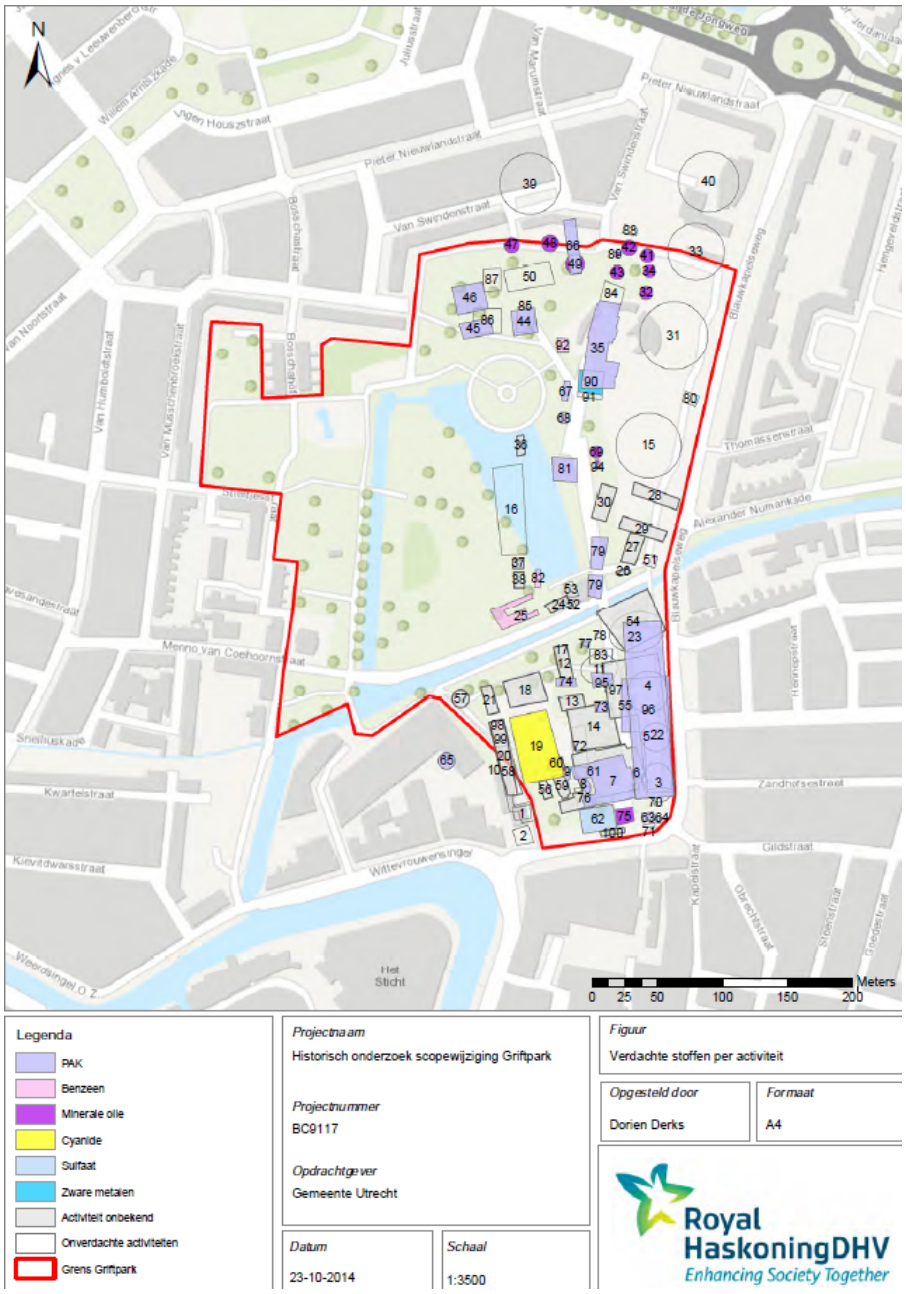

Figure 4: A map of the possible contamination in the Griftpark according to the report of the Royal HaskoningDHV (2014)

The contamination can be divided into mobile and immobile. The immobile contamination is located in the top layer and is caused by coal particles, ash, coke residues and slag that are spread over the terrain in dampings and excavations. The mobile PAH contamination is caused by non-aqueous phase liquid (NAPL) and originates from tar components. There are two kinds of non-aqueous phase liquids (NAPL), grouped according to their comparative density to water. LNAPL (lighter non-aqueous phase liquids) are compounds with a lower density than water and DNAPL (dense non-aqueous phase liquids) are compounds with a higher density than water (National-Research-Council, 2000). The former floats on top of the water surface and the latter is sinks to the bottom (see figure 5). The spreading of the LNAPL contamination by dissolved BTEX and PAH is currently controlled by the groundwater extraction. However, the spreading of the DNAPL contamination cannot be constrained with this method. In light of that, this study will focus on the contamination of the DNAPL aromatic volatile hydrocarbon such as BTEX and PAH.

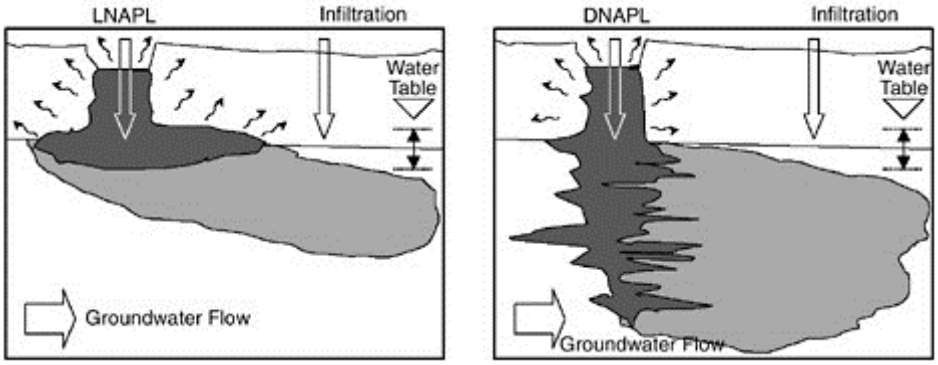

Figure 5: The release of DNAPL and LNAPL in the environment and the migration in the groundwater. The figure was obtained from National-Research-Council (2000).

Benzene forms as a by-product of coal gas separation and was further processed in the benzene plant located north of the Blitsche Grift on the Vaaltterrein (presumabl between number 9 and 11 in figure 3). The core of the benzene contamination is, therefore, expected at the location of this plant and its associated tanks.

Mineral oil, along with tar, are by-products formed during the degassing of coal and coke. The mineral oil was stored in oil reservoirs near the water gas plant (see number 10 and

11 in figure 3). The mineral oil pollution in the soil extends no deeper than 15 meters and is limited to two locations on the site according to the study conducted by Heidemij (1989).The first location is in the top layer at an oil reservoir of the gas plant located at the southern border of the site. The other contaminated area is located at the northern border of the site at the oil reservoirs of the water gas plant. It is striking that in the middle of the site, near the oil-gas plant, where a washing oil tank was present and at the location of the tar wells, no mineral oil contaminants in the soil have been detected by Heidemij (1989).

1.2 BTEXN and alternative oxygen-independent initial activation pathways for hydrocarbon metabolism

The delocalized electrons in the benzene ring stabilize the chemical structure of mono and polycyclic aromatic carbons, hence, these components are difficult to degrade and can persist for decades and centuries (Cerniglia, 1992; Bergmann *et al.*, 2011) in the aquifers. In the absence of oxygen, alternative electron acceptors such as nitrate, sulfate, and iron ions can function as terminal electron acceptors (Langenhoff *et al.*, 1996). In the degradation process molecular oxygen has two functions: (1) it acts as a terminal electron acceptor for the electrons and (2) it acts as a direct oxidant for the cleavage of the aromatic ring. The latter is catalyzed by a dioxygenase (Karthikeyan & Bhandari, 2001). The aerobic degradation pathway is generally considered to proceed more rapidly and more efficiently because it is not only a direct oxidant, it also requires less energy for initiation and yields more energy per reaction (Cookson Jr, 1995; Hinchee *et al.*, 1995). However, the alternative electron acceptors cannot replace oxygen in its second function. Hence, the activation of the aromatic ring differs from those in the aerobic processes. In order to degrade petroleum hydrocarbons, the molecule has to be made accessible for the microorganisms by adding a functional group or fumarate to the molecule. There are different initial activation steps for aromatic hydrocarbons. In principle, four possible

initial activation pathways are known: methylation, carboxylation, hydroxylation and fumarate addition, depending on which component is degraded. The degradation pathway depends on the chemical structure (see figure 6).

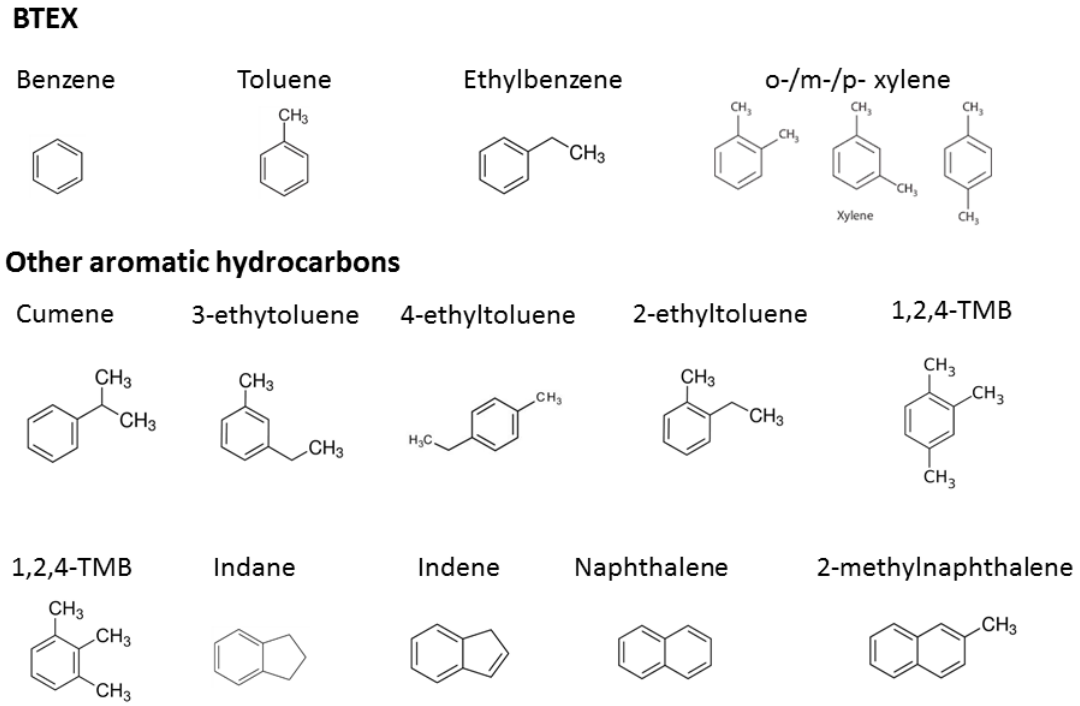

Figure 6: Chemical structure of the studied aromatic hydrocarbons

Benzene

Benzene is considered to be a very stable molecule due to its aromatic ring (Zhang *et al.*, 2010) and is therefore difficult to degrade anaerobically. If the hydrocarbon has no functional group, such as benzene, its degradation is activated by adding a methyl, a carboxyl, or a hydroxygroup. The bacteria *Peptococacceae* sp. is known to degrade benzene (Van der Zaan *et al.*, 2012) and can be targeted with a qPCR assay.

Hydroxylation: If a hydroxyl group is added to the benzene ring it leads to the formation of phenol. Phenol is further degraded along the carboxylation pathway to benzoyl-

CoA (Vogt *et al.*, 2008).

Methylation: Donating a methyl group to the benzene ring using S-adenosyl methionine or methyl-tetrahydrofolate forms toluene (Vogt *et al.*, 2011). Thereafter, it can be further degraded with the addition of fumarate. However, this pathway was only described experimentally in one study (Safinowski & Meckenstock, 2006) and has not been repeated .

Carboxylation: Adding a carboxyl-group to the aromatic ring of benzene in initialized by the putative anaerobic benzene carboxylase (*abc*) and results in benzoate (Abu Laban *et al.*, 2010). Benzoate can be further degraded to benzoyl-CoA, which is then in turn degraded to acetyl CoA and CO2.

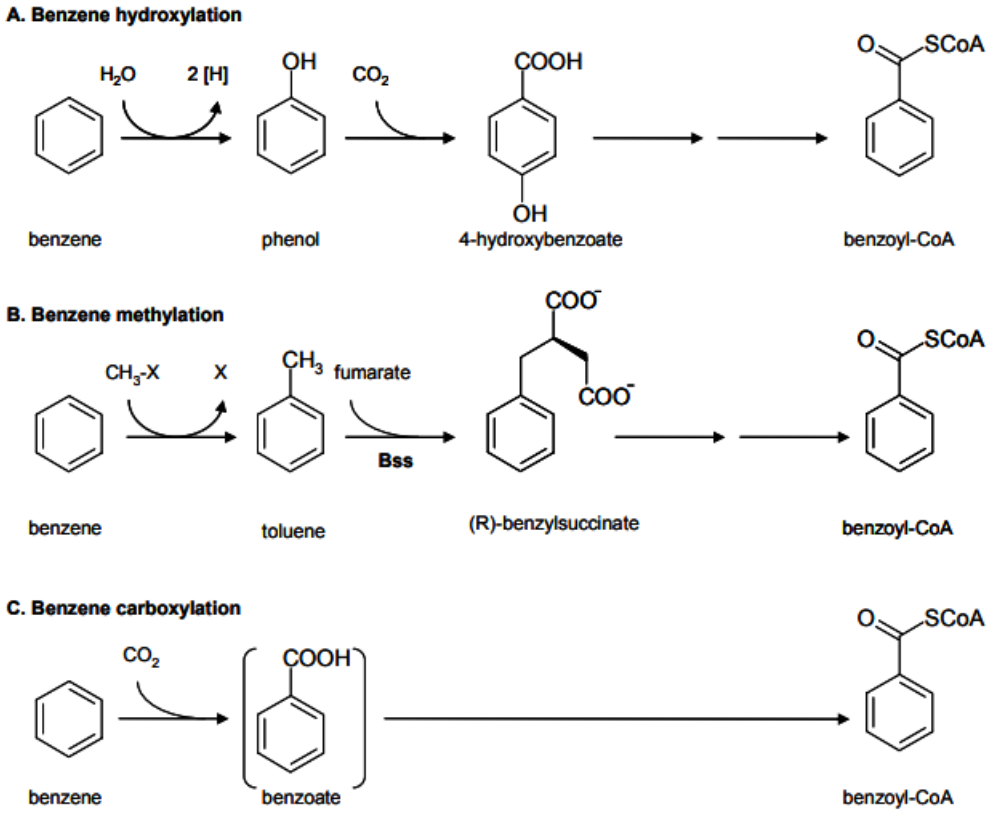

Figure 7: Possible anaerobic degradation pathways of benzene. A: Hydroxylation, B: methylation and C: carboxylation of benzene are illustrated. The figure was adapted from Weelink (2008).

Fumarate addition: If the aromatic hydrocarbon already has a functional group such as an alkyl- or methyl-group the initial activation step is induced by adding fumarate to the functional group. It is catalyzed by the glycyl radical enzyme, benzylsuccinate synthase (*bss*) and others (Callaghan, 2013) and results in the formation of benzoyl-CoA (intermediate in the BTEX degradation). The Benzoyl-CoA is further degraded into acetyl-CoA and CO_2. The degradation of toluene, ethylbenzene, and xylene can follow this pathway.

Toulene

Toluene is among the easiest aromatic hydrocarbons to degrade. Anaerobic degradation has been described under sulfate-, iron- (Beller *et al.*, 1992; Edwards *et al.*, 1992), and manganese reducing conditions as well as for methanogenic conditions (Langenhoff *et al.*, 1996; Vogt *et al.*, 2008). The step for the degradation process is initiated by adding the double bond of fumarate to the methyl group of toluene resulting in benzylsuccinate which is thereafter oxidized to E-phenyl itaconate and eventually benzoyl CoA (Biegert *et al.*, 1996). The presence of the enzyme benzylsuccinate synthase (*bss*) can indicate the potential for the degradation of toluene.

Ethylbenzene

Similar to toluene degradation, the initial step for the anaerobic degradation of ethylbenzene is adding fumarate. This has been described under nitrate (Chakraborty *et al.*, 2005) and sulfate-reducing conditions (Elshahed *et al.*, 2001). Furthermore, Callaghan and colleagues (Callaghan, 2013) described the hydroxylation of the benzylic carbon to form 1-phenylethanol under nitrate-reducing conditions catalyzed by the ethylbenzene dehydrogenase (Johnson *et al.*, 2001; Kniemeyer & Heider, 2001). The molecular oxygen for this reaction is derived from the water molecule (Ball & Reinhard, 1996). Subsequent dehydrogenation of 1-phenylethanol mediates acetophenone and eventually creates the

central aromatic metabolite benzoyl- CoA (Foght, 2008).

Xylene

Xylene is an organic compound which occurs in three isomers: o-, m- and p-xylene. m-xylene is most readily degradable but p-xylene is often resistant to degradation (Vogt *et al.*, 2008). In all cases, the degradation is initialized by adding fumarate to the molecule. In the past nitrate and sulfate have been described as an alternative electron acceptor to oxygen.

Polycyclic aromatic hydrocarbons (PAH)

Naphthalene PAHs are polycyclic aromatic hydrocarbons. They can be divided into small and large PAHs. The large PAHs have the ability to adsorb strongly to particles and are therefore less dangerous (Tsai *et al.*, 2009). Naphthalene is the smallest with two benzoic rings. It is soluble in water and consequently has a high potential to be spread throughout the environment. Anaerobic degradation of naphthalene has been described under nitrate, iron, and sulfate-reducing conditions. The initial activation step to activate naphthalene degradation follows three different pathways. Methylation, fumarate addition, and carboxylation pathways are possible. After adding a methyl group (methylation), it is degraded via 2-naphthoic acid or methylnaphthoic acid into 2-methylnaphthalene (Meckenstock & Mouttaki, 2011). The fumarate can be added after the methylation as the initial step. The carboxylation pathway is initiated by the naphthalene carboxylase enzyme. 2-naphthoic acid is degraded into 5,6,7,8-tetrahydro-2-naphthoic acid and hexahydronaphthoic acid and decalin-2-carboxylicacid (Phelps & Young, 1999). Two signature metabolites are described for naphthalene degradation: naphthyl-2-methyl-succinate and naphthyl-2-methylenesuccinate (Safinowski & Meckenstock, 2006).

2-methylnaphthalene Alkyl-PAHs such as 2-methylnaphthalene seem to be degraded by fumarate addition initiating the formation of naphthyl-2-methylsuccinate and naphthylitaconate (naphthyl-2-methylsuccinate) followed by sequential saturation of the ring system and ring cleavage (Foght, 2008).

1.3 Aim of the research

Due to the variability in organic composition it is necessary to analyze the degradation level for every new contamination sample. To determine whether anaerobic degradation of BTEXN and other mobile aromatics takes place in the groundwater of the former gas plant site, we follow three lines of evidence for natural degradation. The first line of evidence focuses on changes in the concentration and composition of the pollutants, the second on changes in the composition of the groundwater, and the third one on the presence of microorganisms with the potential to degrade the contaminants (Alvarez & Illman, 2006; National-Research-Council, 2000). The aim of the research is first, to analyze the biogeochemical situation and contamination state in the monitoring well in and around the Griftpark in order to select appropriate groundwater types for follow up batch experiments. Second, to investigated what will most presumably happen to the clean groundwater downstream outside of the slurry wall, when it is mixed with contaminated water. And third, to study if degradation of aromatic hydrocarbons occurs in the groundwater of the Griftpark. And if it does, what kind of compounds are degraded and under what conditions does it occur? In light of that, microcosm batch experiments are conducted to test different electron acceptors.

1.3.1 Research objectives summarized

1. Assess the biogeochemistry and state of contamination in the monitoring wells in and around the Griftpark.
   (a) Assess what types of microorganisms, and genes involved in the degradation

of aromatic hydrocarbons are present.

2. Determine the potential implications of contaminated groundwater mixing with clean groundwater by conducting batch experiments

3. Determine if degradation of aromatic hydrocarbons occurs in the groundwater of the Griftpark, and if so, which compounds are degraded under what conditions.

   (a) Assess which electron acceptor achieves the best results in the batches.

2 Methodology

Firstly, field and laboratory analyses of the groundwater from eight monitoring wells located in the Griftpark will reveal the in situ geochemical conditions, the concentration of the contaminant compounds and the presence and potential of biodegradation. Thereafter, three of the wells are selected for follow-up batch culture experiments to study the efficiency of different alternative electron acceptors which are added to the groundwater. The wells are selected according to their contamination and geochemical state and location. The concentration of alternative electron acceptors, anions and cations are measured using DIONEX chromatography and inductively coupled plasma - optical emission spectrometry (ICPOES) analysis. The concentration of aromatic hydrocarbons in the field samples and batches are determined by gas chromatography-mass spectrometry (GC-MS) and gas chromatography-flame ionization detector (GC-FID) analysis. Microbial degradation capacities will be mapped by using quantitative polymerase chain reaction (qPCR) assays.

2.1 Selection of eight monitoring wells in the Griftpark

The aim of the selection of eight monitoring wells in and around the Griftparl was (1) to gain insight into the state of contamination of these different locations and (2) to select three groundwater types for follow up microcosm batch experiments: one type inside the

park containing high concentrations of diverse aromatic hydrocarbons and two 'clean' groundwater types from the 1st and the 2nd aquifer.

The monitoring wells were selected according to the geographic and geohydrological circumstances in the Griftpark area. Important factors to consider were the groundwater flow in the 1st and 2nd aquifer, the location of the source zones of the contamination, the division by the slurry wall and the hole in the aquitard that separates the 1st aquifer from the 2nd one. The groundwater flow in the first aquifer, but not inside the slurry wall is directed from southeast to northwest. The slurry wall prevents most of the groundwater from flowing into the 1st aquifer. The major water input inside the slurry wall is rain and it is completely determined by the pumping activities (van Oorschot, 2015). The groundwater in the 2nd aquifer flows from northeast to southwest (Suzanne Faber, personal communication). The source regions have been described and mapped during the historical research of the Royal Haskoning DHV in 2014. The slurry wall separates, in theory, the contaminated area from the uncontaminated one and hence, constrains the distribution of the contamination. However, there are patches where the clay layer of the aquitard is not entirely present. Due to these patches, the risk of the 2nd aquifer being exposed to the contamination emerges (see figure 8).

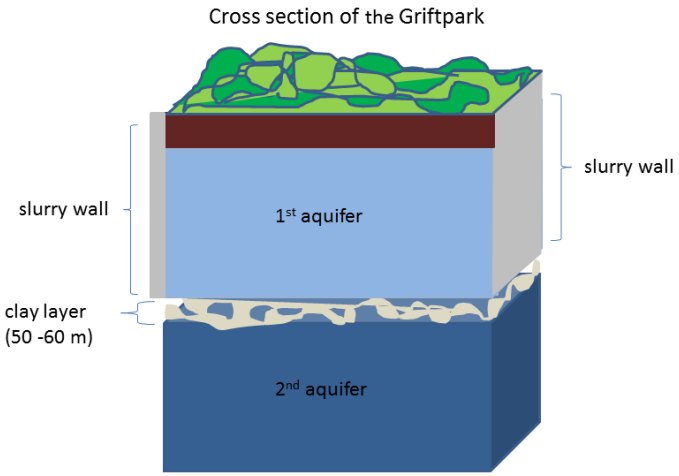

Figure 8: Schematic cross section of the Griftpark, visualization of the aquifers and the incomplete clay layer in between as well as the slurry wall around the Griftpark.

Eight wells were selected. Two wells upstream of the park were selected: one from the 1st aquifer (BW211) and one from the 2nd (BW157) aquifer. They are most likely uncontaminated due to the opposite flow direction of the groundwater. Inside the park, two wells have been selected to sample the source zone in the 1st aquifer in the north (B22) and the plume zone in the south (Pb1) and one well (DV4) to sample the 1st aquifer above the hole of the aquitard. Unfortunately, there was no monitoring well available to sample the 2nd aquifer in the hole inside the slurry wall. Outside, downstream of the park, two wells in the 1st aquifer (BW205 and 37) were selected to investigate the efficiency of the slurry wall and one well in the 2nd aquifer(60) to obtain relatively clean groundwater downstream of the park. Moreover, the monitoring well BW205 is also located in the hole of the aquitard to examine if the contamination could migrate via the 2nd aquifer. Table 1 gives an overview of the locations and the expected contamination state of the wells. Figure 9 shows the selected monitoring wells in and around the Griftpark.

Figure 9: Location of the selected wells in and around the Griftpark. The yellow pinpoints represent the monitoring wells in the 1st aquifer and the blue, the 2nd aquifer. The pink dashed line indicates the presence of the slurry wall. The blue shaded area shows where the patches with incomplete clay layer (aquitard) can be present. The blue arrows visualize the direction of the groundwater flow in the 1st and 2nd aquifer (not inside the slurry wall).

Table 1: Table of the location, depth and assumed contamination state in the selected wells.

ID	Depth (m)	location	expected contamination	DDM N	DDM E
BW211	22-26	1st aq., upstream	no	52 5.924	5 7.910
BW157	63 - 65	2nd aq., upstream	no	52 6.050	5 7.908
B22	44 - 45	1st aq., plume	yes	52 6.088	5 7.623
Pb1	14-19	1st aq., plume	yes	52 5.929	5 7.655
DV4	22	1st aq., hole	yes	52 6.023	5 7.558
37	21 - 25	1st aq., downstream	unknown	52 6.126	5 7.610
60	68 - 72	2nd aq. downstream	unknown	52 6.160	5 7.501
BW205	43-45	Downstream, hole	unknown	52 6.040	5 7.367

2.2 Fieldwork

The fieldwork took place on 8th of May 2018. First, the groundwater level was noted and 11-20 litres were pumped up to measure the pH, oxygen concentration, electric conductivity and the temperature using electrodes under stable conditions. For every monitoring well, six bottles for the analysis by Deltares were prepared. Every bottle was allocated to one analysis. For the detection of anions (Dionex) 2ml vials with 100μl mercury chloride (0.5 g/L stock solution) were prepared and filled with filtered water. For detecting volatile hydrocarbons (via GC-MS, Gas chromatography-mass spectrometry, and GC-FID, gas chromatography-flame ionization detector), 2 x 20ml vials each with 1 ml mercury chloride were filled with unfiltered groundwater and crimp sealed with silicone/PTFE magnetic caps. The groundwater for the ICPOES (Inductively coupled plasma - optical emission spectrometry) analysis was filtered and spiked with 600 μl of HNO_3 retrospectively. Additionally, 50ml groundwater was filtered in a brown glass bottle fixed with 600 μl HCl to determine the concentration of non-purgeable organic carbon (NPOC). Furthermore, 1 litre of unfiltered groundwater was collected for the DNA analysis per monitoring well. Moreover, for the external analyses bottles were prepared and provided by SYNlab Analytics & Services B.V. These bottles were used for the detection of aromatic hydrocarbons, cyanide and total mineral oil.

The groundwater samples from all monitoring wells were analyzed using DNA analysis, Dionex and ICPOES methods and GC-MS, GC-FID, the latter two were compared to the results of the standard analysis performed by SYNlab. After the evaluation of these samples, it was decided to select three monitoring wells for the batch experiments. Two were declared as clean (BW205 and 60) and one of them as very contaminated (B22). Thereafter, a second fieldwork day took place on 22nd of June 2018 to sample groundwater from these monitoring wells. This time, samples for GC-MS and GC-FID analysis were taken as well as six litres of the uncontaminated groundwater and eight litres of the contaminated groundwater. For safety reasons the contaminated monitoring well was sampled by a professionally authorized sampler from the municipality of Utrecht.

2.3 Laboratory batch experiments

For the batch experiments, three groundwater types were selected after evaluating the field samples. For the contaminated groundwater, the water from the B22 monitoring well was used and clean water was obtained from the BW205 and 60 wells. In the batch experiments, the clean groundwater was mixed with the contaminated one and different electron acceptors were tested regarding their degradation potential. To determine the potential degradation of the contamination in the groundwater samples of the batches, eight different conditions were simulated. Anaerobic degradation was described for almost all BTEXN (BTEX + naphthalene) compounds under nitrate, sulfate, iron-reducing and methanogenic conditions. Consequently, these conditions are among the investigated scenarios. As iron electron acceptor ferrihydrite has been selected since it is considered to be the most bioavailable iron oxide for iron-reducing microorganisms (Wu *et al.*, 2015) and thus greatly influences the global cycle of carbon in the environment (Eusterhues *et al.*, 2005; Kiem & Kögel-Knabner, 2002; Borggaard, 1982). To investigate if oxygen can be indirectly introduced by adding chlorate to the groundwater, one batch scenario simulated the situation when chlorate is present. To compare the efficiency of the anaerobic degradation with the aerobic one, two additional scenarios were simulated. Two batches were held under aerobic conditions but one of them contained nutrients (see protocol in the appendix cocerning Brunner medium). Finally, sterile batches were used as negative controls. They were sterilized by adding 12.5 ml of 5g/L mercury chloride and autoclaving them. Throughout the experiment, single use needle tips with size 0.5x16 mm (RW/LB Luer Lock) and mercury chloride stock solution with a concentration of 0.5g/L were used.

2.3.1 Preparation of the alternative electron acceptor stock solutions

For the stock solution of the alternative electron acceptors, 100ml of each 1M Stock solution of sodium nitrate, sodium chlorate, and sodium sulfate and 0.5 M stock solution

of ferrihydrite were prepared anaerobically by flushing with N_2 gas and creating a vacuum inside the bottles. The ferrihydrite was prepared according to the protocol of Straub *et al.* (2005) using 500ml of a 0.4 M FeCl3 solution, which was adjusted to pH 7 by adding NaOH (1M) slowly under constant stirring. Once the pH was stabilized the solution was let rest to precipitate and the supernatant was discarded. Subsequently, the ferrihydrite was washed 3 times with 500ml distilled water to remove any traces of sodium and chloride. The total of 600ml was partitioned into twelve 50 ml centrifuge tubes and centrifuged at 5000 x g for 10 min. Thereafter, the ferrihydrite was resuspended in distilled water in 0.5 M concentration. Subsequently, the solution was transferred in 250 ml glass bottles and sealed with viton rubber stoppers and crimp caps. After flushing the stock solution bottles with N_2 gas to remove any traces of oxygen, they were sterilized by autoclaving. Subsequently, they were stored at 12 °C in the dark.

2.3.2 Preparation of the batches

For the microcosm batch experiments, forty-eight 500-ml serum bottles (Glasgerätebau Ochs GmbH, Bovenden, Germany) with crimp sealed viton rubber stoppers (Rubber BV, Hilversum, The Netherlands) and aluminium crimp caps (Grace, MD, USA) were used and autoclaved prior to the preparation of the batches. To maintain anaerobic conditions, the bottles were placed in a glove bag (Glas-Col X-37-27) which was vacuum pumped (Handsontools electric air pump EP130) and inflated four times with 95% N_2 and 5% CO_2 gas. Thereafter, 250 ml of the highly contaminated water from the source well B22 and 225 ml of the non-contaminated groundwater from the monitoring wells 60 and BW205 were poured into sixteen bottles respectively. Next, 25 ml of the very contaminated B22 water were added to the clean water using a sterile plastic syringe and sterile single-use needle tips, resulting in the final volume of 250 ml groundwater. The aerobic batches were spiked with 50 ml pure O_2 which corresponds to the 20 % oxygen content in the atmosphere. For the scenario called oxygen + nutrients, 1 L of the 457

mineral medium (Brunner) was prepared according to DSMZ (see appendix section 1) and 25 ml were added to the batches. Similar media were used for microbial analysis of fuel-oil contaminated groundwater investigations (Kämpfer *et al.*, 1991). 2.5 ml (100 x dilution of the stock solution) of the alternative electron acceptors were added to the batches respectively using sterile plastic syringes and single-use sterile needles. Furthermore, 15 ml of Ferrihydrite was added to the corresponding batches (30 mM).

2.3.3 Extractions

Immediately after spiking the batches, the first sampling round T0 was extracted from the batches. For this, 2 ml was extracted four times with a sterile plastic syringe (Terumo R Syringe without needle) and a new disposable needle for different analyses. For the DNA analyses, the 2 ml batch water was transferred in a 2ml glass Dionex vial with screw cap (8 mm, with silicon and PTFE septum, Grace Davison Discovery Sciences). For the Dionex analysis, the 2ml were filtered over a 0.45 μm pore size and 25mm diameter nylon syringe filter (Filter-bio) and mixed with 100 μl of mercury chloride. For the ICPOES analysis, the 2 ml were filtered the same way and mixed with 20 μl of HNO_3 68%. For the GC-MS analysis, the 2 ml batch water were diluted 1:2 with 2 ml milliQ water in a 10 ml glass GC vial in order to reach a headspace to volume ratio of 6:4 and crimp sealed with silicone/PTFE magnetic caps. The GC-MS analysis was immediately performed and the DNA was extracted the next day after the sampling round. After 14 days of incubation at 24-25 °C at 100 rpm, the second sampling round t1 was performed. In this report, only the GC-MS analyses are included but all extractions were performed and stored accordingly. The T2 extractions were taken after another 38-39 days of incubation. For T2 all analyses have been exercised and reported.

2.4 Analytical methods

The analyses for the DIONEX (anions, cations), ICP-OES (detection of the composition of elements dissolved in water) and NPOC (non-purgeable organic carbon) were performed by Erik van Vilsteren and Rob van Galen from Deltares and by the Utrecht University. The samples for the ICP-OES analysis were diluted 10 times with 1 M HNO_3. The data was processed using the MATLAB programm versions R2013b and R2016b.

2.4.1 Volatile aromatic hydrocarbons

2.4.1.1 Calibration line for GC analysis Calibration bottles were prepared using an aromatic hydrocarbon mix dissolved in acetone compounded by Johan van Leeuwen. This mix contained benzene, toluene, ethylbenzene, m-/p- and o-xylene, 1,2,4-trimethylbenzene, 1,2,3-trimethylbenzene, indene and naphthalene. Therefrom, a 100x dilution was prepared in 40 ml milliQ water. To this mix, 4 μl of 3-Ethyltoluene (purity), 4-Ethyltoluene (purity), 2-Ethyltoluene (purity), Cumene (purity), and 2-Methylnaphthalene (purity) were added. Subsequently, dilutions of 1x, 2x, 5x, 10x, 20x, 50x, 100x and 200x were prepared using miliQ water and placed on the autosampler of the GC-MS or directly injected in the GC-FID inlet (for details see appendix). For both GC-MS and GC-FID measurements, separate calibration lines were performed. It is ensured that they are only valid for concentrations with a linear correlation and a correlation coefficient R^2 greater than 0.9 and the maximal concentration is below the solubility value of the corresponding compound. See figures 25 and 26 in the appendix for calibration details.

2.4.1.2 GC-FID Gas chromatography equipped with flame ionization detection (FID) is among the most important widely used techniques for oil separation, characterization and identification (Wang *et al.*, 1994). For the GC analysis, the volume of the 20 ml vials filled with groundwater of the field samples and mercury chloride was reduced by half to measure the headspace concentration of volatile compounds. To maintain anaer-

obic conditions, the gas-tight/pressure-lock glass syringe (Vici precision sampling, Baton Rouge, Louisiana) with a disposable needle (0.5mm x 16mm) was flushed 3 times with N_2 gas before extracting 0.5 ml of the headspace for injection in the GC-FID. The GC-FID measurements were performed on a GC system using an Agilent 6850 equipped with an Agilent HP-1 column (0.32 mm x 30 m). The detector was set at 250 °C and the injector at 200 °C with a 5:1 split ratio. The initial oven temperature was 40 °C. After 3 minutes the temperature was increased at a rate of 10 °C/min until it reached 90 °C where it was held constant for 4 minutes followed by an increase of 10 °C/min until 220 °C was reached in the oven. The method was run under a constant pressure of 5 psi with high-purity helium as a carrier gas (flow rate 40 ml/min). The data was processed using the GC-ChemStation software.

2.4.1.3 GC-MS Ever since the GC-MS was invented in the mid-1950s, its applications were and still are restricted by the maximum oven temperature because of the thermal integrity of the separation column (Rabus & Widdel, 1995). For the GC-MS analysis a Agilent 7890A system with a AT^{TM}-624 60m x 0.25 mm x 1.4 μm Heliflex column (Grace) was used. The oven temperature protocol started at 40 °C, and was held for 1 min, with an increase-rate of 10 °C/min rate until 200°C was reached, followed by an increase of 20°C per min until reaching 300 °C. Thistemperature was held for 1 min. The inlet temperature was 200 °C with a pressure of 16.661 psi and the Aux temperature was set to 305°C. A multipurpose sampler (MPS 5975C Gerstel) was used and set to heat up the 1 ml syringe and the agitator to 75 °C. In the agitator the vial was shaken for 10 min clockwise and 10 min anticlockwise before injecting the headspace into the inlet. The injection of the 250 μl headspace had a flow rate of 1 ml/min with a split mode 5:1 (5 ml/min), whereas the septum purge flow was 3 ml/min. After the injection, the syringe was flushed with helium at a rate of 20 ml/min for 3 min. One run took 23 min and the PrepAhead function was on to reduce the time for a whole sequence run. Subsequently, the samples were analyzed in MSD ChemStation software.

2.4.2 Oxygen detection and redox potential in the batches

Following the experiments, two methods were used to test the anaerobic conditions in the batches. Firstly, headspace samples were analyzed in a Gas chromatography - Thermal Conductivity Detector (GC-TCD) using a Varian CP-3800 GC system. 100 μl of headspace was extracted with a gas-tight glass syringe and disposable needles and injected into the column (1041 column). The oven temperature was 65°C, with an actual helium flow rate of 40 ml/min and a column pressure of 44.2 psi. The column oven temperature was set to 45°C and the TCD oven to 80°C. Air was used for the calibration and to calculate the percentage of oxygen in the batches. The data was processed using the Compass CDS software. Due to delays in being able to run the method satisfactorily, the measurements were performed approximately 70 days after the T2 extraction.
Secondly, the batches were spiked with 0.25 ml of the redox indicator stock solution (1 g/L) Resazurin. Resazurin (7-hydroxy-3H-phenoxazin-3-one 10-oxide) is a purple dye that changes colour according to the redox potential in the water. High redox potential is indicated by a pink colour in form of resorufin (Fukushima *et al.*, 2003). It turns colourless after approximately 2 hours when the redox potential is between -200 to -100 mV, indicating anaerobiosis.

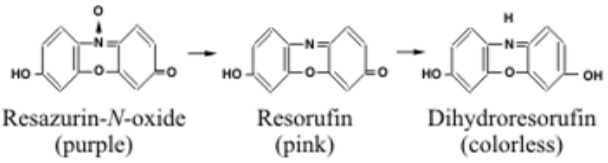

Figure 10: Reduced and oxidized chemical form of resazurin. The figure was directly taken from Fukushima *et al.* (2003)

.

2.4.3 Cyanide test

For the detection of cyanide, a *visocolor*®ECO colorimetric test kit (Macherey-Nagel GMbH & CO. KG) was used. It detects cyanide ions and cyanide complexes in surface water and sewage in concentrations 0.01-0.2 mg/L CN^-. The cyanide ions react with chlo-

ramine T to form cyanogen chloride. By adding isonicoic acid and 1,3-dimethylbarbituric acid a blue polymethine dye is produced. The more intensive the blue coloration is, the higher the concentration in the water is. There was no cyanide detected in the groundwater samples. This was also confirmed by the standard analysis performed by SYNLAB Analytics & Services B.V.

2.4.4 DNA analyses

For the DNA analysis of the field samples, maximal 300 ml of groundwater was vacuum filtered in triplets using the Microfil®filtration funnels with EZ-Pak®and sterile membrane filters (0.22 μm, white gridded 47 mm). The filters were then halved, folded and stored at -80°C. All the following analyses were performed in duplicates. The DNA isolation proceeded according to the Quick-Start protocol provided by the DNeasy®PowerLyzer®PowerSoil®Kit by Qiagen. With a sterile toothpick the filters were torn into small pieces and placed in PowerLyzer Glass Bead Tubes provided by the DNeasy®PowerLyzer®PowerSoil®Kit by Qiagen. Then 60 μl of C1 solution was added and the tubes were placed in the PowerLyzer 24 and run at 2,500 rpm for 45 seconds. Subsequently, the tubes were centrifuged at 10,000 x g for 30 seconds and the supernatant was transferred into a clean 2 ml tube. After adding 250 μl of C2 solution the tubes were vortexed and incubated for 5 min at 4°C. Thereafter, the tubes were centrifuged for 1 min at 10,000 x g as previously and the supernatant was transferred in a clean tube. Once 200 μl of the C3 solution was added another incubation step and centrifugation step followed. Then, the supernatant was transferred in a new tube and 1200 μl of C4 solution was pipetted into the supernatant and vortexted. The next step proceeded in three loads. For each load 675 μl of supernatant was transferred into a MB Spin Column and centrifuged at 10,000 x g for 1 min. Thereafter the the flow through was discarded and another load was added followed by a centrifugation step. Then, 500 μl of solution C5 was added to the MB Spin Column and centrifuged for 30 min at 10,000 x g. After discarding the flow through the tubes were centrifuged for 1 min. Thereafter, the spin filter was placed in

a clean tube and 100 μl of solution C6 was carefully pipetted onto the filter membrane. After centrifuging for 30 seconds at 10,000 x g the MB spin column was removed and the DNA was stored at -80°C.

After isolating the DNA from the samples, it was ready for downstream applications such as qPCR. Dilutions of 10x and 100x, and if necessary, 1000x were prepared prior to the execution of the assays (see table 2). The resulting concentrations were calculated based on the calibration curves prepared and in consideration of the undiluted and diluted (10x and 100x, if necessary, also 1000x) samples. For the calibration curves dilution of 10^7 - 10^1 were prepared prior to the execution of the qPCR assays. The validity of the assays was determined by the melt curve temperature. The melt curve of each assay depends on the abundance of GC and TA base pairs. The more GC base pairs are present the higher the temperature has to be to separate the DNA strains. Therefore, every PCR target has a known meltcurve (if it is detected by SyberGreen). An overview of all performed qPCR assays is given in table 2. For details on the primer and the detection method see table 17 in the appendix.

Firstly, assays targeting the 16s rRNa of bacteria and archaea were performed. Secondly, assays were chosen to detect microorganisms that use sulfate, iron or nitrate as electron acceptors. The assay *drsA* (dissimilatory sulfite reductase) was performed to obtain concentrations of the target gene copies which is present in sulfate-reducing bacteria and catalyzes an important step of the anaerobic sulfate respiration (Dhillon *et al.*, 2003). Targeting the *mcrA* gene (methyl coenzyme M) indicates the presence of methanogenic archaea in the groundwater. For the detection of the iron-reducing bacteria *Geobacter* sp., the 16s rRNA was target and for nitrate-reducing bacteria, the gene *narG* was targeted. Furthermore, the 16s rRNA of *Peptococcaceae* sp. was detected to show benzene degradation. Thirdly, to assess the potential of bacteria to degrade aromatic hydrocarbon, genes that are known to degrade aromatic hydrocarbons were targeted: The NC (naphthalene carboxylase) is known to catalyze the anaerobic degradation of naphthalene; *assA* (Alkylsuccinate synthase) to catalyze the activation of alkane; the *bamA* gene

(6-oxocylcohex-1-ene-1-carbonylCoA hydrolase) is known to catalyze the cleavage of the aromatic ring anaerobically; the *abcA* gene (Benzene Carboxylase) is involved in the anaerobic degradation of benzene; the *bssA* (Benzylsuccinate synthase) of denitrifier and sulfate reducing bacteria (SRB) is a subunit of the enzyme that catalyzes the anaerobic degradation of toluene and xylene.

After running a few assays for the batch experiments unsuccessfully it was obvious that something was inhibiting the PCR. Hence the DNeasy®PowerLyzer®PowerSoil®Kit from Quiagen was used to remove the PCR inhibitors from the purified DNA. Such inhibitors prevent the amplification of the genes through direct interaction with the DNA or interference with the DNA polymerase. Unfortunately, it was not possible to remove the inhibitor from the purified DNA samples. As Gallup (2011) states in his chapter qPCR inhibition and amplification of difficult templates (PCR Troubleshooting and optimization: the essential guide) states "every sample introduces its own degree and assortment of qPCR-inhibitory and qPCR-friendly carryover contaminants, affecting, skewing, influencing and/or enhancing the entire qPCR process". This is known as the sample effect. Retrospectively, using pure groundwater extractions without filtering the sample prior to the DNA isolation leads to the inclusion of contamination in the samples which are most likely responsible for the inhibition of the qPCR processes. However, the qPCR assays worked impeccably on the field samples.

2.4.4.1 qPCR To determine which pathways are used and which enzymes are present in the groundwater samples the following qPCR assays were performed:

Table 2: List of qPCR assays that were performed in order to study the potential of the microorganisms to degrade aromatic hydrocarbons in the fieldsamples of the Griftpark

To study	Gene ID	Gene	References
Total Bacteria	16S rRNA	16s rRNA	Lane (1991); Muyzer & Ramsing (1995)
Total Archaea	16S rRNA	16s rRNA	Vetriani *et al.* (1999)
Methanogenic archaea	*mcrA*	Methyl coenzyme M reductase	Hales *et al.* (1996)
Anaerobic sulfate respiration	*drsA*	dissimilatory sulfite reductase	Dhillon *et al.* (2003)
Geobacter sp. (Iron reducing bacteria)	16S rRNA	16s rRNA	Holmes *et al.* (2002)
Nitrate Reducing Bacteria	*narG*	α-subunit of the membrane bound nitrate reductase	López-Gutiérrez *et al.* (2004)
Peptococcaceae sp. (benzene & naphthalene degradation)	16S rRNA	16S rRNA	van der Waals *et al.* (2017)
Toluene degradation of denitrifiers	*bssA*	α-subunit of benzylsuccinate synthase	Beller *et al.* (2002)
Toluene and Xylene degradation of sulfate reducing bacteria	*bssA* SRB	Benzylsuccinate synthase SRB	Beller *et al.* (2008)
Alkane activation	*assA*	Alkylsuccinate synthase	Callaghan (2013)
Benzoic ring cleavage	*bamA*	6-oxocylcohex-1-ene-1-carbonylCoA hydrolase	Laempe *et al.* (1999)
Naphthalene degradation	NC	Naphthalene carboxylase	see appendix B
Benzene degradation	*abcA*	Benzene carboxylase	van der Waals *et al.* (2017)

3 Results

Firstly, the results from the field samples are presented followed by an evaluation of the chemical, biological and geophysical state of the monitoring well. This leads to a selection of one contaminated monitoring well and two relatively clean ones for follow-up batch experiments. Subsequently, the results of the batch experiments are visualized in section 3.2.

3.1 Results of the field samples

Table 3: Displays the results of the field measurements with the corresponding electrode in the Griftpark (08/05/2018)

ID	Field measurements				
	pH	EC [S/m]	Temperature [°C]	Redox potential [mV]	O_2 [mg/L]
BW211	7.08	1080	14.7	-106	0.07
BW157	7.17	983	14.3	-116	0.12
B22	7.35	1459	13.2	-336	0.03
Pb1	7.26	1541	13.4	-158	0.05
DV4	7.36	1619	12.5	-150	0.05
37	7.1	1037	11.9	-36	0.1
60	7.35	805	13.8	-135	0.18
BW205	7.38	1221	12.6	-195	0.08

Table 3 represents the pH, electrical conductivity, the temperature, redox potential and oxygen concentration measured immediately with electrodes in the field immediatly. The pH in all samples is 7. The temperature of the water varies between 11.9 and 14.7 °C. For all groundwater samples, oxygen concentration remains at least below 0.2 mg/L after pumping up 11-20 litre water. The highest electrical conductivity is observed to occur in the monitoring well DV4 and the lowest in the well 60. The redox potential in the B22 well, considered as the source zone, measures at -336 mV at the highest and the 37 well (downstream) has -36 mV, the lowest potential measured in the groundwater samples.

3.1.1 Abundance of hydrocarbons

Table 4 shows the concentrations of the contamination compounds of the groundwater of the Griftpark samples performed by Deltares in comparison with the external laboratory SYNlab. All investigated compounds are detected in the monitoring well B22 and Pb1 according to the Deltares data sets 1 and 2. For the B22 well, the SYNlab dataset shows similar concentrations for the detected compounds as the Deltares analysis. Whereas, the concentrations found in the groundwater of the PB1 monitoring well differ. Here, the SYNlab values are significantly higher than in the dataset 1 stated. Even higher are the results of the dataset 2 obtained from the GC-FID analysis. The naphthalene concentrations in the BW205 monitoring well differ from each other. In the BW205 monitoring wells, more than 4 mg/L was detected in dataset1 but only 0.033mg/L in the SYNlab data (3) and none was found in dataset 2 but in the BW157 monitoring well. In spite of the different concentrations, it is worth mentioning that both laboratories found naphthalene in the fieldsample of BW205 independently. In the monitoring wells BW211, BW157, 37 and 60, no aromatic hydrocarbons peaks is observed to occur. In the GC-FID measurements, methane is detected in all groundwater samples and especially high in the B22 groundwater with 3882 μg/L.

Table 4: Shows concentrations of compounds from the GC measurements of the groundwater from the eight locations in the Griftpark. Dataset 1 corresponds to the GC-MS measurements (Deltares), dataset 2 to the GC-FID measurements (Deltares) and the third data set represents the results from SYNlab. The red shaded cells indicate concentrations above the intervention level according to Dutch regulations for groundwater (Ministry of Housing & the Environment, 2000). The concentrations with * should only be seen as an indication. This concentration is above the maximal concentration for the linear calibration line of that compound (see appendix figure 25 and 26)for the GC method. 'NA' indicates the compounds that were not mentioned in the SYNlab report. '-' indicates that no peak was detected.

	concentration [ug/L]																							
	BW211			BW157			B22			Pb1			DV4			37			60			BW205		
HC	1	2	3	1	2	3	1	2	3	1	2	3	1	2	3	1	2	3	1	2	3	1	2	3
Benzene	-	-	<0.2	-	-	<0.2	1532	6381	1100	125	1545	300	-	-	<0.2	-	-	<0.2	-	-	<0.2	-	-	<0.2
Toluene	-	-	1.1	-	-	0.4	1173	3131	680	12	104	24	-	-	<0.2	-	-	0.21	-	-	0.58	-	-	0.24
Etb[1]	-	-	<0.2	-	-	¡0.2	1173	4035	1500	5.80	124	24	-	-	<0.2	-	-	<0.2	-	-	<0.2	-	-	0.88
m/p-xyln[2]	-	-	<0.2	-	-	<0.2	1777	7217	1100	15	215	41	1.15	-	-	0.2	-	-	<0.2	-	-	<0.2	-	-	0.89
o-xyln[3]	-	-	<0.2	-	-	<0.1	1029	3260	660	6.83	96	22	-	-	<0.1	-	-	<0.1	-	-	<0.1	-	-	0.37
Cumene	-	-	NA	-	-	NA	333	128	NA	0.51	-	NA	-	-	NA	-	-	NA	-	-	NA	-	-	NA
3Etln[4]	-	-	NA	-	-	NA	1494	1306	NA	0.79	-	NA	-	-	NA	-	-	NA	-	-	NA	-	-	NA
4-Etln[5]	-	-	NA	-	-	NA	366	204	NA	1.70	-	NA	-	-	NA	-	-	NA	-	-	NA	-	-	NA
2-Etln[6]	-	-	NA	-	-	NA	323	141	NA	3.03	-	NA	-	-	NA	-	-	NA	-	-	NA	-	-	NA
1,2,4TMB[7]	-	-	NA	-	-	NA	364	656*	NA	1.42	19	NA	0.24	-	NA	-	-	NA	-	-	NA	-	-	NA
1,2,3TMB[8]	-	-	NA	-	-	NA	11	212	NA	0.04	-	NA	-	-	NA	-	-	NA	-	-	NA	-	-	NA
Indane	-	-	NA	-	-	NA	921	2375	NA	32	266	NA	-	-	NA	-	-	NA	-	-	NA	-	-	NA
Indene	-	-	NA	-	-	NA	1063	64	NA	22	2.86	NA	-	-	NA	-	-	NA	-	-	NA	-	-	NA
Nph[9]	-	-	<0.21	-	421	<0.2	8798*	11174*	8800	64	-	0.42	-	-	0.03	-	-	0.12	-	-	0.24	4155	-	33
2-MNph[10]	-	-	NA	-	-	NA	4113	1302	NA	-	-	NA	-	-	NA	-	-	NA	-	-	NA	-	-	NA
Methane	NA	12	NA	NA	32	NA	NA	3882	NA	NA	216	NA	NA	44	NA	NA	84	NA	NA	82	NA	NA	138	NA
Mineral oil	NA	NA	<50	NA	NA	<50	NA	NA	16000	NA	NA	290	NA	NA	<50	NA	NA	<50	NA	NA	<50	NA	NA	85

[1]Ethylbenzene

[2]m-/p-xylene

[3]o-xylene

[4]3-ethyltoluene

[5]4-ethyltoluene

[6]2-ethyltoluene

[7]1,2,4-trimethylbenzene

[8]1,2,3-trimethylbenzene

[9]naphthalene

[10]2-methylnaphthalene

3.1.2 Abundance of anions and cations

The mutual anions and cations measured in ICPOES and DIONEX analysis are very similar. There is no nitrite and hardly any nitrate present the field samples (see table 5). A high concentration of sulfate is detected in the groundwater of DV4 and Pb1 but none in the B22 well. However, the sulfur concentration in the B22 groundwater is with 118 mg/L the highest concentration measured in the samples. Iron ismeasured as more than 6 mg/L present in the BW211, BW157, and Pb1 wells. Chloride, sodium, and calcium are present in all samples. The highest concentration of these ions is found in the BW205 field samples. Moreover, the highest NPOC was measured here.

Table 5: Table of concentrations of anions, cations, pure elements and NPOC (non-purgeable organic carbon) detected in the groundwater from the eight locations in the Griftpark. The ions that were measured in the DIONEX and ICPOES analysis are listed as the average value. For the raw data see table 20 in the appendix. '<MDL' is given when the concentration is under the detection level and 'NA' if no peak was detected.

monitoring	DIONEX [mg/L]				ICPOES [mg/L]			ICPOES + Dionex [mg/L]				NPOC
well	NO_2^-	NO_3^-	SO_4^{-2}	NH_4^+	Fe	Mn	S	Cl	Na	Ca	Mg	[mg/l]
BW211	NA	<MDL	73	1.23	6.98	1.66	32	62	47	144	12.9	3.42
BW157	NA	<MDL	64	1.18	6.84	0.50	27	47	35	131	15.1	3.07
B 22	NA	<MDL	<MDL	31.00	0.14	0.23	118	72	63	160	19.8	27.13
PB1	NA	<MDL	256	10.50	6.98	1.48	105	70	66	223	18.0	5.28
DV4	NA	<MDL	227	23.40	2.08	0.70	93	60	71	212	21.1	7.96
37	NA	0.47	111	8.38	0.82	1.18	48	43	54	141	14.2	7.92
60	NA	<MDL	31	7.50	2.79	0.33	14	54	35	99	10.3	4.11
BW205	NA	<MDL	21	9.61	1.76	0.44	9	151	112	116	12.0	87.23

3.1.3 DNA analysis

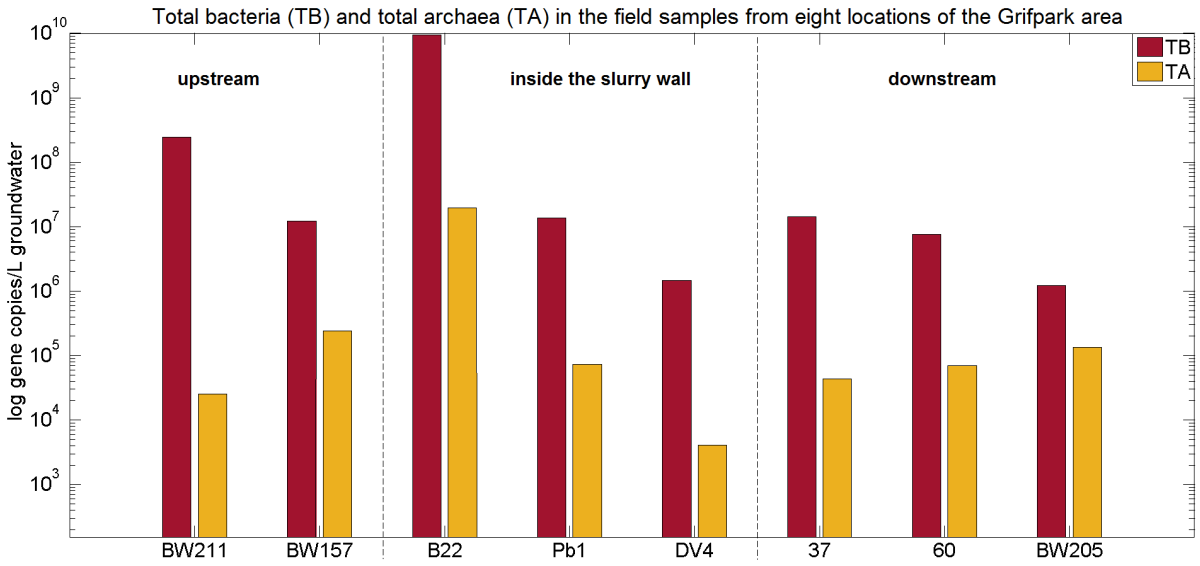

Figure 11: Visualization of the total bacteria (TB) and total archaea (TA) qPCR assay results targeting the 16S rRNA in microorganisms found in 1L groundwater from eight different locations in and around the Griftpark. The different locations are displayed on the x-axis. The y-axis starts at the detection limit. The dotted line separates the samples geographically. The samples in the first part were obtained from the monitoring wells upstream of the slurry wall, the second from inside and the third from downstream.

In figure 11, the concentrations of the genes per copy per liter of groundwater detected in the qPCR assays for total bacteria and total archaea are illustrated. In the groundwater of the B22 monitoring well, the highest concentration of bacteria (10^{10}) and archaea (10^{7}) are found. Similarly, the BW211 has higher bacterial concentrations (10^{8}) than other wells, with the exception of B22, but very low concentrations of archaea (10^{4} gene copies per sample), which is unlike what was found for B22.

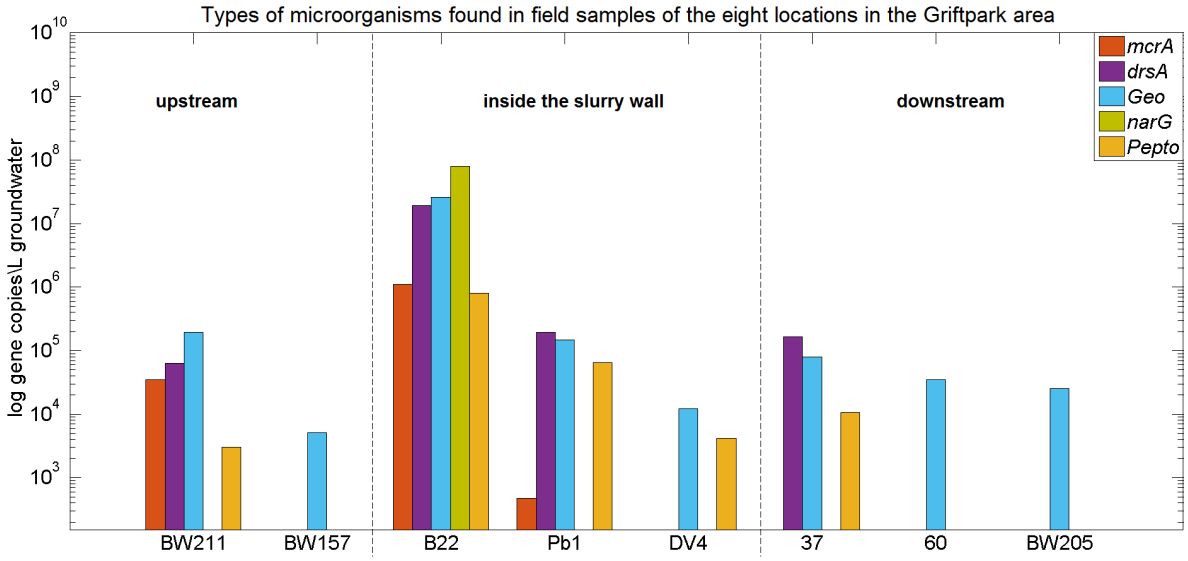

Figure 12: Visualization of the results for the types of microorganisms targeted in qPCR assays found in 1L of filtered groundwater in eight different locations in and around the Griftpark. The different locations are displayed on the x-axis. The y-axis starts at the detection limit. The dotted line separates the samples geographically. The samples in the first part were obtained from the monitoring wells upstream of the slurry wall, the second from inside and the third from downstream. The abbreviations are explained in the following: *mcrA* = methanogenic archaea, *drsA* = *drsA* gene in sulfate-reducing bacteria, Geo = 16s rRNA of *Geobacter* sp. (iron-reducing bacteria), *narG* = *narG* gene in nitrate-reducing bacteria, Pepto= *Peptococcaceae* sp.

Following the determination of the bacterial and archaeal concentrations in the groundwater of the field samples, the diversity of the microorganisms is investigated in the samples. Figure 12 shows the gene copies/L for the enzymes that are present in methanogenic archaea, nitrate-, sulfate-, and iron-reducers, and *Peptococcaceae* sp.. The highest concentrations of the target genes are again found in the B22 groundwater. The assays targeting nitrate-reducing bacteria are displayed in green *narG* and is only present in the B22 water sample (green). To detect sulfate-reducing bacteria, the *drsA* assay was performed (in purple). It is found to occur in the monitoring wells, B22, 37 and Pb1. The genes *mcrA* from methanogenic archaea are only detected in the BW211 and B22 samples (red). The benzene degrading *Peptococcaceae* sp. is found in the BW211, B22m 37, DV4 and PB1 field samples (yellow), whereas the presence of *Geobacter* sp. is found to occur in all field samples (blue).

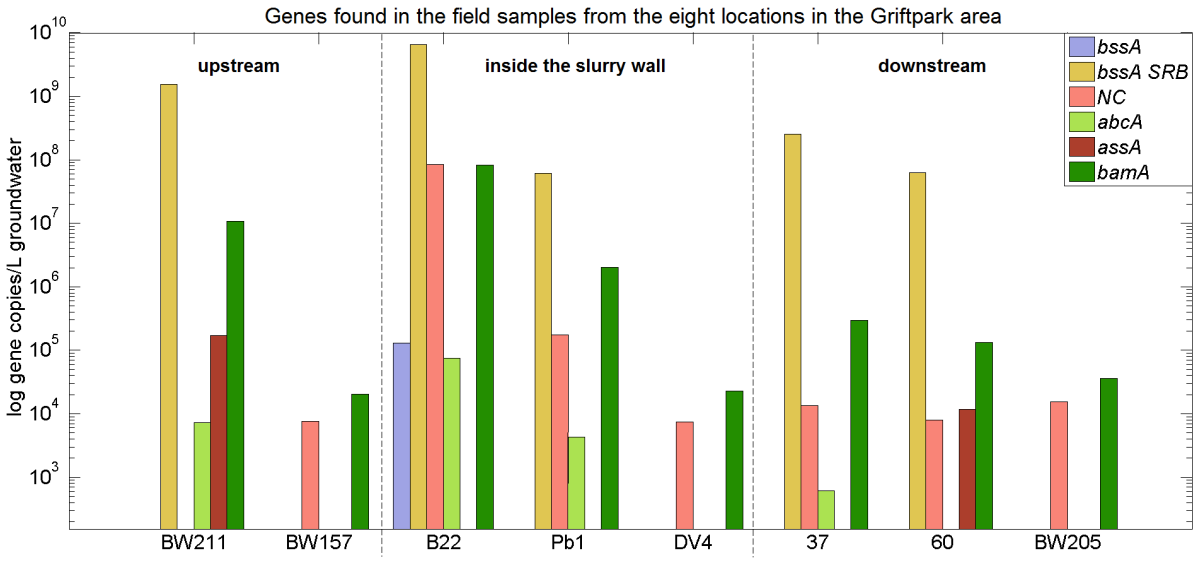

Figure 13: Shows the results of genes targeted in qPCR assays found in 1L groundwater in 8 different location in and around the Griftpark. The different locations are displayed on the x-axis. The y-axis starts at the detection limit. The dotted line separated the samples geographically. The samples in the first part were obtained from the monitoring wells upstream of the slurry wall, the second from inside and the third from downstream. The abbreviation are explained in the following: *bssA* = Benyzlsuccinate synthase for denitrifiers (violet), *bssA* SRB = Benzylsuccinate synthase for sulphate reducing bacteria (yellow), NC = naphthalene carboxylase (rose), *abcA* = benzene carboxylase (light green), *assA* = alkylsuccinate syntase (dark red), *bamA* = 6-oxocylcohex-1-ene-1-carbonylCoA hydrolase (dark green).

To further investigate the potential of the microorganisms to degrade aromatic hydrocarbons, the results of qPCR assays targeting genes associated with the degradation of aromatics in the field samples are presented in figure 13. Very high concentrations of the *bssA* SRB gene ($> 10^7$) are detected in the monitoring wells BW211, B22, 37, 60 and Pb1. The *bamA* gene exists in all samples, but the highest concentration was found for the B22 field samples. The genes for the *bssA*, *assA* and *abcA* are less abundant in the field samples, the *bssA* gene of denitrifying organisms is only present in the B22 field sample. The *assA* gene is more abundant in the field samples. The assay shows revealed the presence of the gene in the BW211 and the 60 samples. Whereby, this assay represents the only gene that was not found in the B22 samples. The *abcA* gene is found in the B22, BW211 and Pb1 groundwater samples in concentrations of more than $<10^4$.

3.2 Results of the batch experiments

Note that all analyses were performed in duplicates. Solely the average values of the analysis are displayed. In the following, the aromatic hydrocarbons are illustrated for the B22, BW205 and 60 batches under the studied scenarios. Special focus is given to the B22 batches. T0 corresponds to the same day the batches were prepared, T1 represents the extraction of the batches after 14 days and T2 after 38-39 days of incubation. The anions and cations presented are selected according to their relevance and changing presence in the analysis. For further details see table 25 in the appendix.

3.2.1 Per scenario

No additives

The first scenario presented is without any additives. The results from the GC-MS analysis are presented in the figure 14 and in the table 22. The aromatic hydrocarbons detected in the B22 batches are illustrated in the scatter plot and split up according to their initital concentration at time T0 (figure 14A, B, C). A total decrease of aromatic hydrocarbons is recorded for the B22 batches, first at 12% in T1 and then 13% in T2 (table 22). In the B22 batches, a moderate decrease of all compounds is observed. The concentration of aromatic hydrocarbons in the BW205 and 60 batches are presented in a bar chart. During the analysis of BW205, no compounds are detected after T1 (figure 14D). In the 60 batches, only o-xylene (2.76 μg/L), 4-ethyltoluene (1.13 μg/L) and indane (2.69 μg/L) show a peak at T1 in the GC-MS analyses. At T2 however, concentrations of toluene (6.68 μg/L), 2-ethyltoluene (1.78 μg/L) are also detected. Moreover, the previously measured compounds (o-xylene (3.57 μg/L), 4-ethyltoluene (1.96 μg/L) and indane (8.31 μg/L) increase slightly in concentrations from T1 to T2. The picture in figure 14E the batches at time T0 and T2 are shown. It is noted that the glass of the B22 batches is less brownish at T2 than at T0, whereas the other batches do not show a significant change in color.

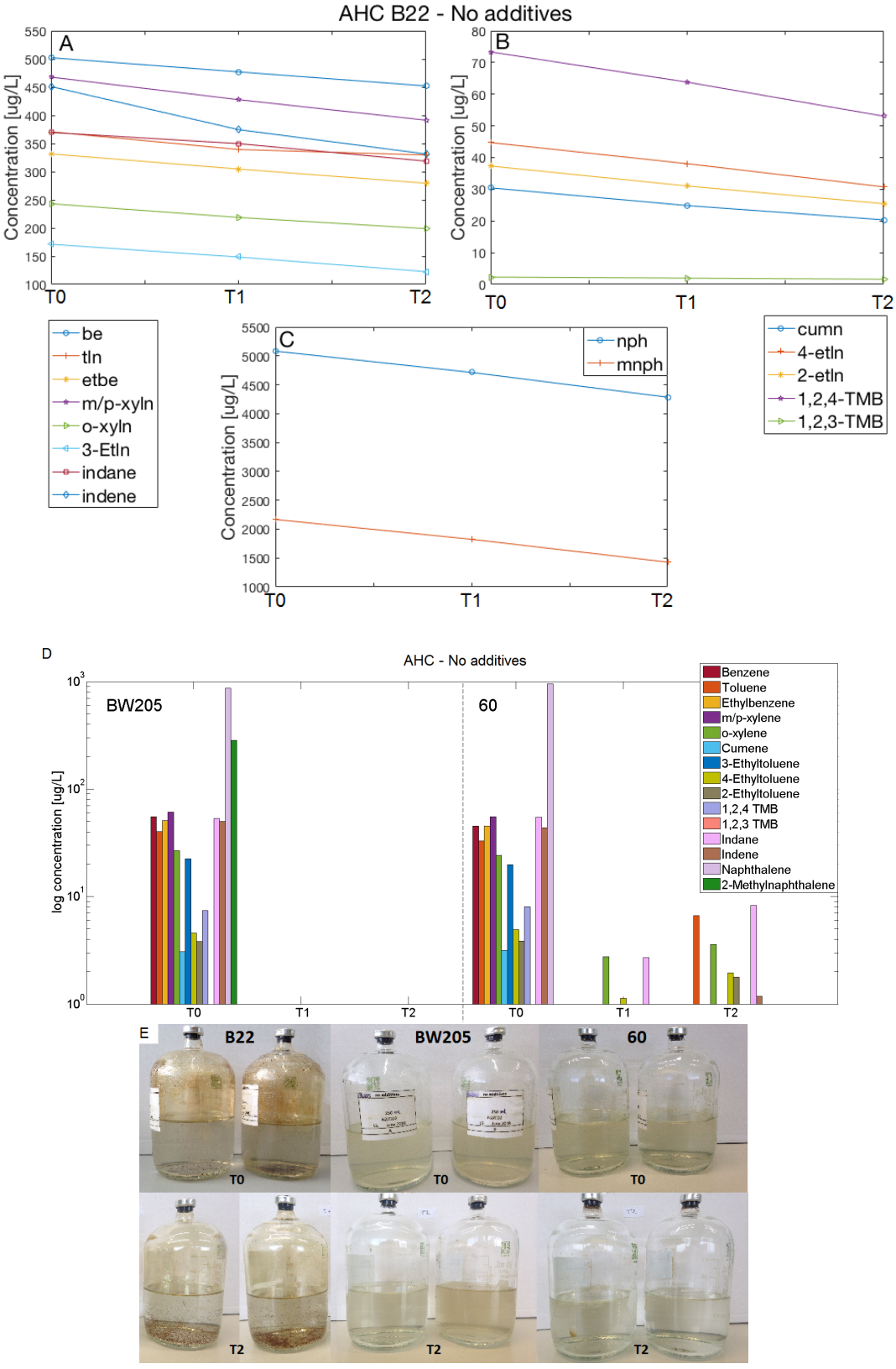

Figure 14: Presentation of the aromatic hydrocarbons detected in the GC-MS measurements and pictures of the No additives batches at the times of T0 and T2. Subfigures A, B, C represent the data of the B22 batches and D the data of the BW205 and 60 batches. The abbreviations are explained in table 4.

Table 6: The results of the Dionex and ICPOES measurements of the no additives batches are displayed. 'NA' indicates that no peak was detected.

Batch	Time	[mg/L]													
		Cl^-	Na^+	Ca^{2+}	K^+	SO_4^{2-}	S^{2-}	NH_4^+	NO_2^-	NO_3^-	Fe^{2+}	Mn^{2+}	Mg^{2+}	P	PO_4^{3-}
B22	T0	78.17	62.70	143.22	19.25	5.83	56.65	26.96	0.11	NA	NA	0.32	18.77	0.95	1.97
	T2	94.85	76.80	121.73	13.61	28.07	33.99	24.81	0.10	3.13	0.21	0.19	15.16	0.76	0.98
BW205	T0	145.66	103.19	102.49	7.85	17.78	6.95	10.54	0.33	0.81	NA	0.44	12.51	0.32	NA
	T2	92.75	72.24	107.83	7.19	21.26	7.94	9.57	0.07	4.51	2.03	0.38	11.82	0.43	NA
60	T0	69.55	38.38	100.46	7.17	30.70	11.44	8.15	0.09	0.73	NA	0.37	11.77	0.33	NA
	T2	32.68	38.75	106.56	6.66	34.20	11.51	7.78	0.09	4.03	2.13	0.27	11.16	0.49	NA

For this scenario, all tested anions and cations are displayed in table 6. In the B22 batches, the amount of sulfate, chloride, and sodium increase but concentrations of chloride, sulfur, potassium, magnesium, and ammonium decrease slightly. The latter, except for chloride show the highest concentrations in the B22 batches. At T2, 3.1 mg/L nitrate is detected which is not initially found. Similar concentrations of nitrate also emerge in the T2 measurement of the BW205 and 60. Here, the chloride concentrations decrease by about 37% and 53% respectively. Moreover, more than 2 mg/L iron is found in the T2 of the BW205 and 60 batches and sulfate and nitrate concentrations increase moderately. All the other concentrations of ions do not change significantly from T0 to T2 in these batches.

Oxygen

Next, the anaerobic batches are studied. The aromatic hydrocarbons in the B22 batches are illustrated in scatter plots (15A,B,C) and the BW205 and 60 batches in bar charts (15D). The data is retrieved from table 22 in the appendix. In the B22 oxygen batches, a rapid decrease of all aromatic hydrocarbons is observed. Already at T1 no ethylbenzene, cumene or naphthalene is found. At T2, the concentration of benzene and toluene, ethylbenzene, indene, cumene, 1,2,3-trimethylbenzene, naphthalene and 2-methylnaphthalene are undetectable and only m-/p-xylene (82.59 μg/L), o-xylene (5.93 μg/L), 3-; 2- and 4-ethyltoluene (48.17 μg/L, 19.62 μg/L and 11.35μg/L), respectively), 1,2,4 trimethylbenzene (19.63 μg/L) indane (66.59 μg/L) and a small concentration of indene (1.19 μg/L) are detected. The decrease of compounds coincides with the mitigating brown coloring of the batches from T0 to T2 (figure 15C). For the BW205 and 60 oxygen batches, no volatile aromatic hydrocarbons are detected at the moment of T1 and T2 (figure 15D).

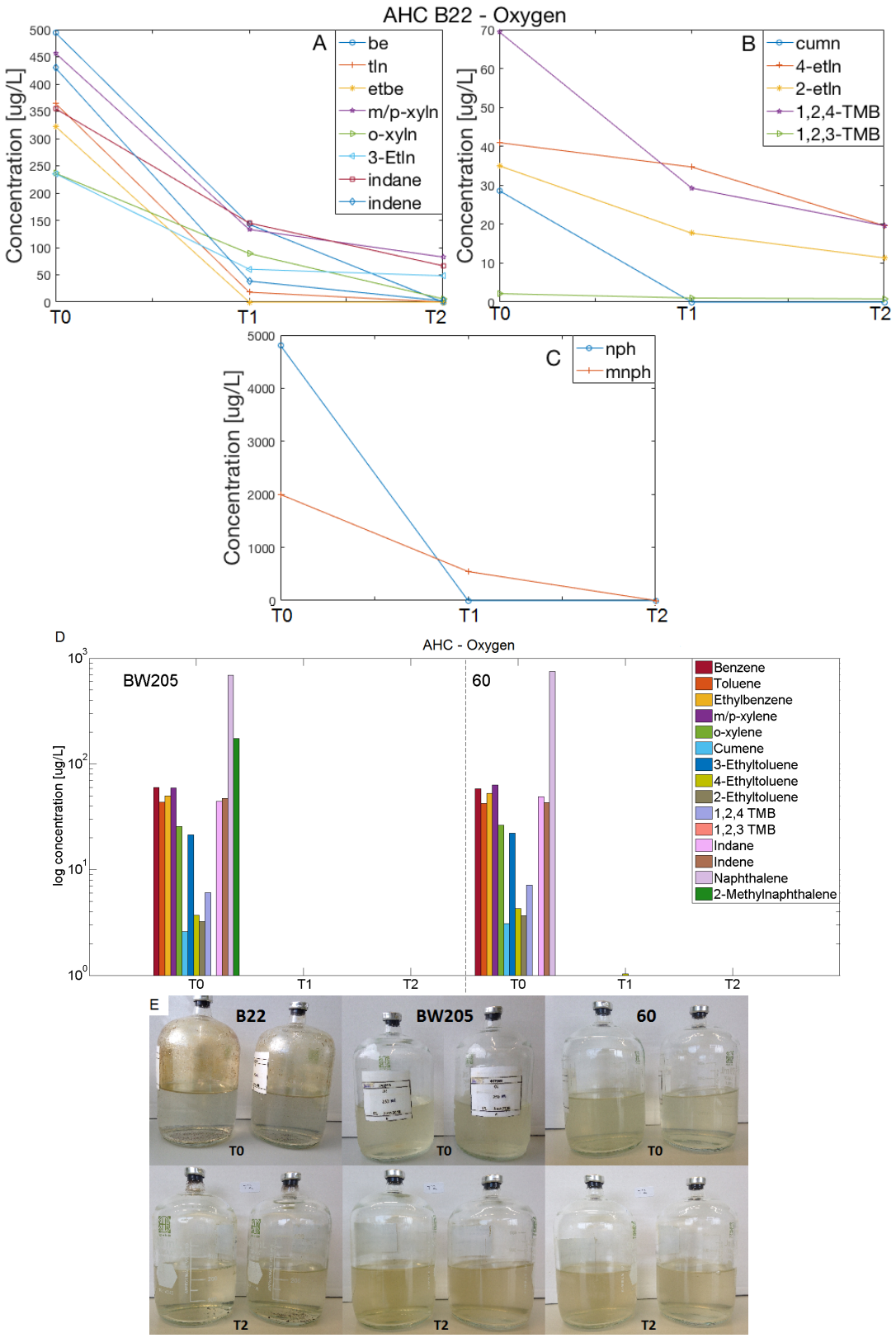

Figure 15: Visualization of the aromatic hydrocarbons (AHC) in the oxygen batches detected by the GC-MS and pictures (E) at time T0 and T2. Subfigures A, B, C represent the data of the B22 batches and D of the BW205 and 60 batches. The abbreviations are explained in table 4.

Table 7: The results of the GC-TCD, Dionex and ICPOES measurements of the oxygen batches are displayed. 'NA' indicates that no peak was detected.

Batch	Time	O_2 [%]	[mg/L]							
			Cl^-	Na^+	Ca^{2+}	SO_4^{2-}	S^{2-}	NH_4^+	NO_2^-	NO_3^-
B22	T0	20.00	142.88	61.51	77.95	5.78	55.59	26.86	0.09	NA
	T2	5.04	68.75	63.15	64.12	44.47	16.13	22.71	0.11	1.21
BW205	T0	20.00	53.79	104.30	106.22	16.42	8.01	10.51	0.17	0.77
	T2	7.18	53.90	101.99	119.94	21.51	8.27	0.26	13.34	18.27
60	T0	20.00	50.77	38.18	87.66	30.68	11.19	8.89	0.10	0.74
	T2	4.85	53.17	39.34	45.69	34.81	12.12	0.14	11.40	14.54

Focusing on the anions and cations (table 7) in the groundwater, it is appaerent that in the B22 batches a rapid decrease of sulfur from T0 (55 mg/L) to T2 (16 mg/L) simultaneous with an increase in the sulfate concentrations from 5 mg/L at T0 to 44 mg/L at T2 occurred. The difference between both concentrations is in both cases 39 mg/L. Moreover, the chloride concentrations decrease to less than half of the initial concentration in the B22 batch. Furthermore, it is striking that the batches with no aromatic hydrocarbons at T1 and T2 (BW205 and 60) show a shift from initially approximately 10 mg/L ammonium to almost 19 mg/L nitrate and 14 mg/L nitrite, whereas in the B22 batch the ammonium concentration are only reduced by 4 mg/L and the nitrate concentration increase from 0 to 1.2 mg/L. The oxygen concentrations (table 7) are initially set to 20 % of the headspace, as the oxygen concentration in the atmosphere, and show a decrease to less than half of the initial concentration in all batches.

Oxygen + Nutrients

In the B22 batches with oxygen and nutrients (table 22 and figure 16A, B and C), a small decrease in the concentration of total compounds to about on average 40 % of the initial concentration is observed. All compounds show a rapid decrease from T0 to T1. From T1 to T2 1,2,4 trimethylbenzene, cumene and 2-ethyltoluene continue to decrease (below 8 μg/L), while the concentrations of the other hydrocarbons remained constant. In BW205, at T1 and T2, no peaks for the compounds are detected by the GC-MS (figure 16D). A similar pattern is observed for the 60 batches. However, at extraction moment T2, more

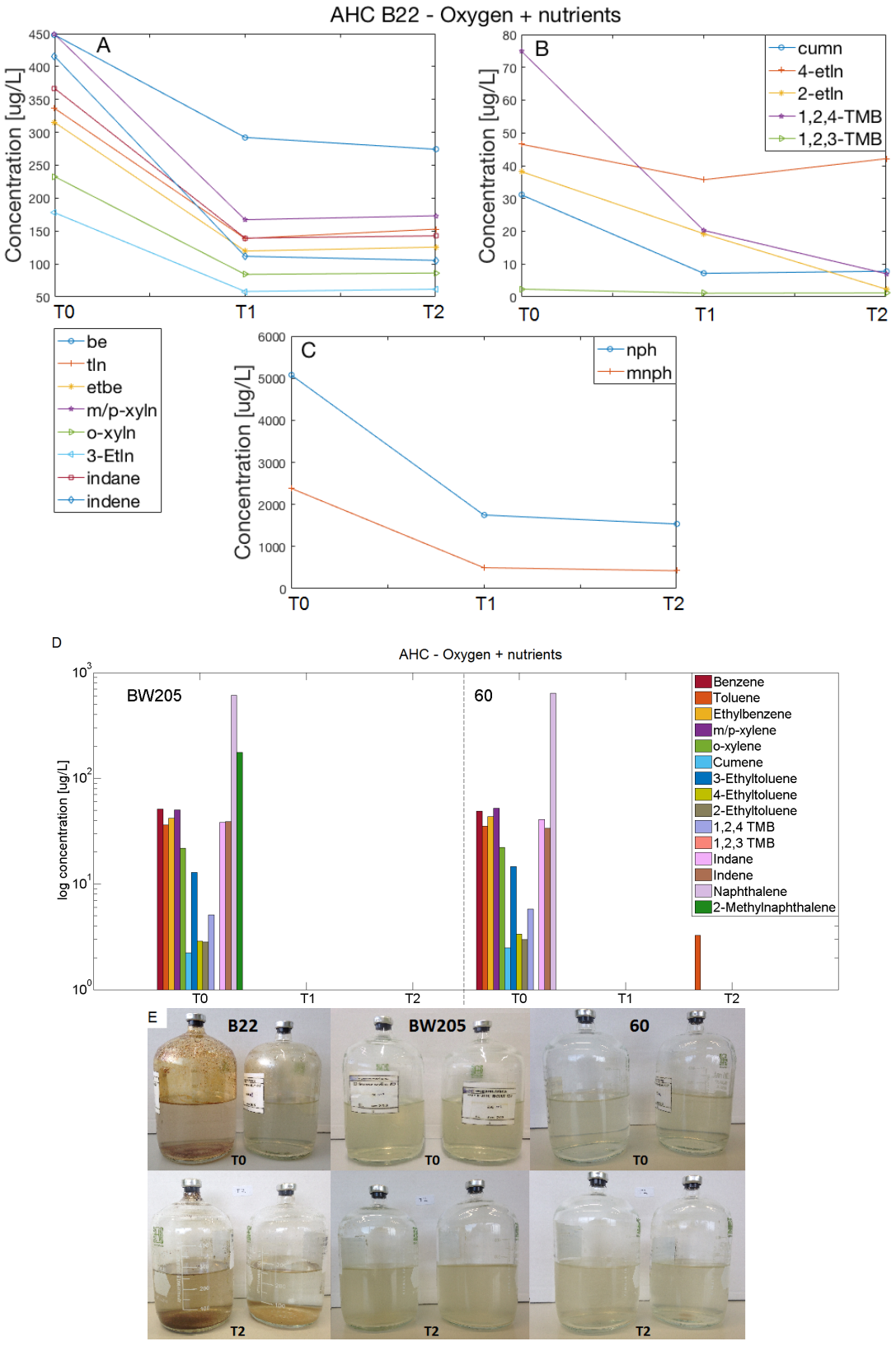

Figure 16: Illustration of the results of the aromatic hydrocarbons detected in the GC-MS measurements and pictures (E) of the oxygen+nutrients batches at the moment of T0 and T2. Subfigures A, B, C represent the data of the B22 batches and D of the BW205 and 60 batches. The abbreviations are explained in table 4.

than 3 μg/L of toluene is measured. Small peaks are detected for other compounds but the concentrations are below 0.5 μg/L and are not visible in the bar chart. A detailed view of concentrations if presented in table 22 in the appendix.

Table 8: The results of the GC-TCD, Dionex and ICPOES measurements of the oxygen and nutrients batches are displayed. 'NA' indicates that no peak was detected.

batch	Time	[mg/L]										
		O_2 [%]	Cl^-	Na^+	Ca^{2+}	SO_4^{2-}	S^{2-}	NH_4^+	NO_2^-	NO_3^-	PO_4^{3-}	P
B22	T0	20.00	74.99	120.189	100.43	38.13	39.06	33.67	0.11	NA	140.41	71.01
	T2	5.46	62.57	122.3929	44.32	50.92	18.94	31.15	0.15	1.11	37.73	24.12
BW205	T0	20.00	139.39	158.9992	97.06	52.68	18.44	20.51	0.25	1.12	148.11	71.86
	T2	5.32	125.61	160.8972	52.98	58.22	19.24	0.39	52.96	2.22	147.49	50.88
60	T0	20.00	66.66	101.5927	92.78	65.11	22.16	19.18	0.10	0.79	222.46	72.61
	T2	9.33	52.52	104.5948	52.53	71.26	22.26	0.35	50.42	1.46	163.43	53.43

The anions and cations measured at T0 and T2 are presented in the table 8. Chloride, calcium and phosphorus concentrations are observed to decrease in all batches. Furthermore, in the B22, the concentrations of sulfur and phosphate are found to decrease as well, whereas in the BW205 batches sulfur and phosphate concentrations are stable. Ammonium concentrations are observed to decrease and in the 60 batches not only ammonium but also phosphate concentrations are observed to decrease. The batches BW205 and 60 have an increase of the concentrations of sulfate, nitrate and nitrite in common. In these batches, the ammonium at T2 is almost completely removed and nitrite concentrations emerge. Whereas in the B22 batches, only the sulfate concentrations increased. Furthermore, the oxygen concentrations measured at T2 were less than half of the initial concentration.

Chlorate

Next, the anaerobic batches are studied. In the chlorate B22 batches, a total reduction from 10342 μg/L to 7926 μg/L is measured from T0 to T1. (table 22 in the appendix). In the B22 batches, presented in scatter plots, first a decrease of compounds from T0 to T1 is observed, followed by an increase from T1 to T2 (figure 17AB). The concentrations of 1,2,3 trimethylbenzene remain relatively steady between 2.34 at 1.50 μg/L. The largest relative

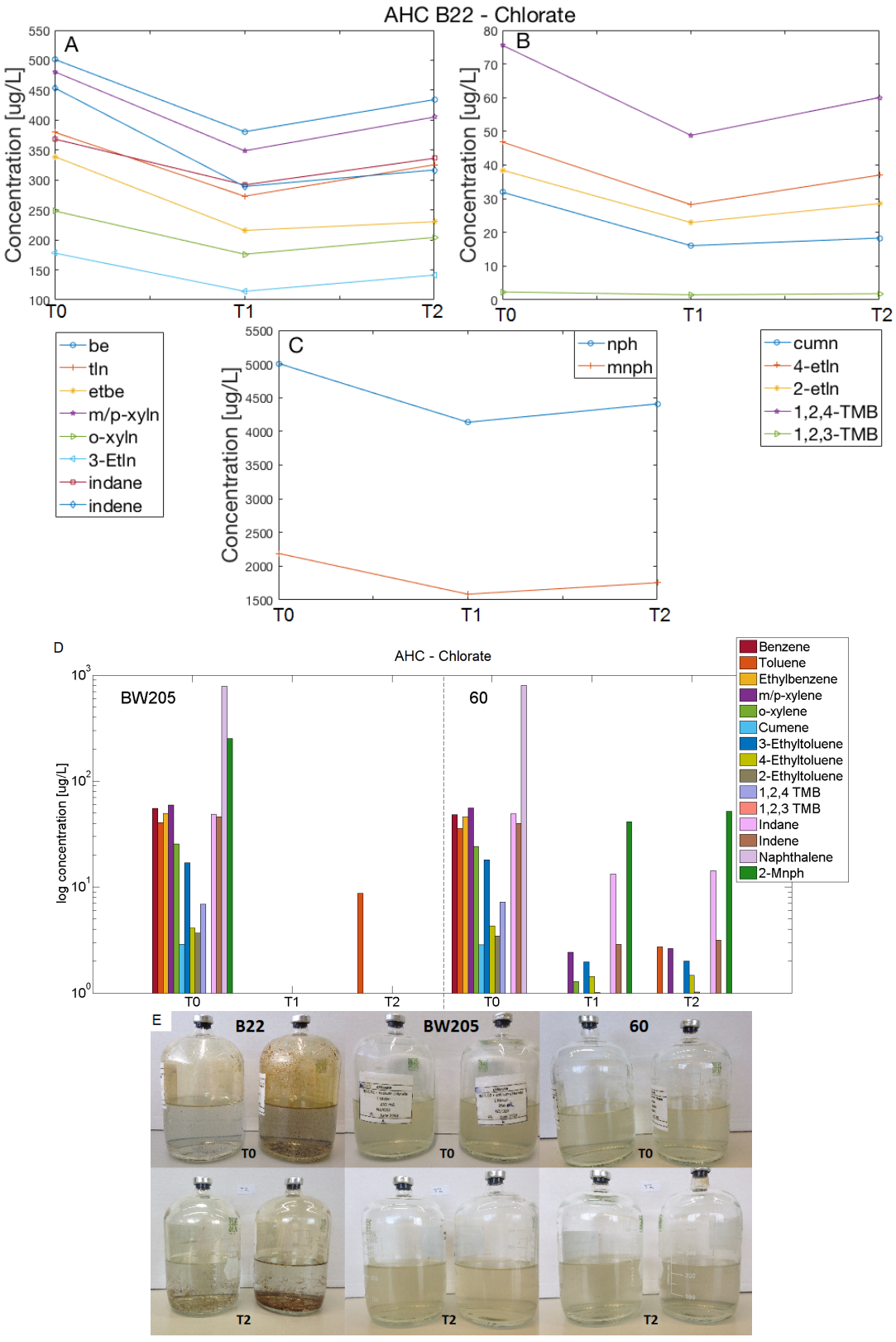

Figure 17: Visualization of the aromatic hydrocarbons detected by the GC-MS and pictures (E) of the chlorate batches at the moment of T0 and T2. Subfigures A, B, C represent the data of the B22 batches and D of the BW205 and 60 batches. The abbreviations are explained in table 4.

change is noted for cumene. Cumene concentrations decrease by almost 50% with an initial concentration of 31 μg/L. In the bar charts of aromatic hydrocarbon concentration found in the BW205, no 1,2,3 trimethylbenzene was found initially (figure 17D). At T1 no compounds in the BW205 batches are detectable but at T2 a toluene concentration of 8.7 μg/L is observed in the BW205 batches. In the 60 batches, no 1,2,3-trimethylbenzene and 2-methylnaphthalene are found in the batches initially. Furthermore, at T1 concentrations of m-/p-xylene (2.42 μg/L), o-xylene (1.28 μg/L), 3-and 4-ethyltoluenen (1.97 and 1.44 μg/L, respectively), indane (13.22 μg/L), indene (2.87 μg/L) and methylnaphthalene (41.17 μg/L) are detected. These concentrations remain relatively constant between T1 and T2. Furthermore, at T2, a toluene concentration of 2.72 μg/L is measured. The picture E in figure 17 shows the batches at T0 and T2. The brown color of the glass of the B22 batches seems to be reduced from T0 to T2. No significant change of the BW205 and 60 batches is observed.

Table 9: The results of the GC-TCD, Dionex and ICPOES measurements of the chlorate batches are displayed. 'NA' indicates that no peak was detected. a - is inserted when no measurement was performed.

Batch	Time		[mg/L]								
		O_2 [%]	ClO_3^-	Cl^-	Na^+	Ca^{2+}	SO_4^{2-}	S^{2-}	NH_4^+	NO_2^-	NO_3^-
B22	T0	6.26	813.25	77.79	290.57	145.70	5.12	8.49	26.04	0.08	NA
	T2	2.50	827.55	269.25	301.09	146.46	22.42	10.67	24.61	0.10	3.10
BW205	T0	-	806.28	148.96	333.80	105.32	17.26	7.61	10.93	0.32	1.16
	T2	5.91	803.18	335.35	337.02	107.68	21.23	7.87	9.99	0.10	4.11
60	T0	-	781.57	76.57	297.01	103.54	30.47	11.72	8.36	0.10	1.02
	T2	2.21	792.72	249.38	265.96	105.26	34.54	12.12	8.15	0.12	3.56

Table 9 demonstrates the concentration of anions and cations measured in the DIONEX and ICPOES analysis and shows the oxygen concentration in percentage compared to 20% atmospheric oxygen. At T0, oxygen measurements were only performed for the B22 batch. For the other batches a '-' indicates that no analysis was performed. For all batches, the oxygen concentrations were measured after the T2 extraction. The chlorate concentrations are only an indication of the concentration. Because the DIONEX analysis did not include the chlorate initially the concentrations were determined in the aftermath of the experiment using a given standard. Nevertheless, the concentrations of chlorate in

the batches do not change over the set time span. The chloride concentrations are lower in T0 but reached similar concentrations as sodium at T2 measurements in all batches. Although sulfate concentrations increased from T0 to T2 in all batches, the B22 samples showed the largest increase from 5 to 22mg/L out of all of them. Moreover, at T2 a small amount of nitrate is measured which does not exists in the T0 measurements.

Nitrate

In the nitrate batches of B22, hardly any change in the aromatic hydrocarbons (figure 18A, B, C and table 23) from T0 to T1 is observed. Afterwards the compouds decrease slightly. The aromatic hydrocarbon measured in T0 for BW205 are beyond detecable limits of the instrument at T1 and T2 (figure 18D). For the 60 batches, only low concentrations of indane (9.54 μg/L) and 2- and 4-ethyltoluene (1.58 and 2.38 μg/L, respectively) are recorded at T1. At the moment of the extraction T2 these concentrations remain the same but additionally, the peak for toluene reappears in the GC-MS measurements corresponding to approximately 7.68 μg/L (see figure 18D and table 23).

Table 10: The results of the Dionex and ICPOES measurements of the nitrate batches are displayed. 'NA' indicates that no peak was detected.

Batch	Time	[mg/L]							
		Cl^-	Na^+	Ca^{2+}	SO_4^{2-}	S^{2-}	NH_4^+	NO_2^-	NO_3^-
B22	T0	77.47	274.36	140.23	4.97	45.09	26.13	0.09	577.41
	T2	65.78	289.65	142.71	43.81	16.08	24.00	21.51	604.93
BW205	T0	147.85	325.44	104.86	17.03	7.27	10.94	0.25	607.78
	T2	128.14	325.66	104.12	20.75	7.47	9.85	1.19	620.68
60	T0	70.45	256.01	99.94	30.07	11.32	9.26	0.11	583.79
	T2	50.82	260.74	103.92	33.71	12.35	8.26	3.05	600.97

In the B22 batches, almost no sulfate (4.9 mg/L) and nitrite (0.09 mg/L) are measured at T0, whereas in the T2 measurements an increase of sulfate of almost 10-fold (43.8 mg/L) is demonstrated (see tabel 10). Furthermore, the nitrite concentration increases up to 21.5 mg/L. The anion and cation concentrations in the BW205 and 60 batches do not change as much as in the B22 batches. However, the sulfate and nitrite concentration increase slightly, whereas, the chloride concentration decreases from T0 to T2. In none of the nitrate spiked batches can a significant change in the concentration of nitrate be

detected.

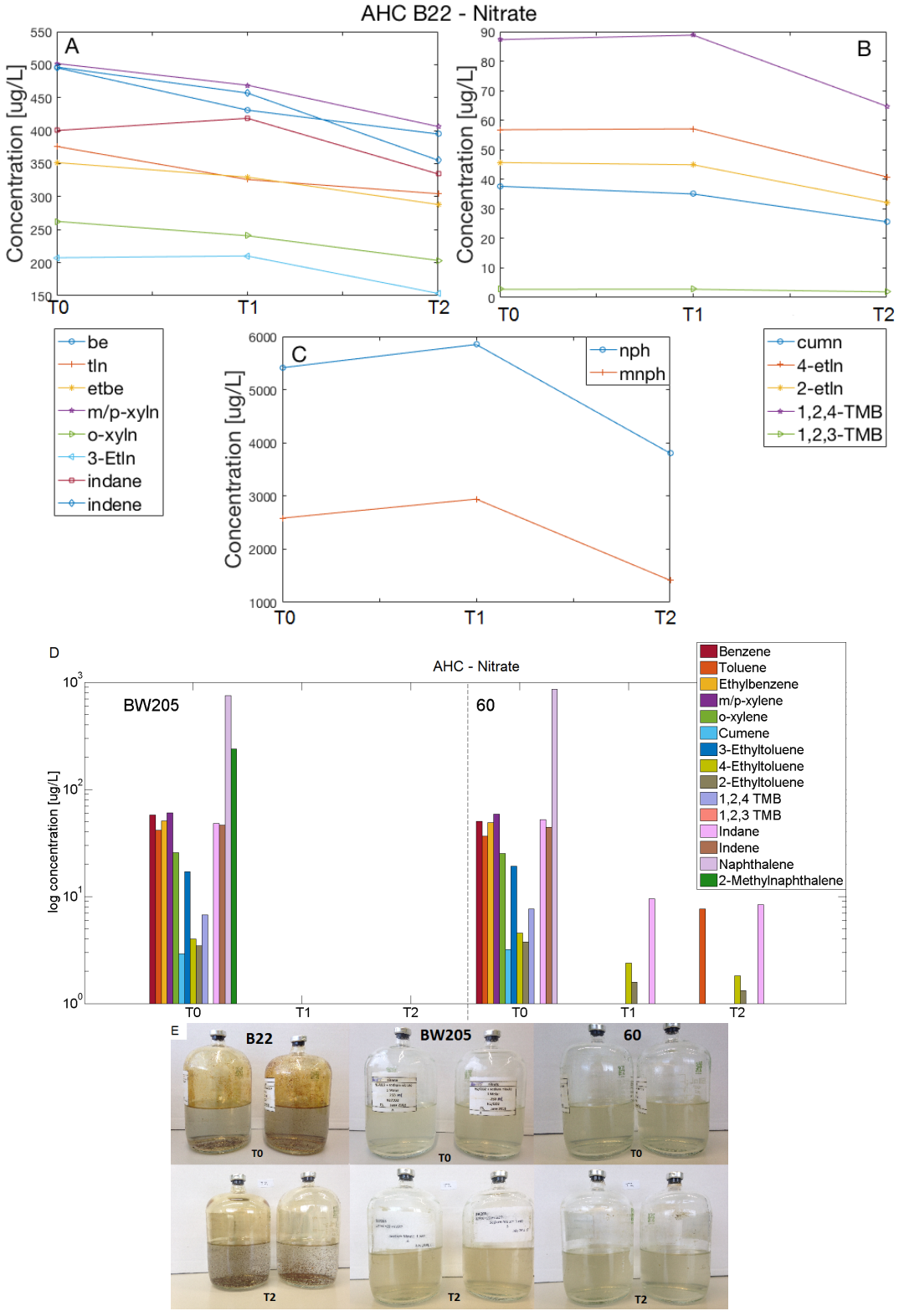

Figure 18: Presentation of the results of the aromatic hydrocarbons detected by the GC-MS and pictures (E) of the nitrate batches at T0 and T2. The subfigures A, B, C represent the data of the B22 batches and D of the BW205 and 60 batches. The abbreviations are explained in table 4.

Sulfate

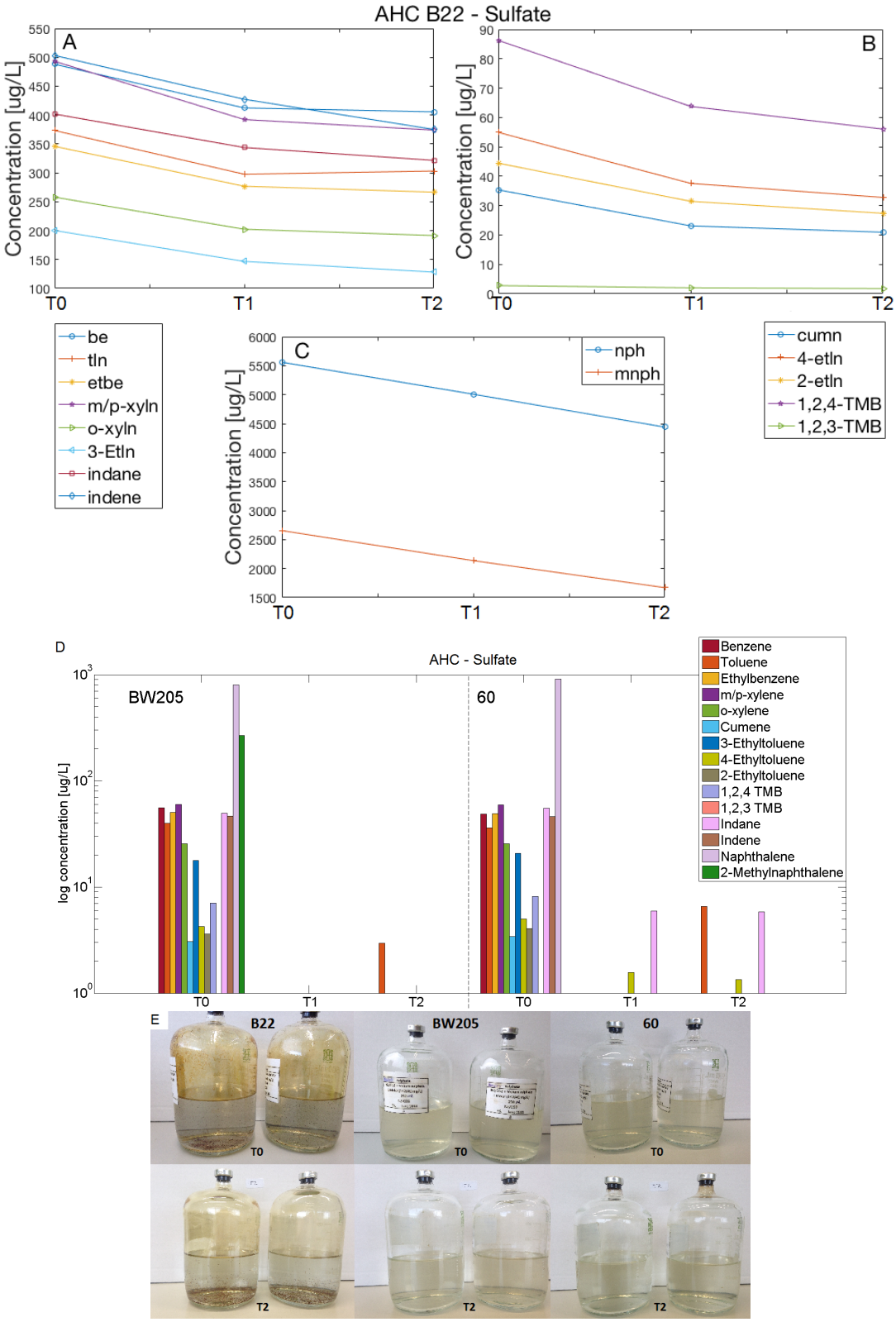

Figure 19: Visualization of the aromatic hydrocarbons detected by the GC-MS and pictures (E) of the sulfate batches at the moment of T0 and T2. The subfigures ABC represent the data of the B22 batches and D of the BW205 and 60 batches. The abbreviations are explained in table 4.

In figure 19, the concentrations of aromatic hydrocarbon in the B22, BW205 and 60 batches are illustrated. A decreased of 22% of the total aromatic hydrocarbon amount is observed in the B22 batches. Detailed values are listed in the table 23 in the appendix. From T0 the concentrations of the compounds decrease at similar ratios. Afterwards from T1 to T2 the difference in concentrations is slightly reduced. Only naphthalene and 2-methylnaphthalee continue to decrease at the same rate (figure 19C). In the BW205 batches, all concentrations of aromatic hydrocarbons at T1 are below the detectable limit of the machine. At T2, an increase of approximately 3 μg/L toluene is observed (figure 19D). In the 60 batches, at T1 and T2 small amounts of 4-ethyltoluene (1.5 μg/L) and indane (5.9 μg/L) are measured. At T2, toluene concentrations areadditionally detected. The picture in figure 19E shows the batches at time T0 and T2. The T0 B22 batches are brownish colored, whereas they appear to be less brown at T2. No significant change is observed for the BW205 and 60 batches.

Table 11: The results of the Dionex and ICPOES measurements of the sulfate batches are displayed. 'NA' indicates that no peak was detected.

Batch	Time	[mg/L]							
		Cl^-	Na^+	Ca^{2+}	SO_4^{2-}	S^{2-}	NH_4^+	NO_2^-	NO_3^-
B22	T0	76.68	537.19	141.13	1014.50	382.19	26.23	0.07	NA
	T2	62.46	560.44	155.09	1096.53	401.56	24.90	0.07	2.81
BW205	T0	147.82	597.60	105.32	1059.87	355.58	10.94	0.19	0.98
	T2	133.46	604.15	107.96	1104.83	359.79	10.27	0.06	3.91
60	T0	69.87	563.61	101.96	1059.04	361.41	9.51	0.08	0.75
	T2	49.99	534.09	104.82	1106.56	356.48	12.19	0.09	2.49

All sulfate batches show a small increase in nitrate concentrations from T0 to T2, whereas, the nitrite concentrations remain unchanged. In all batches, a decrease in chloride concentrations and an increase in sulfate concentrations is observed. Solely, recorded in the B22 batch is an increase of sulfur concentration from T0 to T2.

Ferrihydrite

The results of the batches spiked with ferrihydrite are illustrated in figure 20 and in the table 23 in the appendix. In the B22 batches, all compounds except 3-ethyltoluene, o-

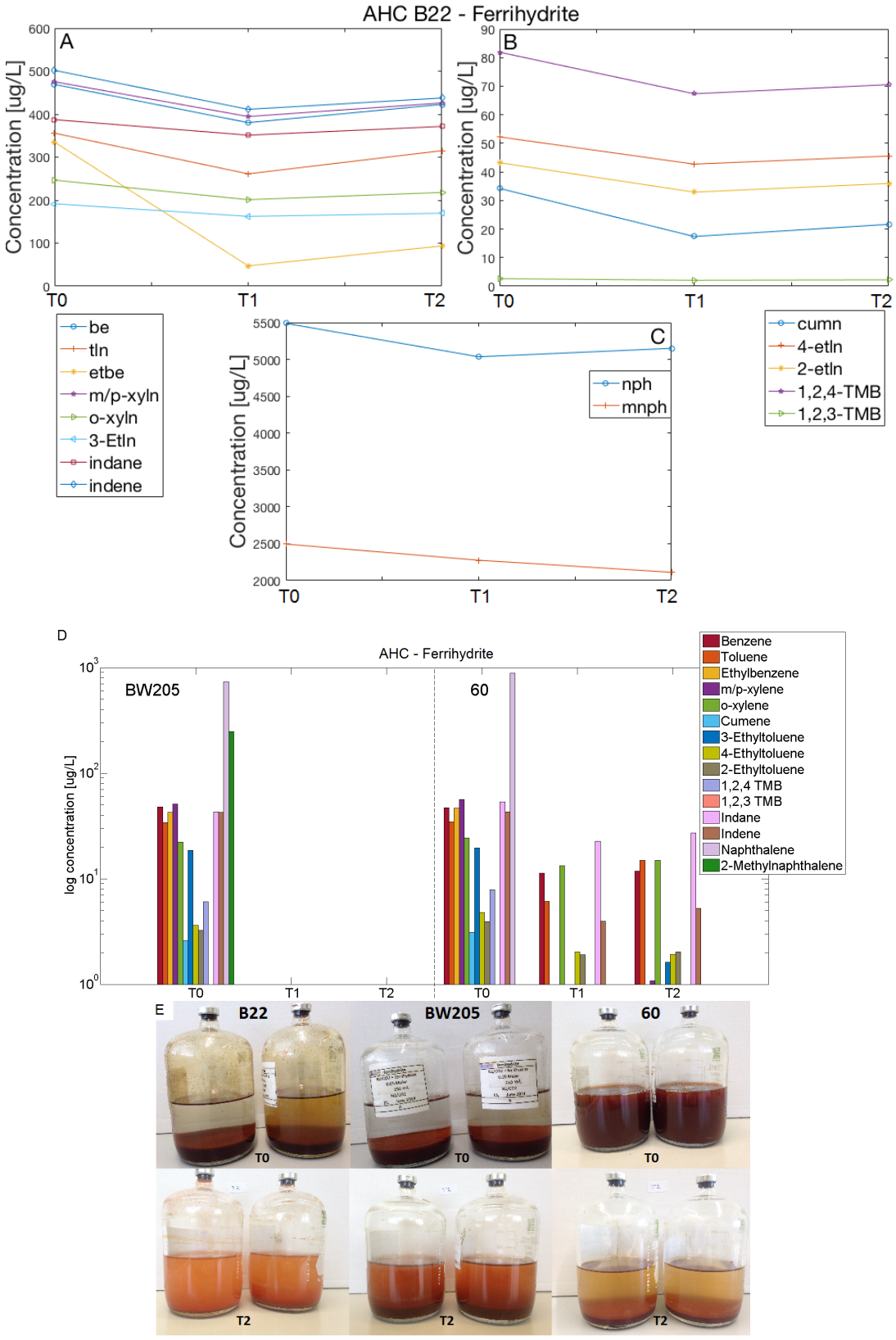

Figure 20: Illustration of the aromatic hydrocarbons detected by the GC-MS and pictures (E) of the ferrihydrite batches at the moment of T0 and T2. The subfigures A, B, C represent the data of the B22 batches and D of the BW205 and 60 batches. The abbreviations are explained in table 4.

xylene and 1,2,3-trimethylbenzene decrease in concentration from T0 to T1. A very rapid decrease is observed to have occurred for ethylbenzene from 335.03 μg/L at T0 to 47.23 μg/L at T1. From T1 to T2 all compounds except 2-methylnaphthelen remain relatively constant or increased slightly. 2-methylnaphthelene continues to decrease in concentration. In the BW205 batches, all compounds are under the detectable limits of the GC-MS machine in the T1 and T2 extraction. In the 60 batches benzene (11.3 μg/L), toluene (6.14 μg/L), o-xylene (13.31 μg/L), 4- and 2-ethyltoluene (2.04 μg/L and 1.91 μg/L, respectively), indane (22.68 μg/L) and indene (3.96 μg/L) are still detected at T1 and remain relatively steady till T2. Moreover, at T2 a small concentration of 3-ethyltoluene (1.63 μg/L) is additionally measured.

Table 12: The results of the Dionex and ICPOES measurements of the ferrihydrite batches are displayed. 'NA' indicates that no peak was detected.

Batch	Time	[mg/L]											
		Fe^{2+}	Mn^{2+}	Mg^{2+}	Si^{4+}	Cl^-	Na^+	Ca^{2+}	SO_4^{2-}	S^{2-}	NH_4^+	NO_2^-	NO_3^-
B22	T0	3.60	1.13	16.93	4.55	115.53	60.38	114.28	4.53	2.67	24.76	0.10	NA
	T2	NA	0.48	17.27	0.26	105.12	64.02	113.40	20.18	7.77	23.85	0.08	2.98
BW205	T0	NA	1.10	11.47	5.06	184.79	101.49	90.54	13.25	5.07	9.91	0.31	1.02
	T2	0.12	0.98	11.20	0.67	171.74	100.97	89.83	16.49	5.89	8.15	1.44	4.34
60	T0	NA	1.00	10.73	4.68	115.28	38.11	89.99	22.95	7.95	7.96	0.09	0.99
	T2	0.16	0.90	10.30	0.43	93.29	39.18	88.30	26.22	8.99	7.78	0.09	4.54

Focusing on the anion and cation results from the DIONEX and ICPOES analysis shown in table 12, it can be noticed that a little iron is detected in the BW205 and 60 batches at T2 but none at T0. On the contrary, a little iron is found initially in the B22 T0 measurements but not at T2. The chloride, silicon, and manganese concentrations are slightly reduced in all T2 extractions. The figure 20E shows pictures of the batches B22, BW205 and 60 at time T0 and T2. At T0 the amount of ferrihydrite, as its manifests itself as a suspended matter that sinks to the bottom (brown-reddish particulates) seems to be similar in all batches (the 60 batch was shaken prior to the picture was taken). At T2 the settled ferrihydrite layer is reduced in all batches but to different degrees. The greatest change appears to have occurred for the B22 batches. Furthermore, the glass of the batches seems to be cleaner at the moment of T2 than at T0. The amount of sulfate and sulfur increase from T0 to T2 in all batches but most significantly in the B22 batches.

Another change is noted for the nitrate concentrations. They increase slightly from T0 to T2 in all batches, whereas the nitrite and ammonium concentrations are fairly stable.

Sterile

The concentrations of aromatic hydrocarbons in the B22 batches show a relatively linear decrease from T0 to T2 (figure 21A, B and C). In the BW205 and 60 batches, the concentrations of aromatic hydrocarbons remain moderately constant throughout the experiment (see figure 21D and table 23 in the appendix). However, there are some changes recorded, for instance, 2-methylnaphthalene concentrations fluctuate over the time in the BW205, while no 2-methylaphthalene is detected in the 60 batches initially.

Table 13: The results of the Dionex and ICPOES measurements of the sterile batches are displayed. 'NA' indicates that no peak was detected. All studied ions are displayed.

Batch	Time	[mg/L]														
		Cl^-	Na^+	Ca^{2+}	SO_4^{2-}	S^{2-}	NH_4^+	NO_2^-	NO_3^-	Fe^{2+}	Mn^{2+}	Mg^{2+}	PO_4^{3-}	P	K^+	Si^{4+}
B22	T0	81.22	60.01	101.10	10.72	7.94	25.77	0.10	NA	NA	0.21	16.15	1.47	0.71	17.94	8.89
	T2	68.98	62.13	111.16	15.54	8.74	23.84	0.10	1.20	0.14	0.09	16.60	1.43	0.62	19.12	7.40
BW205	T0	150.48	98.56	86.04	17.64	5.96	9.75	0.28	1.14	NA	0.26	11.48	NA	0.34	7.65	8.83
	T2	137.53	99.18	94.58	17.39	5.88	9.41	0.29	3.34	0.12	0.21	11.33	NA	0.24	7.14	8.04
60	T0	80.19	52.84	78.00	29.75	9.97	13.71	0.07	1.10	NA	0.21	10.71	NA	0.34	16.29	9.16
	T2	53.91	37.41	99.85	30.27	10.49	7.63	0.11	1.45	0.12	0.20	10.66	NA	0.25	6.53	8.74

There is no major change recorded between the anions and cations from T0 and T2 (table 13). In all batches the chloride concentrations decrease and the calcium concentrations increase slightly. In the B22 batches the sulfate and nitrate concentration increased. The former increases from approximately 10 mg/L to 15 mg/L and the latter from 0 to 1.2mg/L. The concentrations of sulfur, nitrite, iron, manganese, magnesium, phosphate, phosphorus and silicon do not change over the time. Focusing on the pictures in figure 21C, the coloring of the BW205 and 60 batches is similar at T0 and T2. The B22 batches seem to be cleaner at T2 than at T0 and the dark particles appear to be less visible.

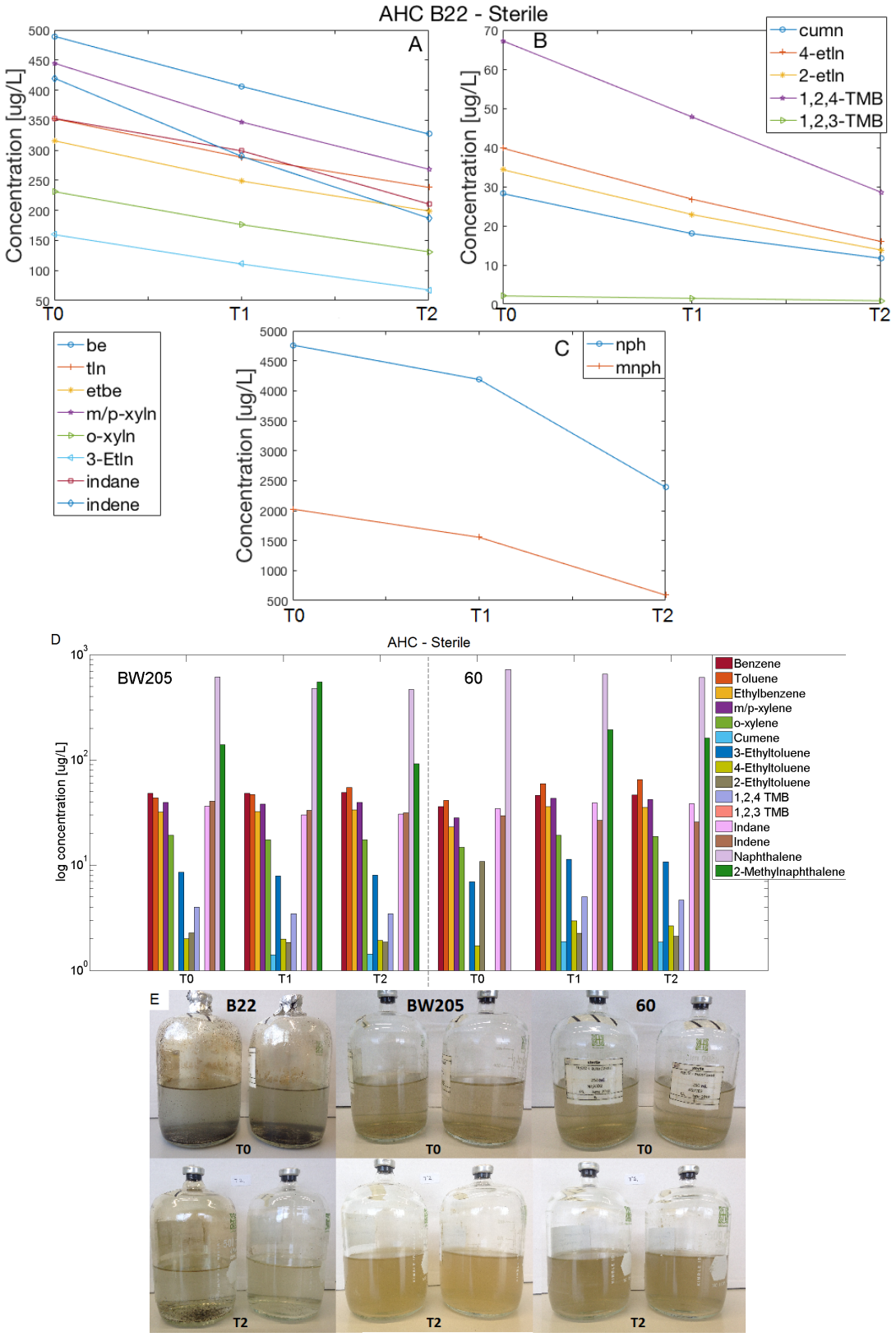

Figure 21: Visualization of the aromatic hydrocarbons detected by the GC-MS, the results and pictures (E) of the sterile batches at the moment of T0 and T2. The subfigures A, B, C represent the data of the B22 batches and D of the BW205 and 60 batches. The abbreviations are explained in table 4.

Table 14: Summary of the removal of aromatic hydrocarbons (AHC) in the batches at time T2.

	% of AHC at T2		
Scenario	B22	BW205	60
No Additives	77.1	0.2	11.7
Oxygen	13.8	0.7	0.3
Oxygen+Nutrients	36.7	0.2	1.1
Chlorate	78.9	2.4	10.4
Nitrate	73.9	0.3	10.0
Sulfate	70.8	2.1	7.0
Ferrihydrite	82.6	0.5	23.0
Sterile	49.7	96.0	96.2

Table 14 displays the percentages of the aromatic hydrocarbons measured at T2 in every scenario. From the sterile scenario the BW205 and 60 batches show the least removal of aromatic hydrocarbons. All the other scenarios comprise the highest remaining amount of aromatic hydrocarbons in the B22 batches. In the B22 oxygen batches, only 13.8 % of the initial aromatic hydrocarbons are found in the T2 extraction.

3.2.2 Methane concentrations

Table 15: Table of methane concentrations detected in the GC-FID measurements of the headspace samples from the batches.

		Methane concentrations [μg/L]							
Batch	Time	NoAdd	O2	O2+Nu	Chl	N	S	Fe	sterile
B22	T0	1734	1615	1555	1610	1300	1317	1675	1612
	T2	2057	1794	1618	1498	710	1365	1323	1514
BW205	T0	95	176	146	115	124	127	111	185
	T2	95	4	8	122	76	112	71	162
60	T0	19	28	29	41	35	37	27	59
	T2	30	37	34	39	38	36	24	47

The methane concentrations measured with the GC-FID are presented in the table 15. Already at time T0, differences in methane concentrations are visible in the same batch types but different scenarios. In the B22 batches spiked with nitrate and sulfate ($\approx$ 1300 μg/L methane) the initial methane concentrations are lower than in the other tested scenarios ($\approx$ 1633 μg/L). The BW205 and 60 batches sterile batches (185 and 59 μg/L) contain the highest initial methane concentrations of the scenarios. In the nitrate batches

of B22 and BW205, the methane concentration decreased to almost half of the T0 concentration at T2. In the oxygen and oxygen + nutrient BW205 batches, the methane is almost completely removed, whereas the concentrations in the oxygen batches of 60 and B22 are slightly increased at T2.

3.2.3 Oxygen detection and redox indication

Table 16 shows the results of the oxygen measurements of the GC-TCD and the corresponding resazurin color of the batches after the experiment. The oxygen percentage is given for the assumption that 20% of the headspace (as it occurs in the atmosphere) is 100%. NA is inserted when no resazurin was added to the batch. The batches with ferrihydrite show the characteristic color of the iron oxide (see figure 20C) and the mercury chloride in the sterile batches prevented the resazurin coloring the batches. Therefore, no information can be given about these batches. In the oxygen bachtes a rapid decrease of oxygen is observed within the first 14 days of incubation. Afterwards the concentrations remain moderately steady. 70 days after the T2 extraction, percentages of between 0.2 to 2.0% oxygen are obtained from the measurements of the batches containing alternative electron acceptors. The highest oxygen percentage of 2.66% is found in the 60 no additive B batch.

Table 16: Oxygen measurements of the GC-TCD in comparison with the colors of the batches one day after adding the redox indicator resazurin. 'NA' is inserted when no resazurin was added. The percentages obtained from the measurements T0, T1 and T2 are only indications. The actual concentration of oxygen cannot exceed these values.

	Batch	Time	% of atmospheric oxygen (20%				
			T0	T1	T2	120 days	Resazurin
No Additives	B22	A	5.96	-	7.02	1.31	colorless
		B	-	-	6.51	0.55	pink
	BW205	A	-	4.87	2.63	0.80	colorless
		B	-	1.56	5.05	1.15	pink
	60	A	-	-	6.16	1.34	colorless
		B	-	-	2.47	2.66	light rose
Oxygen	B22	A	100	-	9.07	0.84	blue
		B	100	-	12.07	1.27	blue
	BW205	A	100	13.47	13.44	0.38	colorless
		B	100	12.21	13.85	2.63	colorless
	60	A	100	-	11.34	0.89	blue
		B	100	-	8.45	1.14	blue
O_2 + nutrinets	B22	A	100	-	8.53	0.95	blue
		B	100	-	14.69	1.34	blue
	BW205	A	100	9.97	10.65	1.48	light blue
		B	100	7.13	9.64	0.75	light blue
	60	A	100	-	8.53	2.35	blue
		B	100	-	8.15	1.56	blue
Chlorate	B22	A	6.26	-	5.65	0.45	pink
		B	-	-	7.24	0.59	pink
	BW205	A	-	4.38	4.77	1.30	purple
		B	-	3.03	5.31	1.18	purple
	60	A	-	-	6.23	0.43	blue
		B	-	-	4.85	0.50	purple
Nitrate	B22	A	-	-	6.45	0.29	purple
		B	-	-	6.49	0.79	purple
	BW205	A	-	1.97	3.26	0.36	blue
		B	-	5.15	5.31	0.25	blue
	60	A	-	6.48	1.88	0.37	purple
		B	-	-	3.22	0.43	purple
Sulfate	B22	A	-	-	6.50	1.11	colorless
		B	-	-	6.59	0.53	colorless
	BW205	A	-	3.52	4.63	2.00	pink
		B	-	3.61	4.75	0.51	pink
	60	A	-	-	3.14	0.30	pink
		B	-	-	3.00	0.44	colorless
Ferrihydrite	B22	A	-	-	6.73	0.86	NA
		B	-	-	6.49	0.60	NA
	BW205	A	-	3.22	3.41	1.11	NA
		B	-	4.09	5.35	1.49	NA
	60	A	-	-	5.68	0.98	NA
		B	-	-	4.20	0.58	NA
Sterile	B22	A	-	-	7.14	0.44	NA
		B	-	-	6.99	0.11	NA
	BW205	A	-	4.47	3.11	0.40	NA
		B	-	3.68	6.01	1.40	NA
	60	A	-	-	5.98	0.11	NA
		B	-	-	3.67	0.07	

4 Discussion

4.1 Field sample assessment and groundwater selection for batch experiments

Following the results, the biogeochemicistry and the state of contamination in the monitoring well are analyzed. The results of the monitoring wells are discussed in geographical order i.e. Upstream of the park, inside the slurry wall and finally, downstream of the park.

Upstream

Wells BW211 and BW157 are located upstream of the park. The field measurements (see table 3) showed that values of the pH, electrical conductivity, temperature and the redox potential were very similar in these groundwater types. Also the results of the Dionex and ICPOES analysis revealed no significant concentrations of nitrate, nitrite or ammonium, although more than 64 mg/L sulfate was found (see table 5). As sulfate is a strong oxidizing agent, this highly suggests dominating sulfate reducing conditions in the upstream well. Iron(II) was also detected in the upstream groundwater. Although iron has a higher redox potential than sulfate, it is likely that the combination of both iron and sulfate reducing conditions are present in the upstream groundwater, hence resulting in the redox potential of -106 mV. This is also supported by the findings of iron-reducing bacteria in the upstream groundwaters and sulfate-reducing bacteria in the BW211 well. The redox potential of -106 mV was also found to be slightly higher compared to other wells, with the exception of well 37. Furthermore, there were no significant concentrations of aromatic hydrocarbons found in the GC analyses from Deltares and Synlab (see table 4), indicating groundwater with no concentrations of the studied contaminating compounds within the detectable limits. The naphthalene detected in the BW157 with the GC-FID is most likely due to the accidental exchange of the vial from the BW205 well. However, the presence

of the naphthalene carboxylase in the sample indicates that there was naphthalene in the BW157 monitoring well. So, the possibility that naphthalene is present in the BW157 cannot be excluded. Maybe there used to be naphthalene in the BW157 well but it had been degraded. In the BW211 more genes and types of microorgansism were detected than in the BW157 well. That included genes coding for methanogenic archaea, nitrate and iron-reducing bacteria, but also *Peptococacceae* sp., a benzene and naphthalene degrading bacteria. Furthermore, genes involved in the anaerobic degradation of aromatic hydrocarbons were found in the BW211 samples. This indicates that the bacteria in the BW211 well could be able to degrade some aromatic hydrocarbons. In summary, sulfate and iron-reducing conditions were found to be present in the samples from the upstream wells but they did most likely not contain monocyclic aromatic hydrocarbon at the time of the sampling. The presence of naphthalene carboxylase in the sample of BW157, however, indicates that naphthalene was presumably present at very low concentrations, or already degraded. Hence the sulfate and iron was used to oxdize other organic material in the upstream wells.

Inside the slurry wall

Inside the slurry wall, the monitoring well B22 contained very high concentrations of aromatic hydrocarbons, according to the GC analyses in table 4. Compared to the B22, the wells Pb1 and DV1 contained less aromatic hydrocarbon. The GC measurements of the B22 showed that especially high concentrations of BTEXN (benzene, toluene, ethylbenzene, xylene and naphthalene), 3-ethyltoluene, indene, indane and 2-methylnaphthalene were present. The large contamination in B22 was also reflected in the electrical conductivity. Comparing the geophysical data from the monitoring wells upstream to the one inside the slurry wall, it is striking that the electrical conductivity was much higher inside the park, where the contamination is present. This is conform with several geoelectrical investigations stating that zones of hydrocarbons coincide with higher bulk conductivities (Atekwana *et al.*, 2004; Sauck *et al.*, 1998; Atekwana *et al.*, 2000; Aal *et al.*, 2003;

Werkema *et al.*, 2003) due to enhanced weathering of minerals from acids produced as by-products of the degradation process (Atekwana *et al.*, 2004). An interesting observation is the even higher electrical conductivity values measured in the less contaminated wells Pb1 and DV4 compared to the B22 well, suggesting the presence of biodegradation by-products and/or hydrocarbons which were not researched in this study. High concentrations of sulfate were found in the Pb1 and DV4 wells, indicating sulfate-reducing conditions. Whereas, in the B22 well, no sulfate (table 5) was detected but a very low redox potential of -336 mV (table 3) suggesting that another very strong oxidizing agent had to be dominant. As such, carbon dioxide could have been reduced to methane, as the very high concentration of methane (3882 μg/L, see table 4) detected by the GC-FID measurements suggest (see figure 22). Methanogenic conditions are present in anoxic systems with a redox potential between -200- and -400 mV (Fetzer & Conrad, 1993; Zehnder & Mitchell, 1978). The redox potential of -336 mV is within this range. Hence, it is concluded that methanogenic conditions were present in the B22 well and the time of sampling. Moreover, high concentrations of sulfur indicate a strong depletion of sulfate (see table 5), following which, its function as an electron acceptor is then replaced by carbon dioxide.

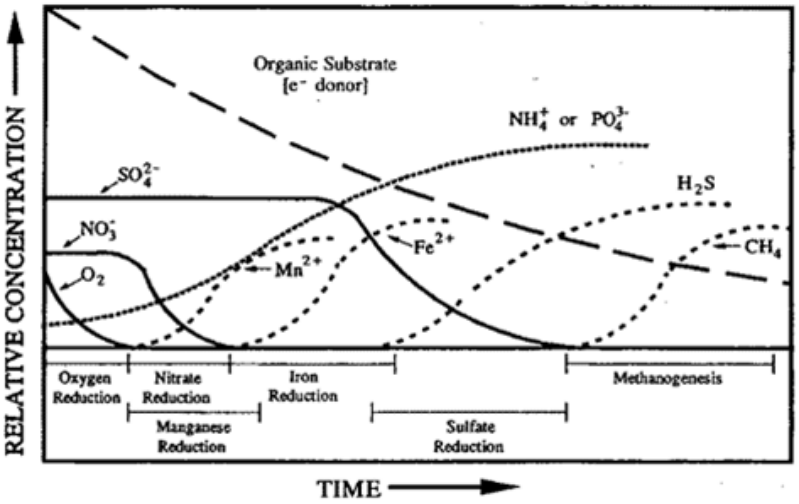

Figure 22: Flowpath of the reduction of electron acceptors in groundwater with an organic carbon source over time. Thermodynamic considerations predict that in a closed aqueous system containing living organisms, after oxygen is removed, biological reduction of alternative electron acceptors nitrate, manganese dioxide, iron hydroxide and sulfate should proceed in order (Ghiorse, 1988). The figure was taken directly from Lorah *et al.* (2012).

Furthermore, the highest concentrations of bacteria and archaea including all investigated types of microorganism and genes, except one, were detected in the field samples from B22 well. Only the *assA* gene coding for the enzyme that is involved in the activation of alkanes was not found.

In summary, inside the slurry wall, aromatic hydrocarbons were found to different degrees. The bulk of the contamination was found to occur in the northern part of the park. It is striking that in 1989 and 2014 according to Heidemij (1989); Royal HaskoningDHV (2014) no contamination was found at this location (see figure 4) Hence, water input by rain and pumping activities must have altered the conditions of the contamination. The contamination inside the slurry wall was most likely exposed to sulfate-reducing conditions, but in the B22 well, the sulfate was already reduced to sulfur and methanogenesis took over. The fact that the sulfate was depleted resulting in methanogenic conditions, suggest that adding sulfate to the groundwater as a remediation strategy could enhance the activity of sulfate-reducing bacteria to degrade aromatic hydrocarbons.

Downstream

At locations BW205, 60, and 37, which are upstream of the park, no monocyclic aromatic hydrocarbons were detected in the analyses. This was again confirmed by the SYNLab analysis. Although the GC-MS and SYNlab (data set 1 and 3 table 4) analyses detected naphthalene in the BW205 well, the GC-FID did not detect any significant peaks in the signal of the compounds. This leads to the suggestion that the vials of the BW205 and BW157 wells for the GC-FID measurements were interconverted, as mentioned before. This is also supported by the comparably high electrical conductivity indicating that hydrocarbons were present in the groundwater from BW205. The high NPOC detected in the BW205 well could originate from other organic material, such as humic acids, amines, or fulvic acids. Strikingly, the redox potential of the well 37 is much higher (-36 mV, see table 3) than of the other groundwater types. This deviation could be explained by focusing on the concentrations of anions and cations in table 5 and the microorganisms

present in the groundwater. Nitrate was only measured in well 37. Nitrate is considered as a mildly reducing electron acceptor corresponding to a higher redox potential. The incomplete removal of nitrate from the water suggests that nitrate-reducing conditions were present. Supporting this, genes coding for an enzyme involved in the nitrate reduction (see figure 12) and a very high concentration of sulfate was found, as sulfate will only be reduced when nitrate is depleted, (see figure 22). In the 60 and BW205 downstream well, most likely sulfate-reducing conditions wer present, as no high concentrations of alternative oxidizing agents were detected. Additionally, a variety of the genes coding for enzymes participating in the anaerobic degradation of aromatic hydrocarbons were detected downstream in all wells, indicating that the microorgansisms in the downstream wells are capable of degrading at least some petroleum-derived hydrocarbons.
In summary, the downstream wells were relatively clean compared to the ones inside the slurry wall. However, naphthalene was found in the BW205 well which could mean that the slurry wall is partly permeable for naphthalene or the naphthalene was already there prior to the slurry wall. Furthermore, sulfate-reducing conditions were found to be present in the 60 and BW205 wells, while in the 37 wells most likely nitrate-reducing conditions prevailed.

Selection of three groundwater types for the batch experiment

For the selection of the groundwater for the batch experiments, it is of great importance that (1) one of the groundwater types contains a variety of aromatic hydrocarbon in high concentrations, the other two groundwater types should not contain any volatile aromatic hydrocarbon to investigate what could happen to clean groundwater upstream of the park when the contamination spreads with the groundwater flow. (2) The groundwater should not contain high concentrations of the alternative electron acceptors (nitrate, sulfate, and iron) because they will be added in the experiment. (3) In favor of the success of the experiment, the microorganisms that are capable of degrading aromatic hydrocarbons

should be present.

Based on the results of the analysis, the groundwater of the B22 well represented the best choice as the contamination source for the batch experiments due to its highest concentrations of aromatic hydrocarbons and microorganisms detected of all the samples. Furthermore, the concentrations of nitrate, sulfate, and iron were very low, which is favorable for the batch experiments. In theory, the microbial community in the B22 groundwater should have the potential to degrade the aromatic hydrocarbons found in the same groundwater sample under nitrate, sulfate, iron-reducing and methanogenic conditions. To investigate the possible implications of clean groundwater coming into contact with contaminated water from B22, two locations downstream of the groundwater flow were chosen (see figure 23). Since the groundwater flows westward, contamination could therefore spread in that direction. The geographical locations of BW205 and 60 therefore make an appropriate source for the batch experiments as they are located westward of B22. Additionally, the small concentrations of sulfate, nitrate, and iron resulted in good conditions for the groundwater batches. Consequently, the batches were prepared using the groundwater from well B22, BW205 and 60.

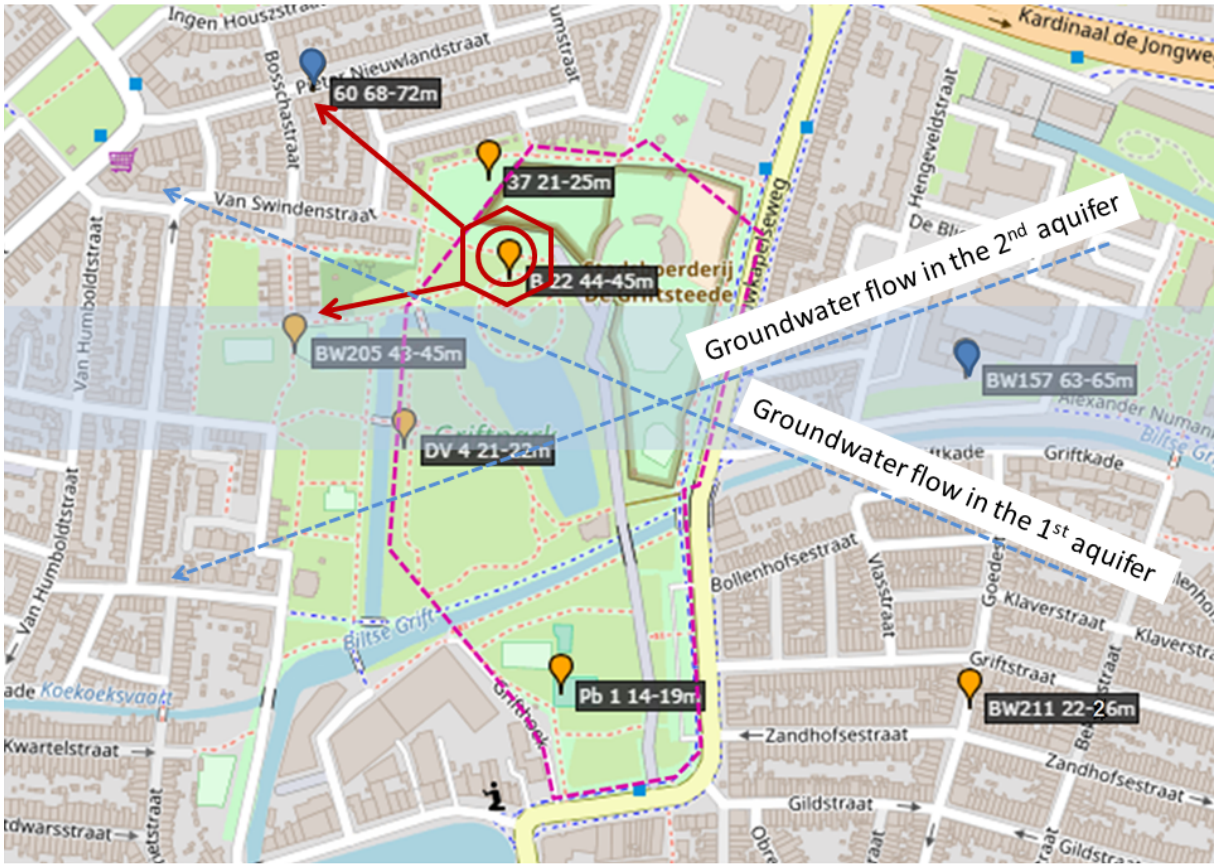

Figure 23: Mapped spreading of the contamination. the Benzoic ring around the B22 location represents the contamination source. The arrows correspond to the direction of the groundwater and points to the location of the clean monitoring wells, visualizing the potential spreading of the contamination to these locations.

4.1.1 Evaluation of the batch experiments

The concentrations of aromatic hydrocarbons in the BW205 and 60 batches were 10 % of the B22 batches on average. This is in agreement with the added volume of B22 to those batches (25 ml B22 water was added to 225 ml of the clean groundwater samples). Hence, it can be concluded that the allocation of the contaminated groundwater onto the clean water proceeded equally. Note that sometimes the 60 and BW205 batches behaved very differently than the B22 batches in this experiment and are therefore analyzed separately. For the BW205 batches, there were almost no aromatic hydrocarbons left at T1 and T2 in any scenario, except in the sterile batches. The given concentrations were very difficult to determine and might have resulted from noise in the GC-MS. They are therefore neglected

in this report. It is noted that an overall decrease of the concentrations of aromatic hydrocarbons was observed in all batches and scenarios, except the sterile BW205 and 60 batches (see table 24, 22 and 23 in the appendix). All studied aromatic hydrocarbons have the ability to be oxidized but in almost all scenarios, cumene, naphthelene, ethylbenzene and 2-methylnaphthalene were the compounds to be removed the fastest, and indane, 4-etln and benzene were the most persistent to degradation. Furthermore, the mass balances of the compounds ammonium-nitrate-nitrite and sulfur-sulfate showed that no significant loss of nitrogen or sulfur occurred in the batches (see table 26).

First, the batches with no additives are evaluated to investigate the possible implications of the clean groundwater coming in contact with contaminated groundwater (source zone groundwater)? Thereafter, all other scenarios were examined to find out under what conditions the aromatic hydrocarbons were removed and which electron acceptor achieved the best results for batches with the contaminated water, and for the clean ones spiked with the contaminated water?

4.2 Scenarios:

No additives

First of all, the no additives (figure 14) batches are focused on to get an impression of what happenes to the groundwater of the 60 and BW205 locations when it comes into contact with the contaminated B22 groundwater. Despite no alternative electron acceptors being added to the groundwater, the aromatic hydrocarbons are observed to drastically decrease in BW205. In the 60 batches some more persistent compounds such as indane and o-xylene remain in small concentrations (<8 μg/L). The toluene emerging at T2 in BW205 and 60 batches may be a result of cross-contamination between the vials placed in the autosampler of the GC system and is therefore neglected in the discussion. Since a total removal of aromatic hydrocarbons of almost 23 % occurred (see table 14), the increase in chloride and sodium concentrations observed in the B22 batch might be related

to the emerging by-products that result from biodegradation, as mentioned in section 4.1. However, no such increase in ions was observed in the other batches. Strikingly, in all three batch types a small amount of nitrate ($\sim$ 0.05 mmol/L) was measured with a similar decrease in the ammonium concentration ($\sim$ 0.06 mmol/L) in the T2 extraction (see table 26 in the appendix), indicating the oxidation of ammonium. Furthermore, the sulfate concentration in batches BW205 and 60 but especially in the B22 batch increased from T0 to T2. The increase in sulfate concentration of the B22 batch coincided with a decrease in sulfur concentrations, indicating the oxidation of inorganic elemental sulfur to organic sulfate by the sulfur oxidizer. A possible explanation of both oxidizing processes occurring might be the presence of oxygen. If dissolved oxygen concentrations are above 1-2 mg/L, sulfate and nitrate concentrations are then expected to be higher. Moreover, the large decrease in aromatic hydrocarbons in the BW205 and 60 batches was not in agreement with the small change in the amount of anions and cations in the batches. Furthermore, the results from the GC-TCD analysis support the idea of oxygen being responsible for the degradation of aromatic hydrocarbons, as approximately 70 days after the experiment maximal 1.3 % of the air oxygen were detected in the headspace (see table 16). At time T2 the approximate oxygen concentration could not have exceeded 7.02 % in the batches. Furthermore, the resazurin colored the water pink to colorless which corresponds to a redox potential of higher than -200 mV and the semi-reduced (resorufin) to reduced (dihydroresorufin) form of resazurin. The reduced form of resazurin dihydroresorufin is present under anoxic conditions. Since the batches were not completely colorless, supposedly little oxygen was present. Based on the results, it can be concluded that the presence of another electron acceptor, such as oxygen, was responsible for the removal of the aromatic hydrocarbons.

In conclusion, the mixing of the clean groundwater of the monitoring wells 60 and BW205 with the contaminated water of B22 led to a short time contamination. The concentrations in the batches were supposedly not high enough to resist the degradation under hypoxic

conditions in the headspace accelerating the degradation of aromatic hydrocarbons.

Oxygen

The largest removal of aromatic hydrocarbons was found to have occurred in the batches with oxygen (see figure 15). Naphthalene, cumene, 1,2,3-trimethylbenzene, ehtylbenzene, and toluene were especially removed rapidly from the headspace after 14 days. So far toluene is known as a pollutant that is rapidly degraded relative to other compounds (Hanson *et al.*, 1999; Langenhoff *et al.*, 1996; Phelps & Young, 1999). The removal of toluene is mediated by the *bssA* SRB (Foght, 2008), which was very prominent in the initial groundwater samples of B22 and 60. For the degradation of cumene, not much literature is available, whereas, the degradation of naphthalene has been studied intensively. Naphthalene, with its two aromatic rings, is more resistant to degradation because the persistence increases with increasing molecular weight (Haritash & Kaushik, 2009). Of the studied aromatic hydrocarbons, naphthalene and 2-methylnaphthalene were the largest molecules and therefore had therefore the highest molecular weight. This rapid removal of compounds under oxic condition was also found in the study by Hinchee *et al.* (1995). They recorded a complete removal of benzene, toluene, ethylbenzene, m-xylene and 1,2,4-trimethylbenzene within 7 days under aerobic conditions. Unfortunately, no assay targeting the enzyme deoxygenase, which is involved in aerobic degradation of BTEX and PAHs was performed here. Hence, no detailed information on the aerobic degradation potential of microorganism can be given. Moreover, not only bacteria but also fungi are capable of degrading PAHs (Haritash & Kaushik, 2009), broadening the possibility of biodegradation in the groundwater.

Measuring errors also have to be taken into consideration. Throughout the experiment, we encountered problems detecting the PAHs because of the mitigating signal in the GC. The weak signal towards the end of the run made the identification of the peaks difficult (see figure 27). The complete removal of the naphthalene at T1 in the B22 batches could be such a mistake but since the peak for 2-methylnaphthalene was detected and its

molecular weight is heavier then that of naphthalene, it is assumed that this outcome is correct. However, the possibility of hydrophobicity and adsorption of the compounds to the rubber stopper and/or glass of the bottles cannot be excluded as an explanation for the removed compounds.

In all oxygen batches, a decrease in oxygen was measured (see table 7). Consequently, the aromatic hydrocarbons were most likely removed by the microorganism using oxygen as the electron acceptor. In addition to this, in the B22 batches, sulfur oxidation was observed to occur. Calculating the mass balances (see table 26in the appendix), a loss of 0.83 mmol/L of sulfur occurred between T0 to T2. This sulfur could be converted into hydrogen sulfide. Since no analysis was performed to determine the amount of hydrogen sulfide in the batches, it cannot be determined if the loss of sulfur could have been converted into hydrogen sulfide. Increases in sulfate were observed for the other batches, with no decrease in sulfur occurring. This could be explained by the oxidation of sulfide anions to sulfate. In the batches with BW205 and 60 groundwater, the ammonium at T0 was used up and most likely oxidized to nitrate and nitrite. *Nitrosomonas* are bacteria that can oxidize ammonium to nitrite. The oxidation of nitrite to nitrate is done by the genus *Nitrobacter*. Both genera had to be present in the Bw205 and 60 groundwater since no such change was observed for the B22 batches.

Another notable event is the remarkable removal of methane in the BW205 batches (see figure 28. A possible explanation could be the activity of methane-oxidizing bacteria (methanotrophs). The decrease of methane was only observed for the BW205 batches, suggesting that methanotrophs are only active of present in this groundwater. However, without testing for methanotrophic bacteria, their presence cannot be determined.

Based on the results of the analysis, adding oxygen to the contaminated groundwater resulted in a rapid removal of all compounds to different degrees. The oxygen added was quickly utilized by the bacteria to degrade the aromatic hydrocarbons, but also for oxidation of sulfur (B22 batch) ammonium (BW205 and 60 batches) and methane

(BW205). Consequently, adding oxygen as a remediation strategy for the Griftpark is recommended.

Oxygen + nutrients

The initial idea of adding nutrients to the batches was to increase the concentration of microorganisms, thus potentially enhancing the biodegradation. Comparing the total removal of aromatic hydrocarbons in the oxygen + nutrients batches of B22 (table 14) of 63.3% to the one with only oxygen of 86% it is likely that adding nutrients did not enhance the degradation, moreover, it mitigated the removal of aromatic hydrocarbons. However, a removal of compounds of the nutrient mix (Brunner) is visible in the table 8. Chloride, calcium, phosphorus decreased in concentration indicating that these ions have been utilized by the bacteria or precipitated. Furthermore, in the B22 batch, again the sulfur had been oxidized to sulfate. A striking finding is that in the BW205 and 60 batches the ammonium was oxidized into solely nitrite meaning that ammonium oxidizing bacteria or archaea had to be present. The concentrations of nitrite were above 50 mg/L and were therefore 50 times above the drinking water limit (WHO, 2011). Nitrite is a toxic intermediate due to two reasons. Firstly, it can react with secondary amines to produce nitroamines which can be carcinogenic (Tiedje, 1988). Secondly, nitrite in humans interferes with the oxidation of normal haemoglobin and forms methaemoglobin, which binds oxygen irreversibly and inhibits transport to the tissues (Schlegel, 1981; WHO, 2011). The accumulation of nitrite in the batch raised the impression that factors were present affecting the nitrification as described by Tiedje (1988). Presumably there is a lack of enzymes that oxidize the nitrite further to nitrate or the activity is inhibited by the presence of toxic chemicals or limited electron donors.

In conclusion, adding the nutrients to the batches did not only decrease the degradation compared to the batches without nutrients, it also produced toxic levels of nitrite in the groundwater. Considering the results of the batch experiments so far, it appears that

adding oxygen alone to the groundwater is, by far, the preferred method for the potential bioremediating of the Griftpark.

Chlorate

Since the conclusion of the batch experiments indicate a strong potential for the use of oxygen as a groundwater remediation strategy, another way of introducing oxygen to the groundwater is by the addition of chlorate. Chlorate (ClO_3^-) is used to produce chlorine dioxide in bleaching and disinfection processes and as a precursor for the production of perchlorate (Wang & Coates, 2017; Weelink, 2008). Molecular oxygen is released by the transformation of chlorate to chloride. The chlorate reductase (ClrABC) reduces chlorate to chlorite which is further transformed by the chlorite dismutase (Cld) to chloride, producing molecular oxygen (Vanwijk & Hutchinson, 1995) (see figure 24).

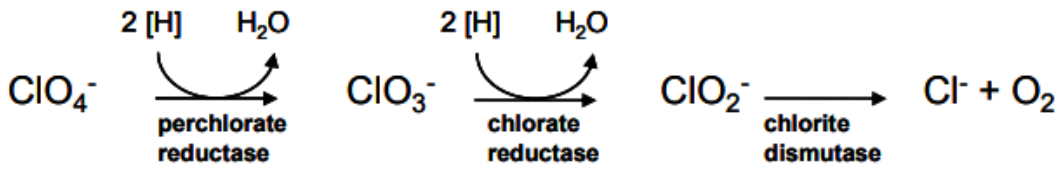

Figure 24: The reduction and dismutation of (per)chlorate to chloride and oxygen. The scheme was directly taken from Weelink (2008).

This oxygen can be used by aerobic and facultative anaerobic microorganisms to degrade the aromatic hydrocarbons. Yet, it was only observed that 21.1 % (table 14) of the compounds were removed, which was approximately four times less than what was observed in the oxygen batches. Furthermore, it was found that the concentrations of aromatic hydrocarbons in the B22 batches further increased. Therefore, this disqualifies the possibility of using chlorate to bioremediate the Griftpark as it most likely contributes to an accumulation of the aromatic hydrocarbons in the long-run.

In table 9 a very prominent increase of chloride concentration at T2 was observed in all batches. This could be the result of the chlorate reduction to chloride. However, no

change in chlorate concentration was observed. This is also confirmed by looking at the mass balances in table 26 in the appendix, a gain of approximately 5. mmol/L occurred in all batches from T0 to T2. This suggests that chloride was introduced via a different pathway than chlorate reduction. One possible explanation could be the presence of chlorite in the batches which is via a dismutase converted into chloride and oxygen or as previously described chloride also accumulates as a consequence of biodegradation. Furthermore, in theory, chlorate can also be used as a substrate for respiratory or assimilatory nitrate reductases ($NO_3^- \rightarrow NO_2^- \rightarrow NH_4^+$ (Tiedje, 1988)). However, the opposite was observed in the chlorate batches of B22. The ammonium concentrations decreased slightly and therefore low nitrate concentrations emerged, indicating ammonium oxidating conditions as has been described in the oxygen batches.

Based on these results, adding chlorate to the groundwater as a remediation strategy for the Griftpark is not recommended because aromatic hydrocarbons started to accumulate after 14 days of incubation and so far, no chlorate was utilized by the microorganisms, suggesting that chlorate-reducing bacteria were not present or inactive.

Alternative electron acceptors

Nitrate

Many studies described the degradation of aromatic hydrocarbons under nitrate-reducing conditions. To investigate if denitrifiers in the Griftpark are capable of degrading the contamination in the source zone, nitrate was added to the batches. The reduction of nitrate to nitrite is known as part of the denitrification occurring in anoxic environments. Nitrate is reduced to nitrite which is further reduced to NO and N_2O and elemental nitrogen. The first step is catalyzed by the enzyme nitrate reductase (Schlegel, 1981). Under nitrate-reducing conditions, the nitrate would be removed and nitrite and ammonium concentration are expected to rise. However, the nitrate concentrations did not change

in any of the batches. On the contrary, in all batches, the ammonium was oxidiez to nitrite, as it happened in the oxygen + nutrient batches. According to the mass balances (see table 26 in the appendix) a gain of almost 0.8 mmol/L nitrogen occurred in the B22 batch. This could indicate the presence of bacteria fixing nitrogen gas to nitrogenous compounds such as nitrite or nitrate in this case. However, without testing for the detection of nitrogen fixing bacteria, their presence cannot be concluded. The greatest increase in nitrite concentrations was observed for the B22 batches with a concentration of 21.51 μg/L. Ammonium oxidation as part of the nitrification process only occurs under oxic conditions. Since oxygen reduction is thermodynamically more favorable than nitrate reduction, oxygen is consumed first (see figure 22). The sulfate concentration increased in all batches but the greatest change was observed for the B22 batches. indicating that sulfur was likely oxidized under aerobic conditions. Yet a loss of 0.5 mmol/L of sulfur was calculated in the mass balances (table 26). This loss could result from hydrogen sulfide formation. Interestingly, the aromatic hydrocarbon concentrations were relatively steady at T0 and T1 but then decreased more rapidly from T1 to T2. This suggests that an electron acceptor, such as oxygen, was introduced to the batches at time T1. Unfortunately, no oxygen measurements were performed at T1 for the nitrate batches B22. Hence, no information on the oxygen content at that moment can be given. A rapid decrease of aromatic hydrocarbons was observed for the BW205 and 60 batches, presumably due to oxygen in the batches. At T1, a maximal 6.48 % of oxygen was measured in the headspace of the BW205 and 60 (only A batch) batches. Although these concentrations are only seen as an indication, it is assumed that the actual concentrations were not higher than these.

In summary, all aromatic hydrocarbons were slightly reduced. However, due to oxygen in the batches, no nitrate was reduced but ammonium was oxidized to nitrite and sulfur oxidized to sulfate and presumably hydrogen sulfide. In theory, the microorganisms were present and capable of reducing nitrate in the groundwater (see figure 12) but because of

the hypoxic conditions, no information of the efficiency of nitrate as an oxidizing agent can be given.

Sulfate

In all field samples except the monitoring well B22, sulfate concentrations were detected, indicating that the microorganism community in the groundwater worked well under sulfate-reducing conditions. Every aromatic hydrocarbon in batch B22 showed a decreasing trend in concentration in the batches with added sulfate. From T0 to T2 almost 30% of the initial concentration was removed. That was slightly more than it was observed for the nitrate batches, but much less than for the anaerobic batches. In the BW205 and 60 batches, almost all petroleum-derived hydrocarbons were oxidized at T2. Indane was one of the more persistent compounds in the 60 batches. But in the B22 batches also, indane did only decreased by 19.9 %. Even more resistant were benzene and toluene to degradation with a decrease of less than 18.79% (calculated from table23). Benzene is already known as one of the most stable aromatic hydrocarbons (Zhang *et al.*, 2010), toluene, however, has been described as a rapidly degradable aromatic hydrocarbon.
Initially, the groundwater of B22 did not contain any sulfate (see table 5) but high concentrations of sulfur, whereas in BW205 and 60 small amounts of sulfate were detected. But only in the field samples of the 60 and B22 monitoring wells, the presence of sulfate-reducing bacteria was confirmed by performing qPCR assays targeting the *bssA* SRB and the *drsA* genes. Subsequently, adding the B22 groundwater to all batches introduced sulfate-reducing bacteria in the BW205. Yet, the sulfate concentrations did not decrease from T0 to T2, although aromatic hydrocarbon concentrations decreased. Meaning that another electron acceptor had to be present. Since a small amount of ammonium was oxidized, the presence of oxygen in the batches is suggested. The GC-TCD measurements of the sulfate batches showed that the oxygen concentration at T2 was lower than 6.49 % of the atmospheric oxygen. After 120 days of incubation, only a maximal of 0.79 % oxygen was detected in the headspace. Since sulfate-reducing bacteria are strictly anaer-

obic (Widdel, 1988), the oxygen had to be consumed before sulfate could undertake its position as a oxidizing agent.
Although the reduction of sulfate was not observed during the experiment, a 'rotten egg' -like odor was noted afterwards. Furthermore, black coloring of the media was also observed to occur in the B22 batches (figure 19E), suggesting the formation of ferrous sulfide (Widdel, 1988). Despite these being characteristics of the presence of hydrogen sulfide, this cannot be concluded without concrete analytical results obtained. For the B22 batch no iron was measured in T0 but a small concentration was detected at T2. However, it needs to be stressed out that without testing for ferrous sulfide, the presence cannot be concluded.

Based on the results, the aromatic hydrocarbons in the B22 sulfate batches were slightly reduced in concentration over an incubation time of 53 days. Since most experiments with sulfate-reducing bacteria lasted longer than 2 months (Weelink, 2008; Rueter *et al.*, 1994), and oxygen was present, the duration of the experiment was presumably too short for the bacteria to adapt to the presence of sulfate in the water. Resulting in a delay in the response of the microorganisms to sulfate in the batches. Hence, no information on the efficiency of degrading aromatic hydrocarbons with sulfate as the electron acceptor can be given.

Ferrihydrite

As the last alternative electron acceptor for the degradation of aromatic hydrocarbons, adding ferrihydrite to the batches was tested. Again, all aromatic hydrocarbons slightly decreased in concentrations. With a removal of only 18% of the total aromatic hydrocarbons in the B22 batches, this represents the scenario with the lowest removal. The largest decrease on concentration was observed for ethylbenzene of 85% from T0 to T1 of the B22 batches. The degradation of ethylbenzene in iron-reducing enrichment cultures was also studied by Jahn & Meckenstock (2005). First of all, iron-reducing bacteria such

as *Geobacter* sp. were found in the field samples of all three monitoring wells. They are constrained to anoxic environments (Schlegel, 1981). Unfortunately, it could not be determined if the batches were anoxic the whole time but the GC-TCD measurements of the ferrihydrite batches concluded that there was less than 1.5 % oxygen in the headspace after 120 days incubation and less than 6.6% at the T2 measurements. It can therefore be assumed that little oxygen was present throughout the experiment, which might have inhibited the reduction of iron. Although the amount of ferrihydrite appeared to be less at T2 than at T0 when looking at the pictures of figure 20E, no such change in iron concentration was observed when focusing on the anions and cations of the table 25 in the appendix. While measuring iron, some problems were encountered that might explain the insufficient information on the iron concentrations: The iron was added in form of a ferric iron III oxide which is practically insoluble in water (Schlegel, 1981) but its reduced form ferric iron II oxide is more soluble (Cornell & Schwertmann, 2003). Hence, only iron II was detected by the ICPOES. Furthermore, if the precipitation of iron II occurred, it would have been filtered out prior the preparation of the ICPOES samples. Another possibility is that during the preparation of the ICPOES samples the groundwater was exposed to oxygen from the air which leads to precipitation in the ICPOES sample. Hence the ICPOES results of the iron concentrations are not representative of the actual concentration. Despite potential iron reduction, ammonium oxidation was observed in small amounts in this scenario, which also indicates oxic conditions. Furthermore, an increase in sulfate with a simultaneous increase in sulfur occurred in the B22 batches. This might suggest that sulfide was present and then oxidized to sulfate and reduced to sulfur.

In conclusion, the presumable reduction of FeIII to FeII did not coincide with a rapid decline in aromatic hydrocarbon concentrations in the B22 ferrihydrite batches. The iron could have been reduced using natural organic matter. Presumably, little oxygen was present to oxidize a small percentage of the aromatic hydrocarbons and inhibit the enforcement of iron as a oxidant. Therefore, no information on adding ferrihydrite to the

Griftpark contamination as a remediation strategy can be given.

4.2.1 Summary of the scenarios

An interesting observation was the occurrence of ammonium oxidation in all of the batches. This means that at least in the beginning some oxygen was present. This is supported by the oxidation of methane in the BW205 oxygen and nitrate batches, and the B22 nitrate batches. Furthermore, sulfur oxidation to sulfate occurred in almost all B22 batches. Presumably due to the high sulfur and low sulfate concentrations initially. As mentioned, in the B22 and 60 batches the largest removal of aromatic hydrocarbons was achieved in the oxygen scenario (86.2% and 99.7% respectively, in the table 14).

The second-best removal result in the B22 and 60 batches was achieved under oxic conditions with nutrients, however, the high amount of nitrite resulting from the oxidation of ammonium led to undesired toxic conditions in the groundwater. Adding the chlorate to the batches did not have the same effect on the aromatic hydrocarbons degradation as adding oxygen to the batches showed. Moreover, it resulted in an accumulation of aromatic hydrocarbons at T2.

Regarding the alternative electron acceptors, no decrease was observed during the experiment. Presumably oxygen was present and consequently, no alternative electron acceptor was utilized from the microorganisms to degrade the aromatic hydrocarbons in the batches. Of the batches with aromatic hydrocarbons, the ones with sulfate obtained the best removal of aromatic hydrocarbons. However, the removal of aromatic hydrocarbons in these batches most likely originates from the oxygen inside and cannot be credited to the sulfate as a oxidizing agent. Furthermore, this scenario showed less success than the sterile batches. This introduces the idea that the sterilization might have been insufficient and/or oxygen was present, whereas, the sterile batches of BW205 and 60 represent a removal of only approximately 4%. This difference presumably resulted from measuring differences and can be neglected. Hence it can be asummed that the sterilization of these batches was successful, and the batches did not leak and no abiotic removal of aromatics

occurred.

4.3 Remarks

Throughout the experiment, oxygen presented a problem. The GC-TCD measurements during the experiment revealed themselves to be false due to the needles used for the injection. The needles were too small to penetrate the column in the GC which lead to the injection of additional oxygen and false results. Furthermore, after the termination of the experiment, it was realized that the viton rubber stoppers used to seal the batches were flawed in their production. Consequently, the crimp-sealing of the batches was insufficient and enabled oxygen to enter the batches. Another problem arose during the GC-FID calibration. The signal towards the end of the run was very weak so that independent of the concentration tested in the headspace, the peak areas stayed small. Hence, the concentrations obtained are genuinely too high and not representative, for example, the naphthalene and 2-methylnaphthalene in the headspace. Consequently, onlye the methane concentrations obtained from the GC-FID were used in this study. Another shortcoming of the experiment was to only take duplicates. This constrained the dataset in performing statistical analysis.

5 Conclusion

Field samples were taken to investigate the presence and extent of the contamination in and around the Griftpark. The groundwater upstream and downstream of the slurry wall appeared to be relatively clean, although small concentrations of toluene, ethylbenzene, xylene and a slightly higher concentration of naphthalene were detected in the groundwater very close to the slurry wall downstream. Indicating that either the compounds were already there prior the construction of the slurry wall or the slurry wall was slightly permeable. In all monitoring wells except the B22, sulfate was measured. Inside the

slurry wall, the monitoring wells contained the highest concentrations indicating sulfate-reducing conditions. No sulfate but high concentrations of sulfur and methane were found in the B22 well, suggesting that the sulfate was depleted and methanogenic conditions were present in the heavy polluted groundwater. This suggested that sulfate is a favorable oxidant in the B22 groundwater. The microorganisms detected in the field samples of the B22 monitoring well are in theory, able to degrade the aromatic hydrocarbons.

Batch experiments were performed to study the removal of contamination compounds from the source zone in the park under different electron acceptors. First of all, it was noted that in all scenarios, except for the sterile BW205 and 60 batches, the concentrations of aromatic hydrocarbons decreased during the experiment. In the BW205, all compounds were removed within 14 days in every scenario. The outcome of the batch experiments with no added electron acceptors led to the conclusion that firstly, adding the contaminated groundwater B22 to the clean water 60 and BW205 under presumably anaerobic conditions led to a short time contamination which was rapidly removed from the batches. The concentrations added to the batches were presumably too low to persist in the groundwater. For the B22 batches and 60 batches, adding oxygen achieved the best removal of aromatic hydrocarbons, indicating a high potential for aerobic biodegradation as a remediation strategy for the Griftpark. Under aerobic conditions, ethylbenzene, cumene, 2-methylnaphthalene and naphthalene were the most rapidly degraded compounds, whereas 4-ethyltoluene, indane and benzene showed to be very resistant to degradation. Secondly, none of the tested alternative electron acceptors was reduced by the microorganisms during the batch experiment. The best results were given by the sulfate batches. However, the removal was most likely due to oxygen in the batches. Furthermore, the duration of the experiment was too short to investigate the efficiency of alternative electron acceptors because most presumably oxygen was present and had to be depleted before alternative electron acceptors could undertake its function as an oxidizing agent. Furthermore, ammonium was oxidized to nitrate or/and nitrite in all batches confirming the presence of oxygen.

In conclusion, all scenarios achieved lower concentrations of aromatic hydrocarbons in the batches, but the largest removal was observed to occur in the oxygen batches. Adding nutrients did not accelerate the degradation of compounds. the addition of chlorate, as an indirect source of oxygen, to the batches was expected to increase the removal but resulted in an accumulation of compounds. Moreover, both scenarios led to high and toxic concentrations of nitrite in the groundwater and are therefore not recommended as remediation strategies for the Griftpark. No conclusion can be given for the efficiency of the alternative electron acceptors because hypoxic conditions were present initiating ammonium oxidation and sulfur oxidation. As a remediation strategy for the removal of the contamination in the Griftpark, adding elemental oxygen to the groundwater shows high potential. However, this is a very cost-intensive strategy. Therefore, future work should emphasize anaerobic remediation strategies.

Note that here, the given conclusions only represent possibilities as the presented data was derived from batch experiments at a higher temperature than in the field. In the field, more factors influence biodegradation such as water flow, sediment adsorption and temperature. Hence, characterizing an entire site by analyzing only a few monitoring wells is not completely representative of the actual situation on site and remains one of the major obstacles for bioremediation projects (Jahn & Meckenstock, 2005). Consequently, more reserach is needed.

6 Future research

This study gives insight in the biogeochemical situation of wells upstream and downstream of the Griftpark and inside the slurry wall. But to gain a better overview of the situation in the Griftpark, it is important to study the site in detail. Therefore, more monitoring wells have to be investigated and extensive communication between the parties of the research consortium is necessary. For the future, it would be interesting to compare the

results obtained in this research to other studies on the Griftpark, but so far nothing has been published. For instance, it would be interesting to study the soil and groundwater from the Griftpark in batch experiments and assess the potential of biodegradation of aromatic hydrocarbons but also adsorption properties of the compounds to the sediment. Moreover, studying the groundwater flow, time frame and speed of possible contamination and applying this to the batches or larger scale experiments could give more insight in the actual situation in the case that the contamination spreads.

Another interesting objective to study, is the fast removal of cumene, naphthalene and 2-methylnaphthalene against the slow removal of indane and benzene as is seems to occurr in the batches. In light of this, a small batch experiment could be conducted with the microorganisms from the B22 well with added aromatic hydrocarbons. Another possibility could be to test the growth of the microorganisms from the B22 well on media containing these compounds.

Furthermore, the here performed batch experiments should continue in order to determine the efficiency of the alternative electron acceptors in the experiment. For this purpose, it is recommended to flush the batches with N_2 and CO_2 gas again before reintroducing heavy polluted groundwater from B22 to the BW205 and 60 batches at a higher concentration than is mentioned in this report (for example 50 ml instead of 25 ml) and use new viton rubber stoppers and crimp seals.

Additonally, to improve this experiment, adding a qPCR assay to detect chlorate-reducing bacteria and methanotrophic bacteria to the methods represents a possibility. So far, it is uncertain if the bacteria in the batches can reduce chlorate. Adding DAX-8 as an adsorbent to remove humic acids prior to qPCR Schriewer *et al.* (2011) to increase the efficiency of the qPCR for the batch DNA is also suggested. In addition to the DNA analysis, headspace measurements of volatile aromatic hydrocarbon isotope fractionation should be used to determine the actual degradation rate of the compounds. To reduce the extraction amount, manual injections of headspace samples for the GC-MS are recommended. For further analysis, it is recommended to perform triplet or quadruple repetitions to remove anomalous values from the dataset and to enable statistical analytical tests.

Bibliography

Aal, G. Z. A., Atekwana, E. A., Slater, L. D., & Ulrich, C. 2003. Induced polarization (IP) measurements of soils from an aged hydrocarbon contaminated site. *Pages 190–201 of: Symposium on the Application of Geophysics to Engineering and Environmental Problems 2003*. Society of Exploration Geophysicists.

Abu Laban, N., Selesi, D., Rattei, T., Tischler, P., & Meckenstock, R. U. 2010. Identification of enzymes involved in anaerobic benzene degradation by a strictly anaerobic iron-reducing enrichment culture. *Environmental microbiology*, **12**(10), 2783–2796.

Alvarez, P.J.J., & Illman, W.A. 2006. Bioremediation technologies. *Bioremediation and natural attenuation: Process fundamentals and mathematical models*, 351–455.

Anderson, R. T., & Lovley, D.R. 1997. Ecology and biogeochemistry of in situ groundwater bioremediation. *Pages 289–350 of: Advances in microbial ecology*. Springer.

Atekwana, E. A., Sauck, W. A., & Werkema Jr, D. D. 2000. Investigations of geoelectrical signatures at a hydrocarbon contaminated site. *Journal of applied Geophysics*, **44**(2-3), 167–180.

Atekwana, E. A., Atekwana, E. A., Rowe, R. S., Werkema Jr, D. D., & Legall, F. D. 2004. The relationship of total dissolved solids measurements to bulk electrical conductivity in an aquifer contaminated with hydrocarbon. *Journal of Applied Geophysics*, **56**(4), 281–294.

Ball, H. A., & Reinhard, M. 1996. Monoaromatic hydrocarbon transformation under

anaerobic conditions at Seal Beach, California: laboratory studies. *Environmental Toxicology and Chemistry*, **15**(2), 114–122.

Beller, H. R., Grbić-Galić, D., & Reinhard, M. 1992. Microbial degradation of toluene under sulfate-reducing conditions and the influence of iron on the process. *Applied and Environmental Microbiology*, **58**(3), 786–793.

Beller, H. R., Kane, S. R., Legler, T. C., & Alvarez, P. J.J. 2002. A real-time polymerase chain reaction method for monitoring anaerobic, hydrocarbon-degrading bacteria based on a catabolic gene. *Environmental science & technology*, **36**(18), 3977–3984.

Beller, H.R., Kane, S. R., Legler, T. C., McKelvie, J. R., Sherwood Lollar, B., Pearson, F., Balser, L., & Mackay, D. M. 2008. Comparative assessments of benzene, toluene, and xylene natural attenuation by quantitative polymerase chain reaction analysis of a catabolic gene, signature metabolites, and compound-specific isotope analysis. *Environmental science & technology*, **42**(16), 6065–6072.

Bergmann, F., Selesi, D., Weinmaier, T., Tischler, P., Rattei, T., & Meckenstock, R.U. 2011. Genomic insights into the metabolic potential of the polycyclic aromatic hydrocarbon degrading sulfate-reducing Deltaproteobacterium N47. *Environmental microbiology*, **13**(5), 1125–1137.

Berner, R.A. 2003. The long-term carbon cycle, fossil fuels and atmospheric composition. *Nature*, **426**(6964), 323.

Biegert, T., Fuchs, G., & Heider, J. 1996. Evidence that anaerobic oxidation of toluene in the denitrifying bacterium Thauera aromatica is initiated by formation of benzylsuccinate from toluene and fumarate. *The FEBS Journal*, **238**(3), 661–668.

Boll, M., Fuchs, G., & Heider, J. 2002. Anaerobic oxidation of aromatic compounds and hydrocarbons. *Current opinion in chemical biology*, **6**(5), 604–611.

Borggaard, O.K. 1982. The influence of iron oxides on the surface area of soil. *European Journal of Soil Science*, **33**(3), 443–449.

Callaghan, A. V. 2013. Enzymes involved in the anaerobic oxidation of n-alkanes: from methane to long-chain paraffins. *Frontiers in microbiology*, **4**, 89.

Carmona, M., Zamarro, M. T., Blázquez, B., Durante-Rodríguez, G., Juárez, J. F., Valderrama, J. A., Barragán, M. J.L., García, J. L., & Díaz, E. 2009. Anaerobic catabolism of aromatic compounds: a genetic and genomic view. *Microbiology and Molecular Biology Reviews*, **73**(1), 71–133.

Cerniglia, C.E. 1992. Biodegradation of polycyclic aromatic hydrocarbons. *Pages 227–244 of: Microorganisms to combat pollution*. Springer.

Chakraborty, R., & Coates, J.D. 2004. Anaerobic degradation of monoaromatic hydrocarbons. *Applied Microbiology and Biotechnology*, **64**(4), 437–446.

Chakraborty, R., O'Connor, S. M., Chan, E., & Coates, J. D. 2005. Anaerobic degradation of benzene, toluene, ethylbenzene, and xylene compounds by Dechloromonas strain RCB. *Applied and Environmental Microbiology*, **71**(12), 8649–8655.

Chapelle, F.H. 1999. Bioremediation of petroleum hydrocarbon-contaminated ground water: the perspectives of history and hydrology. *Groundwater*, **37**(1), 122–132.

Christensen, T. H., Kjeldsen, P.and Albrechtsen, H.-J., Heron, G., Nielsen P. H., Bjerg, P. L., & Holm, P.E. 1994. Attenuation of landfill leachate pollutants in aquifers. *Critical reviews in environmental science and technology*, **24**(2), 119–202.

Cookson Jr, J. T. 1995. Bioremediation engineering: Design and application.

Cornell, R. M., & Schwertmann, U. 2003. *The iron oxides: structure, properties, reactions, occurrences and uses*. John Wiley & Sons.

Dhillon, A., Teske, A., Dillon, J., Stahl, D. A., & Sogin, M.L. 2003. Molecular characterization of sulfate-reducing bacteria in the Guaymas Basin. *Applied and Environmental Microbiology*, **69**(5), 2765–2772.

DiDonato Jr, R.J., Young, N. D., Butler, J. E., Chin, K.J., Hixson, K. K., Mouser, P., Lipton, M.S., DeBoy R., & Methé, B. A. 2010. Genome sequence of the deltapro-

teobacterial strain NaphS2 and analysis of differential gene expression during anaerobic growth on naphthalene. *PloS one*, **5**(11), e14072.

Edwards, E.A., Wills, L.E., Reinhard, M., & Grbić-Galić, D. 1992. Anaerobic degradation of toluene and xylene by aquifer microorganisms under sulfate-reducing conditions. *Applied and Environmental Microbiology*, **58**(3), 794–800.

Ehrlich, G.G., Schroeder, R.A., & Martin, P. 1985. *Microbial populations in a jet-fuel-contaminated shallow aquifer at Tustin, California.* Tech. rept. US Geological Survey,.

Elshahed, M. S., Gieg, L. M., McInerney, M. J., & Suflita, J. M. 2001. Signature metabolites attesting to the in situ attenuation of alkylbenzenes in anaerobic environments. *Environmental science & technology*, **35**(4), 682–689.

Eusterhues, K., Rumpel, C., & Kögel-Knabner, I. 2005. Organo-mineral associations in sandy acid forest soils: importance of specific surface area, iron oxides and micropores. *European Journal of Soil Science*, **56**(6), 753–763.

Fetzer, S., & Conrad, R. 1993. Effect of redox potential on methanogenesis by Methanosarcina barkeri. *Archives of Microbiology*, **160**(2), 108–113.

Foght, J. 2008. Anaerobic biodegradation of aromatic hydrocarbons: pathways and prospects. *Journal of Molecular Microbiology and Biotechnology*, **15**(2-3), 93–120.

Fredrickson, J.K., Brockman, F.J., Workman, D.J., Li, S.W., & Stevens, T.O. 1991. Isolation and characterization of a subsurface bacterium capable of growth on toluene, naphthalene, and other aromatic compounds. *Applied and environmental microbiology*, **57**(3), 796–803.

Fukushima, R. S., Weimer, P. J., & Kunz, D. A. 2003. Use of photocatalytic reduction to hasten preparation of culture media for saccharolytic Clostridium species. *Brazilian Journal of Microbiology*, **34**(1), 22–26.

Gallup, J.M. 2011. qPCR inhibition and amplification of difficult templates. *PCR troubleshooting and optimization: the essential guide*, **1**, 59.

Ghiorse, C. W. 1988. Microbial reduction of manganese and iron. *Biology of anaerobic microorganisms.*, 305–327.

Gibson, J., & Harwood, C. 2002. Metabolic diversity in aromatic compound utilization by anaerobic microbes. *Annual Reviews in Microbiology*, **56**(1), 345–369.

Grbić-Galić, D., & Vogel, T.M. 1987. Transformation of toluene and benzene by mixed methanogenic cultures. *Applied and Environmental Microbiology*, **53**(2), 254–260.

Hales, B.A., Edwards, C., Ritchie, D. A., Hall, G., Pickup, R. W., & Saunders, J. R. 1996. Isolation and identification of methanogen-specific DNA from blanket bog peat by PCR amplification and sequence analysis. *Applied and environmental Microbiology*, **62**(2), 668–675.

Hanson, J. R., Macalady, J. L., Harris, D., & Scow, K. M. 1999. Linking toluene degradation with specific microbial populations in soil. *Applied and Environmental Microbiology*, **65**(12), 5403–5408.

Haritash, A.K., & Kaushik, C.P. 2009. Biodegradation aspects of polycyclic aromatic hydrocarbons (PAHs): a review. *Journal of hazardous materials*, **169**(1-3), 1–15.

Heidemij. 1989. Voorbereiding sanering Griftpark te Utrecht Aanvullend onderzoek omgeving en noordelijk deel van het park. *Rapportnummer 929-88/3.*

Heider, J., & Fuchs, G. 1997. Anaerobic metabolism of aromatic compounds. *The FEBS Journal*, **243**(3), 577–596.

Heitkamp, M.A., & Cerniglia, C. E. 1988. Mineralization of polycyclic aromatic hydrocarbons by a bacterium isolated from sediment below an oil field. *Applied and environmental microbiology*, **54**(6), 1612–1614.

Hem, J. D. 1985. *Study and interpretation of the chemical characteristics of natural water.* Vol. 2254. Department of the Interior, US Geological Survey.

Herder, H., & Kolkman, H. 2000. De Utrechtse gasfabriek. *op de rails.*

Hinchee, R.E., Kittel, J.A., & Reisinger, H. J. 1995. Applied bioremediation of petroleum hydrocarbons.

Holmes, D.E., Finneran, K. T., O'neil, R. A., & Lovley, D. R. 2002. Enrichment of members of the family Geobacteraceae associated with stimulation of dissimilatory metal reduction in uranium-contaminated aquifer sediments. *Applied and Environmental Microbiology*, **68**(5), 2300–2306.

Hutchins, S.R. 1991. Biodegradation of monoaromatic hydrocarbons by aquifer microorganisms using oxygen, nitrate, or nitrous oxide as the terminal electron acceptor. *Applied and Environmental Microbiology*, **57**(8), 2403–2407.

Jahn, M. K.and Haderlein, S. B., & Meckenstock, R.U. 2005. Anaerobic degradation of benzene, toluene, ethylbenzene, and o-xylene in sediment-free iron-reducing enrichment cultures. *Applied and environmental microbiology*, **71**(6), 3355–3358.

Johnson, H. A., Pelletier, D. A., & Spormann, A. M. 2001. Isolation and characterization of anaerobic ethylbenzene dehydrogenase, a novel Mo-Fe-S enzyme. *Journal of bacteriology*, **183**(15), 4536–4542.

Kämpfer, P.M, Steiof, M, & Dott, W. 1991. Microbiological characterization of a fuel-oil contaminated site including numerical identification of heterotrophic water and soil bacteria. *Microbial ecology*, **21**(1), 227–251.

Karthikeyan, R., & Bhandari, A. 2001. Anaerobic biotransformation of aromatic and polycyclic aromatic hydrocarbons in soil microcosms: a review. *Journal of hazardous substance research*, **3**(1), 3.

Kiem, R., & Kögel-Knabner, I. 2002. Refractory organic carbon in particle-size fractions of arable soils II: organic carbon in relation to mineral surface area and iron oxides in fractions¡ 6 μm. *Organic Geochemistry*, **33**(12), 1699–1713.

Kniemeyer, O., & Heider, J. 2001. Ethylbenzene dehydrogenase, a novel hydrocarbon-oxidising molybdenum/iron-sulfur/heme enzyme. *Journal of Biological Chemistry*.

Laempe, D., Jahn, M., & Fuchs, G. 1999. 6-Hydroxycyclohex-1-ene-1-carbonyl-CoA dehydrogenase and 6-oxocyclohex-1-ene-1-carbonyl-CoA hydrolase, enzymes of the benzoyl-CoA pathway of anaerobic aromatic metabolism in the denitrifying bacterium Thauera aromatica. *European journal of biochemistry*, **263**(2), 420–429.

Lane, D.J. 1991. 16S/23S rRNA sequencing. *Nucleic acid techniques in bacterial systematics*, 115–175.

Langenhoff, A.A.M., Zehnder, A.J.B., & Schraa, G. 1996. Behaviour of toluene, benzene and naphthalene under anaerobic conditions in sediment columns. *Biodegradation*, **7**(3), 267–274.

Loibner, A.P., Szolar, O.H.J., Braun, R., & Hirmann, D. 2004. Toxicity testing of 16 priority polycyclic aromatic hydrocarbons using Lumistox®. *Environmental toxicology and chemistry*, **23**(3), 557–564.

López-Gutiérrez, J. C., Henry, S., Hallet, S., Martin-Laurent, F., Catroux, G., & Philippot, L. 2004. Quantification of a novel group of nitrate-reducing bacteria in the environment by real-time PCR. *Journal of Microbiological Methods*, **57**(3), 399–407.

Lorah, M.M., Cozzarelli, I.M., & Bohlke, J.K. 2012. Evaluating nutrient fate and redox controls in groundwater in riparian areas. *USGS National Research Program, Virginia, SIR*, **5235**.

Lovley, D.R., & Lonergan, D.J. 1990. Anaerobic oxidation of toluene, phenol, and p-cresol by the dissimilatory iron-reducing organism, GS-15. *Applied and Environmental Microbiology*, **56**(6), 1858–1864.

Lovley, D.R., Baedecker, M.J.and Lonergan, D.J., Cozzarelli, I.M., Phillips, Elizabeth J.P., & Siegel, D.I. 1989. Oxidation of aromatic contaminants coupled to microbial iron reduction. *Nature*, **339**(6222), 297.

Lu, X.-Y., Zhang, T., & Fang, H. H.-P. 2011. Bacteria-mediated PAH degradation in soil and sediment. *Applied microbiology and biotechnology*, **89**(5), 1357–1371.

MacRae, J.D., & Hall, K.J. 1998. Biodegradation of polycyclic aromatic hydrocarbons (PAH) in marine sediment under denitrifying conditions. *Water Science and Technology*, **38**(11), 177–185.

Meckenstock, R. U., Morasch, B., Griebler, C., & Richnow, H. H. 2004. Stable isotope fractionation analysis as a tool to monitor biodegradation in contaminated acquifers. *Journal of Contaminant Hydrology*, **75**(3-4), 215–255.

Meckenstock, R.U., & Mouttaki, H. 2011. Anaerobic degradation of non-substituted aromatic hydrocarbons. *Current Opinion in Biotechnology*, **22**(3), 406–414.

Menzie, C. A., Potocki, B. B., & Santodonato, J. 1992. Exposure to carcinogenic PAHs in the environment. *Environmental science & technology*, **26**(7), 1278–1284.

Miao, Z., Brusseau, M.L., Carroll, K. C., Carreón-Diazconti, C., & Johnson, B. 2012. Sulfate reduction in groundwater: characterization and applications for remediation. *Environmental geochemistry and health*, **34**(4), 539–550.

Ministry of Housing, Spatial Planning, & the Environment. 2000. Annex A: Target values, soil remediation intervention values and indicative levels for serious contamination.

Muyzer, G., & Ramsing, N. B. 1995. Molecular methods to study the organization of microbial communities. *Water Science and Technology*, **32**(8), 1–9.

National-Research-Council. 2000. *Natural attenuation for groundwater remediation*. National Academies Press.

Phelps, C. D., & Young, L.Y. 1999. Anaerobic biodegradation of BTEX and gasoline in various aquatic sediments. *Biodegradation*, **10**(1), 15–25.

Rabus, R., & Widdel, F. 1995. Anaerobic degradation of ethylbenzene and other aromatic hydrocarbons by new denitrifying bacteria. *Archives of microbiology*, **163**(2), 96–103.

Rockne, K. J., Chee-Sanford, J. C., Sanford, R. A., Hedlund, B. P., Staley J. T, & Strand, S. E. 2000. Anaerobic naphthalene degradation by microbial pure cultures

under nitrate-reducing conditions. *Applied and Environmental Microbiology*, **66**(4), 1595–1601.

Royal HaskoningDHV, enhancing Society Together. 2014. Griftpark scopeverandering. Historisch onderzoek ten behoeve van nader onderzoek grondwater. *Derks, Dorien and Rood, Peter and Manders, Bart.*

Rueter, P., Rabus, R., Wilkest, H., Aeckersberg, F., Rainey, F.A., Jannasch, H.W., & Widdel, F. 1994. Anaerobic oxidation of hydrocarbons in crude oil by new types of sulphate-reducing bacteria. *Nature*, **372**(6505), 455.

Safinowski, M., & Meckenstock, R. U. 2006. Methylation is the initial reaction in anaerobic naphthalene degradation by a sulfate-reducing enrichment culture. *Environmental Microbiology*, **8**(2), 347–352.

Sauck, W.A., Atekwana, E.A., & Nash, M.S. 1998. High conductivities associated with an LNAPL plume imaged by integrated geophysical techniques. *Journal of Environmental and Engineering Geophysics*, **2**, 203–212.

Schlegel, H.G. 1981. *Allgemeine Mikrobiologie.*

Schriewer, A., Wehlmann, A., & Wuertz, S. 2011. Improving qPCR efficiency in environmental samples by selective removal of humic acids with DAX-8. *Journal of microbiological methods*, **85**(1), 16–21.

Shao, M., Zhang, T., & Fang, H. H.P. 2009. Autotrophic denitrification and its effect on metal speciation during marine sediment remediation. *Water research*, **43**(12), 2961–2968.

Sharp, P.A., Sugden, B., & Sambrook, J. 1973. Detection of two restriction endonuclease activities in Haemophilus parainfluenzae using analytical agarose-ethidium bromide electrophoresis. *Biochemistry*, **12**(16), 3055–3063.

Shuman, S. 1991. Site-specific interaction of vaccinia virus topoisomerase I with du-

plex DNA. Minimal DNA substrate for strand cleavage in vitro. *Journal of Biological Chemistry*, **266**(17), 11372–11379.

Shuman, S. 1994. Novel approach to molecular cloning and polynucleotide synthesis using vaccinia DNA topoisomerase. *Journal of Biological Chemistry*, **269**(51), 32678–32684.

Statistics Netherlands, CBS. 2015. *Number of contaminated sites Statistics Netherlands (CBS), The Hague; PBL Netherlands Environmental Assessment Agency, The Hague; RIVM National Institute for Public Health and the Environment, Bilthoven; and Wageningen University and Research, Wageningen.*

Straub, K. L., Kappler, A., & Schink, B. 2005. Enrichment and isolation of ferric-iron-and humic-acid-reducing bacteria. *Methods in enzymology*, **397**, 58–77.

Tiedje, J.M. 1988. Ecology of denitrification and dissimilatory nitrate reduction to ammonium. *Biology of anaerobic microorganisms*, **717**, 179–244.

Tsai, C.-J., Chen, M.-L., Chang, K.-F., Chang, F.-K., & Mao, I.-F. 2009. The pollution characteristics of odor, volatile organochlorinated compounds and polycyclic aromatic hydrocarbons emitted from plastic waste recycling plants. *Chemosphere*, **74**(8), 1104–1110.

Uribe-Jongbloed, A., & Bishop, P. L. 2007. Comparative study of PAH removal efficiency under absence of molecular oxygen: effect of electron acceptor and hydrodynamic conditions. *Journal of Environmental Engineering and Science*, **6**(4), 367–376.

van der Waals, M.J., Atashgahi, S., Da Rocha, U. N., van der Zaan, B.M., Smidt, H., & Gerritse, J. 2017. Benzene degradation in a denitrifying biofilm reactor: activity and microbial community composition. *Applied microbiology and biotechnology*, **101**(12), 5175–5188.

Van der Zaan, B.M., Saia, F.T., Stams, A.J.M., Plugge, C.M., de Vos, W.M., Smidt, H., Langenhoff, A.A.M., & Gerritse, J. 2012. Anaerobic benzene degradation under

denitrifying conditions: Peptococcaceae as dominant benzene degraders and evidence for a syntrophic process. *Environmental microbiology*, **14**(5), 1171–1181.

van Oorschot, H.J. 2015. *The remediation of soil and groundwater at the Griftpark in Utrecht Geohydrological and solute transport modeling of the Griftpark pollution Scenarios that could lead to a finite remediation approach.* M.Phil. thesis.

Vanwijk, D.J., & Hutchinson, T. H. 1995. The ecotoxicity of chlorate to aquatic organisms: a critical review. *Ecotoxicology and Environmental safety*, **32**(3), 244–253.

Vetriani, C., Jannasch, H. W., MacGregor, B. J., Stahl, D. A., & Reysenbach, A.-L. 1999. Population structure and phylogenetic characterization of marine benthic archaea in deep-sea sediments. *Applied and Environmental Microbiology*, **65**(10), 4375–4384.

Vogt, C., Cyrus, E., Herklotz, I., Schlosser, D., Bahr, A., Herrmann S., Richnow, H.-H., & Fischer, A. 2008. Evaluation of toluene degradation pathways by two-dimensional stable isotope fractionation. *Environmental science & technology*, **42**(21), 7793–7800.

Vogt, C., Kleinsteuber, S., & Richnow, H.-H. 2011. Anaerobic benzene degradation by bacteria. *Microbial biotechnology*, **4**(6), 710–724.

Wang, O., & Coates, J. 2017. Biotechnological applications of microbial (Per) chlorate reduction. *Microorganisms*, **5**(4), 76.

Wang, Z., Fingas, M., & Li, K. 1994. Fractionation of a light crude oil and identification and quantitation of aliphatic, aromatic, and biomarker compounds by GC-FID and GC-MS, part II. *Journal of chromatographic science*, **32**(9), 367–382.

Weelink, S.A.B. 2008. *Degradation of benzene and other aromatic hydrocarbons by anaerobic bacteria.*

Werkema, D. D., Atekwana, E. A., Endres, A. L., Sauck, W. A., & Cassidy, D. P. 2003. Investigating the geoelectrical response of hydrocarbon contamination undergoing biodegradation. *Geophysical Research Letters*, **30**(12).

WHO. 2011. nitrite in drinking-water. Background document for preparation of WHO Guidelines for drinkingwater quality. *World Health Organization, Geneva*.

Widdel, F. 1988. Microbiology and ecology of sulfate-and sulfur-reducing bacteria. *Biology of anaerobic microorganisms.*, 469–585.

Widdel, F., & Rabus, R. 2001. Anaerobic biodegradation of saturated and aromatic hydrocarbons. *Current opinion in biotechnology*, **12**(3), 259–276.

Wilson, B.H., Smith, G.B., & Rees, J.F. 1986. Biotransformations of selected alkylbenzenes and halogenated aliphatic hydrocarbons in methanogenic aquifer material: a microcosm study. *Environmental science & technology*, **20**(10), 997–1002.

Wu, Y.and Zhang, W., Yu, W., Liu, H., Chen, R., & Wei, Y. 2015. Ferrihydrite preparation and its application for removal of anionic dyes. *Frontiers of Environmental Science & Engineering*, **9**(3), 411–418.

Zehnder, A.J.B., & Mitchell, R. 1978. Ecology of methane formation. *Water pollution microbiology*, **2**, 349–376.

Zhang, T., Gannon, S. M., Nevin, K. P., Franks, A. E., & Lovley, D. R. 2010. Stimulating the anaerobic degradation of aromatic hydrocarbons in contaminated sediments by providing an electrode as the electron acceptor. *Environmental microbiology*, **12**(4), 1011–1020.

1 Appendix A

1.1 Additional information on the methods used

1.1.1 qPCR assay - additional information

Table 17: Details on the qPCR assays performed in this study. The primer pair, minimal and maximal concentrations, melt-curve temperature and the detection method are listed. * BSA stock solution 20 μ/μg.

Gene ID	Primers	Conc. min	Conc max.	Melt curve	Detection	Notes
16S rRNA total bacteria	519F/907R	7.29E+07	7.29E+02	87-88	SYBR®Green	
16S rRNA total archaea	Arch0025F/Arch364R	5.19E+07	5.91E+01	86-87	SYBR®Green	
mcrA	ME1F/ME3R	6.65E+07	6.65E+01	86-89	SYBR®Green	
drsA	DrsA1F/DrsA500R	4.00E+07	4.00E+01	90-92	SYBR®Green	
16S rRNA *Geobacter* sp.	GEO564F/GEO840R	5.55E+07	5.55E+01	86-88	SYBR®Green	
narG	NarGGF/NarGGR	3.36E+07	3.36E+01	90-92	SYBR®Green	
16S rRNA *Peptococcaceae*	Pepto F/ Pepto R	1.47E+07	1.47E+01	82-85	SYBR®Green	
bssA	bssAF/bssAR	4.13E+07	4.13E+01	-	Taqman	BssA probe
bssA SRB	BssA SRBF/ BssA SRB R	2.24E+07	2.24E+06	81-84	SYBR®Green	
assA	1432assA F/Ass/bss R	1.92E+07	1.92E+02	87-90	SYBR®Green	
bamA	oahF/oahR	8.16E+07	8.16E+01	87-91	SYBR®Green	BSA 0.4 μ/μg*
NC	NaftcarboF2/NaftcarboR2	1.95E+07	1.95E+01	84.5	SYBR®Green	
abcA	BenzCarb F1/ Benzcarb R1	1.51E+07	1.51E+01	83-86	SYBR®Green	BSA 0.4 μ/μg*

1.1.2 457. Mineral medium (Brunner) - 2012 DSMZ GmbH

- Na2HPO4 2.44 g
- KH2PO4 1.52 g
- (NH4)2SO4 0.50 g
- MgSO4 x 7 H2O 0.20 g
- CaCl2 x 2 H2O 0.05 g
- Trace element solution SL-4 (see below) 10.00 ml
- Distilled water 1000.00 ml
- Adjust pH to 6.9.

Prepare a separate solution of the phosphates and autoclave separately. Combine the two solutions after cooling.

Trace element solution SL-4:

- FeSO4 x 7 H2O 0.20 g
- Trace element solution SL-6 (see below) 100.00 ml
- Distilled water 900.00 ml

Trace element solution SL-6:

- ZnSO4 x 7 H2O 0.10 g
- MnCl2 x 4 H2O 0.03 g
- H3BO3 0.30 g
- CoCl2 x 6 H2O 0.20 g
- CuCl2 x 2 H2O 0.01 g
- NiCl2 x 6 H2O 0.02 g
- Na2MoO4 x 2 H2O 0.03 g
- Distilled water 1000.00 ml

1.1.3 Preparation of the calibration line for the GC measurements

Table 18: Calculation of the concentrations in the dilution of the HC acetone in milliQ water and of the added compounds. The dilutions 1-200x are the concentrations that were used for the GC-MS and GC-FID calibration lines. The grey shaded cells represent the concentrations until the peak area and show a linear correlation and a correlation coefficient 0.9 (see figure 25 and 26). From the linear trendline the slope is used to calculate the concentrations obtained from the analysis of this report.

Chemical		molar mass	density					undiluted	100x dilution
HC mix in acetone	[ul/500mL]	g/mol	kg/m³	g/ml	ml/500ml	g/500ml	g/l	ug/L	
benzene	3000	78.11	876	0.876	3.000	2.628	5.256	5256000	52560
toluene	2500	92.14	867	0.867	2.500	2.168	4.335	4335000	43350
ethylbenzene	350	106.17	866	0.866	0.350	0.303	0.606	606200	6062
mp xylene	900	106.16	861	0.861	0.900	0.775	1.550	1549800	15498
o xylene	1650	106.16	861	0.861	1.650	1.421	2.841	2841300	28413
1,2,4 TMB	140	120.19	876	0.876	0.140	0.123	0.245	245280	2452.8
1,2,3 TMB	200	120.20	864	0.864	0.200	0.173	0.346	345600	3456
indene	830	116.16	997	0.997	0.830	0.828	1.655	1655020	16550.2
naphthalene	1510	128.17	1140	1.140	1.510	1.721	3.443	3442800	34428
added compounds	ul/500ml	g/mol	kg/m³	g/ml	ml/500ml	g/500ml	g/l	ug/L	
cumene	50	120.19	862	0.862	0.050	0.043	0.086	86200	-
3-ethyltoluene	50	120.20	865	0.865	0.050	0.043	0.087	86500	-
4-Ethyltoluene	50	120.20	861	0.861	0.050	0.043	0.086	86100	-
2-Ethyltoluene	50	120.20	887	0.887	0.050	0.044	0.089	88700	-
Indane	50	118.18	962	0.962	0.050	0.048	0.096	96200	-
2-Methylnaphthalene	50	142.20	1000	1.000	0.050	0.050	0.100	100000	-

	dilution [µg/l]							
HC mix in acetone	1x	2x	5x	10x	20x	50x	100x	200x
benzene	52560	26280	10512	5256	2628	1051.2	525.6	262.8
toluene	43350	21675	8670	4335	2167.5	867	433.5	216.75
ethylbenzene	6062	3031	1212.4	606.2	303.1	121.24	60.62	30.31
mp xylene	15498	7749	3099.6	1549.8	774.9	309.96	154.98	77.49
o xylene	28413	14206.5	5682.6	2841.3	1420.65	568.26	284.13	142.065
1,2,4 TMB	2452.8	1226.4	490.56	245.28	122.64	49.056	24.528	12.264
1,2,3 TMB	3456	1728	691.2	345.6	172.8	69.12	34.56	17.28
indene	16550.2	8275.1	3310.04	1655.02	827.51	331.004	165.502	82.751
naphthalene	34428	17214	6885.6	3442.8	1721.4	688.56	344.28	172.14
added compounds								
cumene	86200	43100	17240	8620	4310	1724	862	431
3-ethyltoluene	86500	43250	17300	8650	4325	1730	865	432.5
4-Ethyltoluene	86100	43050	17220	8610	4305	1722	861	430.5
2-Ethyltoluene	88700	44350	17740	8870	4435	1774	887	443.5
Indane	96200	48100	19240	9620	4810	1924	962	481
2-Methylnaphthalene	100000	50000	20000	10000	5000	2000	1000	500

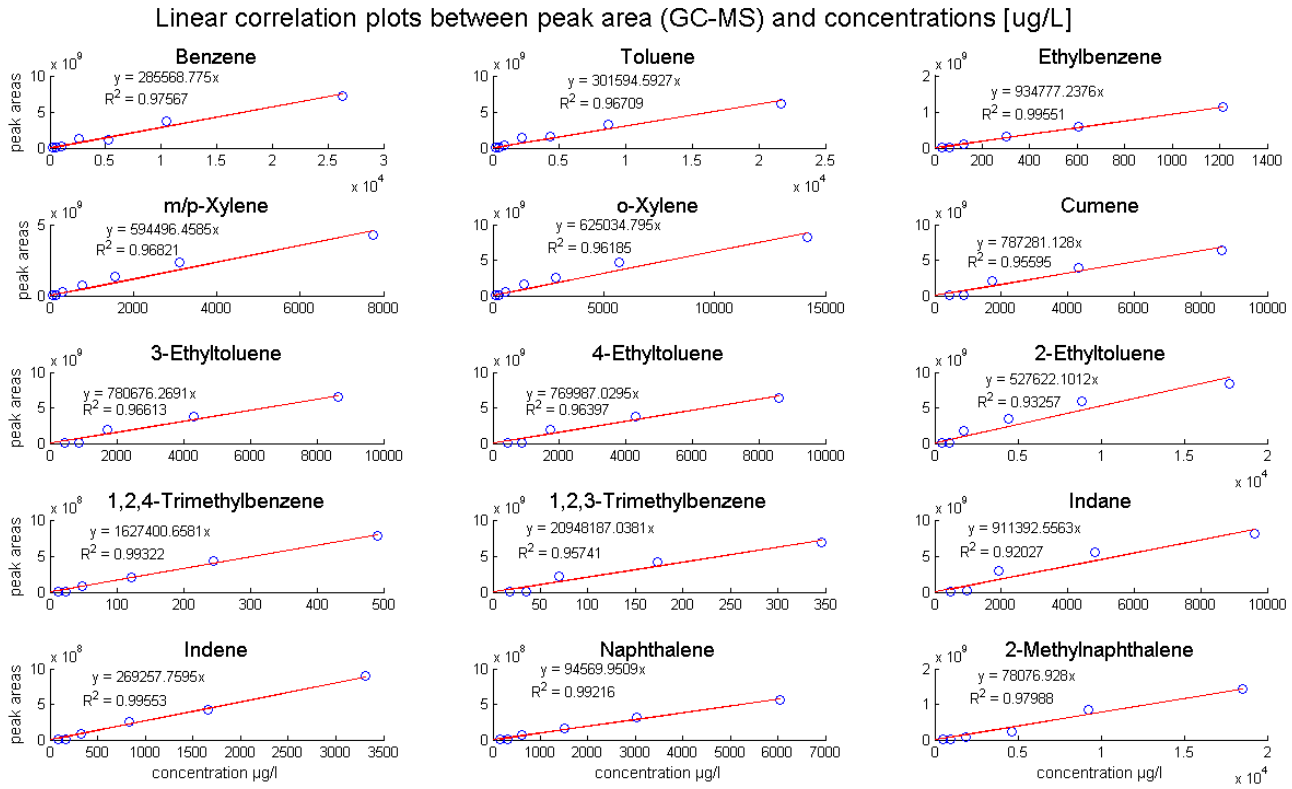

Figure 25: GC-MS calibration line for aromatic hydrocarbons

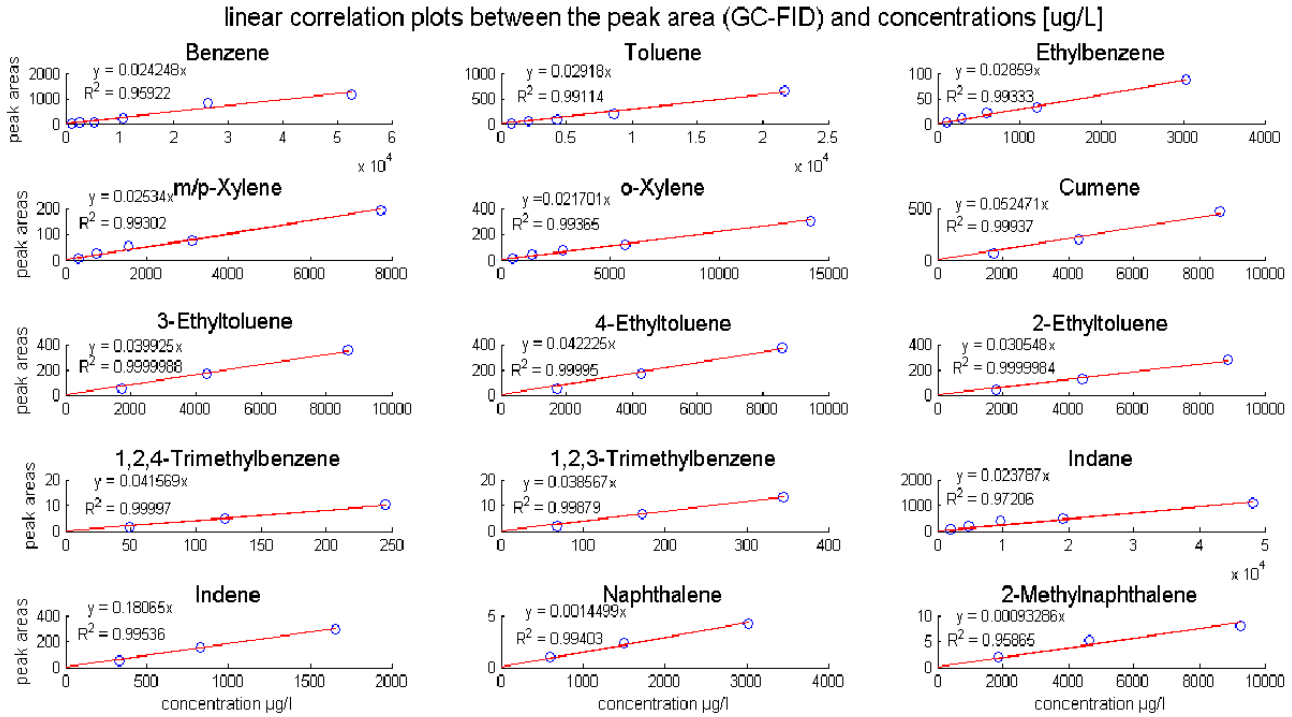

Figure 26: GC-FID calibration line for aromatic hydrocarbons

Table 19: Additional information on the calibration of the concentration of compounds for the GC measurements.

Compound	y=mx slope with P(0—0)	ug/L valid for conc. up to	conc.<solubility	ug/L Solubility in water
Benzene	285568.78	26280.00	TRUE	1815000
Toluene	301594.59	21675.00	TRUE	520000
Ethylbenzene	934777.24	1212.40	TRUE	150000
m/p-xylene	594496.46	7749.00	TRUE	insoluble
o-xylene	625034.80	14206.50	TRUE	insoluble
cumene	78728112.80	86.20	TRUE	insoluble
3-Ethyltoluene	78067626.91	86.50	TRUE	insoluble
4-Ethyltoluene	76998702.95	86.10	TRUE	94000
2-Ethyltoluene	52762210.12	177.40	TRUE	74640
1,2,4-TMB	1627400.66	490.56	TRUE	75200
1,2,3-TMB	20948187.04	345.60	TRUE	57000
Indane	91139255.63	96.20	TRUE	109000
Indene	269257.76	3310.04	TRUE	insoluble
Naphthalene	94569.95	6040.00	TRUE	31600
2-Methylnaphthalene	7807692.80	185.00	TRUE	24600

1.2 Additional information for the results

1.2.1 Field samples

Table 20: Detailed table of the anions and cations measured in the Dionex and ICPOES analyses of the field samples.

					DIONEX				
Sample	Cl^-	Ca^{2+}	Na^+	Mg^{2+}	SO_4^{2-}	NH_4^+	NO_2^-	NO_3^-	K^+
BW211	68.95	134.18	47.79	12.90	73.39	1.23	n.a.	< MDL	16.88
BW157	57.53	109.47	35.30	15.06	63.99	1.18	n.a.	< MDL	9.10
B 22	79.84	148.25	64.70	19.80	< MDL	31.03	n.a.	< MDL	16.82
PB 1	85.70	213.46	66.68	17.99	255.76	10.46	n.a.	< MDL	13.58
DV-4	76.41	209.61	71.65	21.10	227.32	23.42	n.a.	< MDL	14.43
37	54.50	137.67	54.52	14.21	111.21	8.38	n.a.	0.47	5.42
60	60.54	99.01	36.21	10.27	31.15	7.50	n.a.	< MDL	5.33
BW205	151.43	111.84	108.41	12.01	21.03	9.61	n.a.	< MDL	6.28
					ICPOES				
	Cl^-	Ca^{2+}	Na^+	Mg^{2+}	S^{2-}	Mn^{2+}	Si	Fe^{2+}	K^+
BW211	54.05	154.42	46.30	12.36	31.81	1.66	6.65	6.98	11.21
BW157	37.14	153.04	33.86	14.49	26.74	0.50	8.80	6.84	4.42
B 22	63.61	171.84	61.56	18.35	117.83	0.23	7.18	0.14	11.53
PB 1	54.27	232.01	65.72	17.38	104.85	1.48	7.98	6.98	9.40
DV-4	43.41	215.18	70.11	20.25	93.07	0.70	7.44	2.08	10.11
37	30.61	143.99	54.03	13.95	48.13	1.18	8.95	0.82	0.66
60	48.36	98.99	33.46	9.93	14.08	0.33	7.83	2.79	0.14
BW205	149.61	120.41	116.03	12.17	9.04	0.44	8.41	1.76	2.22

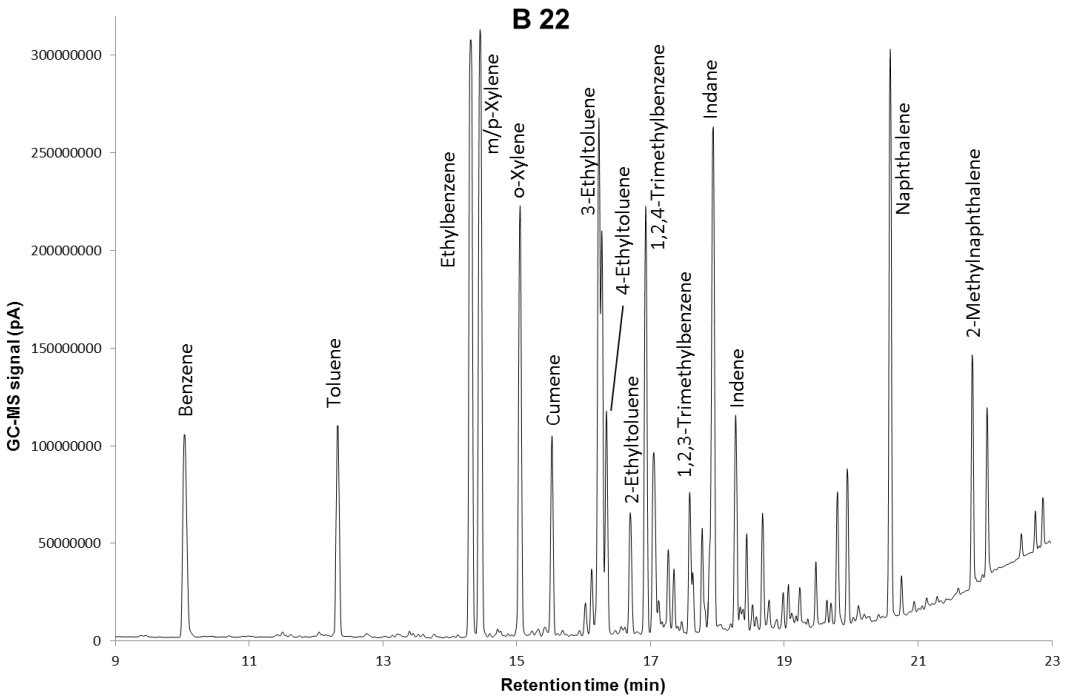

Figure 27: Illustration of the GC-MS signal of the aromatic hydrocarbons in the field sample of the monitoring well B22. The signal over the retention time is shown. The studied aromatic hydrocarbons are labelled according to their retention time.

Table 21: The results of the DNA analysis are displayed in gene copies/L

	gene copies/L						
Well	TB	TA	*mrcA*	*drsA*	Geo	*narG*	*bssA*
BW211	2.45E+08	2.52E+04	3.49E+04	NA	1.94E+05	NA	NA
BW157	1.22E+07	2.42E+05	NA	NA	5.08E+03	NA	NA
B22	9.43E+09	1.97E+07	1.09E+06	1.94E+07	2.58E+07	7.95E+07	1.30E+05
Pb1	1.37E+07	7.25E+04	NA	1.95E+05	1.47E+05	NA	NA
DV4	1.46E+06	4.06E+03	NA	NA	1.21E+04	NA	NA
37	1.43E+07	4.33E+04	NA	1.64E+05	7.96E+04	NA	NA
60	7.65E+06	7.04E+04	NA	NA	3.53E+04	NA	NA
BW205	1.22E+06	1.35E+05	NA	NA	2.53E+04	NA	NA

	bssA SRB	Pepto	NC	*abcA*	*assA*	*bamA*
BW211	1.53E+09	NA	NA	7.31E+03	1.69E+05	1.06E+07
BW157	NA	NA	7.51E+03	NA	NA	2.01E+04
B22	6.62E+09	7.94E+05	8.38E+07	7.47E+04	NA	8.22E+07
Pb1	6.07E+07	6.52E+04	1.75E+05	4.33E+03	NA	2.02E+06
DV4	NA	NA	7.47E+03	NA	NA	2.26E+04
37	2.51E+08	1.06E+04	1.35E+04	6.18E+02	NA	2.93E+05
60	6.32E+07	NA	7.95E+03	NA	1.16E+04	1.31E+05
BW205	NA	NA	1.53E+04	NA	NA	3.64E+04

1.2.2 batch experiments

Table 22: Concentration of aromatic hydrocarbons detected with the GC-MS at extraction time T0, T1 and T2 in the first 4 scenarios. For the explanation of the abbreviations see table 4.

			conc														
	batch	time	Be	Tln	Eb	m/p-xyln	o-xyln	cumn	3-Etln	4-etln	2-etln	1,2,4 TMB	1,2,3 TMB	indane	indene	nph	2-mnph
No Additives	B22	T0	502.24	370.73	331.51	467.81	243.01	30.45	171.16	44.73	37.33	73.34	2.29	369.57	451.06	5082.77	2167.26
		T1	477.12	339.32	304.62	427.79	218.73	24.85	148.45	38.07	31.03	63.81	1.96	349.74	374.57	4713.99	1824.12
		T2	452.13	329.54	279.44	391.34	198.84	20.34	122.45	30.75	25.44	53.06	1.61	318.65	331.35	4284.77	1428.67
	BW205	T0	55.44	40.30	50.82	61.04	26.72	3.07	22.49	4.58	3.82	7.41	0.23	53.23	50.25	869.64	283.63
		T1	0.00	0.00	0.00	0.33	0.32	0.13	0.00	0.12	0.00	0.00	0.01	0.07	0.00	0.00	0.00
		T2	0.00	0.00	0.00	0.30	0.12	0.00	0.00	0.00	0.00	0.00	0.00	0.06	0.00	0.00	0.00
	60	T0	45.25	32.82	45.48	55.35	24.12	3.17	19.87	4.93	3.85	8.08	0.25	54.65	43.52	951.29	0.00
		T1	0.00	0.00	0.00	0.31	2.76	0.00	0.00	1.13	0.75	0.00	0.05	2.69	0.00	0.00	0.00
		T2	0.00	6.68	0.05	0.55	3.57	0.22	0.34	1.96	1.78	0.07	0.08	8.31	1.19	0.00	0.00
O2	B22	T0	494.33	364.68	322.34	456.69	236.39	28.61	235.74	40.96	35.01	69.39	2.16	354.94	429.63	4805.66	1998.04
		T1	142.65	18.04	0.00	133.16	89.07	0.00	60.33	34.69	17.68	29.27	1.05	145.08	38.48	0.00	546.21
		T2	0.00	0.00	0.00	82.59	5.93	0.00	48.17	19.62	11.35	19.63	0.82	66.59	2.11	0.00	0.00
	BW205	T0	60.06	43.41	49.96	59.36	25.72	2.60	21.32	3.69	3.24	6.09	0.19	44.40	47.15	693.68	174.60
		T1	0.00	0.00	0.00	0.62	0.41	0.29	0.00	0.00	0.00	0.04	0.01	0.19	0.23	0.00	0.00
		T2	0.00	0.00	0.10	0.42	0.25	0.00	0.00	0.00	0.09	0.08	0.01	0.12	0.00	0.00	0.00
	60	T0	58.53	42.41	52.80	62.99	26.41	3.08	22.12	4.28	3.68	7.12	0.21	49.04	42.97	750.79	0.00
		T1	0.00	0.00	0.00	0.40	0.55	0.00	0.00	1.03	0.11	0.05	0.01	0.00	0.00	0.00	0.00
		T2	0.00	0.00	0.00	0.23	0.17	0.00	0.00	0.00	0.00	0.06	0.00	0.00	0.00	0.00	0.00
O2 + Nutrients	B22	T0	448.02	336.37	315.00	448.98	232.76	31.13	177.88	46.54	38.21	74.96	2.36	366.62	415.29	5078.31	2383.19
		T1	292.27	138.69	119.65	167.24	84.08	7.16	58.13	35.71	19.26	20.26	1.10	139.26	111.58	1749.24	496.99
		T2	274.22	152.90	125.52	173.19	86.24	7.82	61.57	42.13	2.33	7.07	1.19	142.70	105.40	1535.29	424.67
	BW205	T0	51.33	36.17	41.83	50.19	21.74	2.23	12.85	2.88	2.82	5.09	0.16	38.12	39.01	610.27	175.17
		T1	0.00	0.00	0.00	0.50	0.43	0.19	0.00	0.00	0.26	0.00	0.01	0.06	0.00	0.00	0.00
		T2	0.00	0.00	0.00	0.20	0.34	0.00	0.00	0.00	0.00	0.00	0.00	0.04	0.00	0.00	0.00
	60	T0	49.11	35.14	43.47	52.03	22.19	2.49	14.63	3.37	3.00	5.80	0.18	40.93	33.82	635.34	0.00
		T1	0.00	0.00	0.00	0.25	0.44	0.00	0.00	0.00	0.00	0.00	0.00	0.00	0.00	0.00	0.00
		T2	0.00	3.28	0.00	0.34	0.22	0.00	0.00	0.06	0.00	0.05	0.01	0.00	0.00	0.00	0.00
Chlorate	B22	T0	501.41	379.73	339.12	480.75	248.38	31.94	178.04	46.81	38.49	75.54	2.34	368.43	453.70	5007.59	2189.68
		T1	380.59	272.95	215.83	348.74	176.14	16.07	114.21	28.24	22.95	48.81	1.50	291.88	289.29	4135.43	1583.87
		T2	434.22	325.50	230.35	405.18	204.13	18.34	141.27	37.01	28.55	60.03	1.83	336.31	316.76	4408.01	1754.27
	BW205	T0	55.46	40.49	49.38	59.52	25.59	2.89	17.04	4.12	3.67	6.89	0.21	48.91	46.17	783.99	251.83
		T1	0.00	0.00	0.00	0.33	0.30	0.18	0.00	0.00	0.00	0.13	0.00	0.00	0.00	0.00	0.00
		T2	0.00	8.76	0.11	0.51	0.30	0.10	0.13	0.00	0.10	0.06	0.01	0.21	0.00	0.00	0.00
	60	T0	48.06	35.70	46.21	55.59	24.16	2.86	18.11	4.30	3.45	7.23	0.22	49.32	39.96	800.41	0.00
		T1	0.00	0.00	0.00	2.42	1.28	0.00	1.97	1.44	1.02	0.00	0.06	13.22	2.87	0.00	41.17
		T2	0.00	2.72	0.00	2.62	0.70	0.27	2.00	1.47	1.02	0.07	0.06	14.22	3.17	0.00	51.91

Table 23: Concentration of aromatic hydrocarbons detected with the GC-MS at extraction time T0, T1 and T2 in the last 4 scenarios. For the explanation of the abbreviations see table 4.

			conc														
scenario	batch	time	Be	Tln	Eb	m/p-xyln	o-xyln	cumn	3-Etln	4-etln	2-etln	1,2,4 TMB	1,2,3 TMB	indane	indene	nph	2-mnph
Nitrate	B22	T0	495.28	376.09	351.66	501.70	262.54	37.64	207.51	56.79	45.68	87.29	2.78	400.18	496.31	5412.60	2584.25
		T1	431.07	325.95	329.56	468.83	240.77	35.04	210.12	57.08	44.92	88.81	2.79	418.72	456.93	5849.86	2942.01
		T2	394.85	304.43	288.13	406.14	203.39	25.62	153.41	40.83	32.17	64.74	1.90	334.39	355.17	3805.44	1414.69
	BW205	T0	57.47	41.69	50.74	60.39	25.62	2.92	17.01	4.02	3.45	6.71	0.21	48.01	46.22	752.00	237.84
		T1	0.00	0.00	0.00	0.35	0.39	0.14	0.00	0.00	0.00	0.03	0.00	0.00	0.00	0.00	0.00
		T2	0.00	0.00	0.00	0.31	0.30	0.00	0.00	0.00	0.00	0.06	0.00	0.10	0.00	0.00	0.00
	60	T0	50.35	36.50	48.75	58.87	25.29	3.20	19.11	4.56	3.74	7.65	0.23	52.22	44.25	856.85	0.00
		T1	0.00	0.00	0.00	0.64	0.47	0.00	0.31	2.38	1.58	0.07	0.10	9.54	0.34	0.00	0.00
		T2	0.00	7.68	0.04	0.56	0.25	0.35	0.31	1.81	1.32	0.07	0.08	8.35	0.00	0.00	0.00
Sulfate	B22	T0	488.05	373.35	345.89	493.15	257.94	35.35	200.17	54.93	44.44	86.25	2.77	401.87	503.30	5560.09	2655.12
		T1	412.37	297.57	276.79	392.30	202.39	23.10	146.66	37.56	31.46	63.76	2.02	343.84	427.41	5008.28	2136.64
		T2	405.64	303.18	266.53	374.03	191.43	20.94	128.14	32.78	27.37	56.04	1.75	321.60	375.19	4440.57	1670.56
	BW205	T0	55.71	40.01	50.32	60.11	25.56	3.07	17.77	4.23	3.59	7.03	0.21	49.43	46.40	798.12	267.90
		T1	0.00	0.00	0.00	0.33	0.46	0.00	0.00	0.00	0.00	0.00	0.01	0.00	0.00	0.00	0.00
		T2	0.00	2.95	0.00	0.87	0.83	0.00	0.35	0.28	0.21	0.07	0.01	0.23	0.15	0.00	0.00
	60	T0	48.57	35.93	49.18	59.45	25.66	3.41	20.77	4.98	4.05	8.15	0.26	55.14	46.19	908.38	0.00
		T1	0.00	0.00	0.00	0.44	0.34	0.00	0.30	1.57	0.99	0.03	0.06	5.93	0.31	0.00	0.00
		T2	0.00	6.58	0.05	0.56	0.39	0.26	0.16	1.34	0.93	0.07	0.06	5.81	0.23	0.00	0.00
Ferrihydrite	B22	T0	469.21	355.83	335.03	475.46	246.57	34.23	191.68	52.25	43.22	81.90	2.62	387.31	501.95	5488.52	2494.57
		T1	380.30	261.21	47.23	394.45	201.19	17.39	162.34	42.72	32.93	67.35	2.07	351.12	411.20	5035.48	2275.81
		T2	422.67	315.15	93.55	426.11	217.95	21.64	169.58	45.55	35.95	70.54	2.23	371.51	437.62	5149.84	2111.84
	BW205	T0	47.79	34.10	42.63	51.01	22.29	2.60	18.49	3.61	3.25	6.07	0.19	42.93	42.54	731.22	247.03
		T1	0.00	0.00	0.00	0.28	0.31	0.00	0.00	0.00	0.00	0.03	0.01	0.00	0.00	0.00	0.00
		T2	0.00	0.00	0.00	0.37	0.31	0.07	0.00	0.00	0.00	0.05	0.00	0.09	0.00	0.00	0.00
	60	T0	47.17	34.74	46.74	56.55	24.31	3.11	19.66	4.78	3.91	7.88	0.24	53.26	43.18	887.73	0.00
		T1	11.33	6.14	0.00	0.73	13.31	0.00	0.91	2.04	1.91	0.07	0.11	22.68	3.96	0.00	0.00
		T2	11.85	14.95	0.00	1.08	14.99	0.25	1.63	1.92	2.03	0.05	0.12	27.18	5.23	0.00	0.00
Sterile	B22	T0	489.52	352.48	315.81	444.83	231.15	28.23	159.67	39.83	34.33	67.24	2.10	353.07	419.85	4762.15	2025.36
		T1	406.28	288.23	248.77	346.99	176.26	18.00	110.78	26.81	22.89	47.82	1.48	299.07	289.90	4188.33	1555.45
		T2	326.92	238.24	198.98	268.35	131.12	11.70	67.74	16.00	13.83	28.58	0.86	210.55	187.08	2391.43	590.14
	BW205	T0	48.45	43.84	32.12	39.41	19.24	0.80	8.60	2.00	2.28	4.01	0.15	36.40	40.47	615.67	139.28
		T1	48.34	46.93	32.23	38.21	17.46	1.40	7.94	1.99	1.84	3.46	0.11	29.98	33.21	478.46	549.58
		T2	49.12	54.73	33.43	39.60	17.48	1.43	8.03	1.93	1.86	3.46	0.11	30.62	31.50	469.01	92.32
	60	T0	36.15	41.50	23.17	28.15	14.78	0.00	6.93	1.71	10.84	0.00	0.14	34.53	29.54	722.42	0.00
		T1	46.28	59.64	35.92	43.39	19.25	1.88	11.38	2.96	2.26	5.03	0.16	39.18	26.70	653.05	193.81
		T2	46.46	65.41	35.49	42.04	18.79	1.87	10.82	2.66	2.11	4.68	0.15	38.46	25.71	611.65	161.50

Table 24: Shows if the concentration of the aromatic hydrocarbons increased (+), decreased (-) or remained the same (=) from time T0 to T2 in the batches. For the explanation of the abbreviations see table 4.

		Be	Tln	Eb	m/p-xyln	o-xyln	cumn	3-Etln	4-etln	2-etln	1,2,4 TMB	1,2,3 TMB	indane	indene	nph	2-mnph
No Add	B22	-	-	-	-	-	-	-	-	-	-	-	-	-	-	-
	BW205	-	-	-	-	-	-	-	-	-	-	-	-	-	-	-
	60	-	-	-	-	-	-	-	-	-	-	-	-	-	-	-
O_2	B22	-	-	-	-	-	-	-	-	-	-	-	-	-	-	-
	BW205	-	-	-	-	-	-	-	-	-	-	-	-	-	-	-
	60	-	-	-	-	-	-	-	-	-	-	-	-	-	-	-
O_2 + Nutrients	B22	-	-	-	-	-	-	-	=	-	-	-	-	-	-	-
	BW205	-	-	-	-	-	-	-	-	-	-	-	-	-	-	-
	60	-	-	-	-	-	-	-	-	-	-	-	-	-	-	-
Chlorate	B22	-	-	-	-	-	-	-	-	-	-	-	-	-	-	-
	BW205	-	-	-	-	-	-	-	-	-	-	-	-	-	-	-
	60	-	-	-	-	-	-	-	-	-	-	-	-	-	-	-
Nitrate	B22	-	-	-	-	-	-	-	-	-	-	-	-	-	-	-
	BW205	-	-	-	-	-	-	-	-	-	-	-	-	-	-	-
	60	-	-	-	-	-	-	-	-	-	-	-	-	-	-	-
Sulfate	B22	-	-	-	-	-	-	-	-	-	-	-	-	-	-	-
	BW205	-	-	-	-	-	-	-	-	-	-	-	-	-	-	-
	60	-	-	-	-	-	-	-	-	-	-	-	-	-	-	-
Ferrihydrite	B22	-	-	-	-	-	-	-	-	-	-	=	=	-	-	-
	BW205	-	-	-	-	-	-	-	-	-	-	=	-	-	-	-
	60	-	-	-	-	-	-	-	-	-	-	-	-	-	-	-
Sterile	B22	-	-	-	-	-	-	-	-	-	-	-	-	-	-	-
	BW205	=	+	=	=	=	+	=	=	=	=	=	-	-	-	-
	60	+	+	+	+	+	+	+	+	+	+	=	+	-	-	+

Table 25: Concentrations [mg/L] of the anions and cations measured in the DIONEX and ICPOES analysis of the batch experiments

Scenario	Batch	Time	Chloride	Na	Ka	Mg	Ca	Sulfate	Phosphate	Ammonium	Nitrite	Bromide	Nitrate	Fe	Mn	P	S	Chlorate
Oxygen	B22	T0	77.95	61.51	19.00	18.61	142.88	5.78	1.98	26.86	0.09	0.39	NA		0.31	0.96	55.59	
		T2	66.10	63.15	19.91	18.50	137.16	44.47	<DL	22.71	0.11	0.22	1.21	0.13	0.21	0.53	16.13	
	BW205	T0	148.22	104.30	7.94	12.74	107.22	16.42	<DL	10.51	0.17	0.23	0.77		0.46	0.30	8.01	
		T2	134.01	101.99	7.79	12.32	107.62	21.51	<DL	0.26	13.34	0.29	18.27	0.13	0.35	0.15	<8.27	
	60	T0	70.08	38.18	7.13	11.60	101.30	30.68	<DL	8.89	0.10	0.21	0.74		0.37	0.33	11.19	
		T2	53.64	39.34	7.00	11.40	106.19	34.81	<DL	0.14	11.40	0.22	14.54	0.12	0.25	0.15	12.12	
O2 + Nutrients	B22	T0	74.99	120.19	53.24	17.94	100.43	38.13	140.41	33.67	0.11	0.33	NA	0.19	0.29	71.01	39.06	
		T2	62.57	122.39	55.02	16.74	44.32	50.92	37.73	31.15	0.15	0.26	1.11	0.13	<DL	24.12	18.94	
	BW205	T0	139.39	159.00	44.09	12.82	97.06	52.68	148.11	20.51	0.25	0.26	1.12		0.40	71.86	18.44	
		T2	125.61	160.90	45.65	11.87	52.98	58.22	147.49	0.39	52.96	0.23	2.22	0.20	<DL	50.88	19.24	
	60	T0	66.66	101.59	43.71	12.17	92.78	65.11	222.46	19.18	0.10	0.17	0.79		0.34	72.61	22.16	
		T2	52.52	104.59	45.34	11.25	52.53	71.26	163.43	0.35	50.42	0.18	1.46	0.15	<DL	53.43	22.26	
Sterile	B22	T0	81.22	60.01	17.94	16.15	101.10	10.72	1.47	25.77	0.10	0.31	NA		0.21	0.71	7.94	
		T2	68.98	62.13	19.12	16.60	111.16	15.54	1.43	23.84	0.10	0.19	1.20	0.14	0.09	0.62	8.74	
	BW205	T0	150.48	98.56	7.65	11.48	86.04	17.64	NA	9.75	0.28	0.21	1.14		0.26	0.34	5.96	
		T2	137.53	99.18	7.14	11.33	94.58	17.39	<DL	9.41	0.29	0.14	3.34	0.12	0.21	0.24	5.88	
	60	T0	80.19	52.84	16.29	10.71	78.00	29.75	<DL	13.71	0.07	0.15	1.10		0.21	0.34	9.97	
		T2	53.91	37.41	6.53	10.66	99.85	30.27	<DL	7.63	0.11	0.12	1.45	0.12	0.20	0.25	10.49	
Nitrate	B22	T0	77.47	274.36	18.60	18.04	140.23	4.97	2.14	26.13	0.09	0.34	577.41		0.30	0.96	45.09	
		T2	65.78	289.65	20.12	18.42	142.71	43.81	1.00	24.00	21.51	0.25	604.93	0.40	0.20	0.81	16.08	
	BW205	T0	147.85	325.44	7.90	12.42	104.86	17.03	<DL	10.94	0.25	0.21	607.78		0.44	0.31	7.27	
		T2	128.14	325.66	7.34	11.89	104.12	20.75	<DL	9.85	1.19	NA	620.68	0.14	0.35	0.15	7.47	
	60	T0	70.45	256.01	7.12	11.39	99.94	30.07	<DL	9.26	0.11	0.21	583.79		0.36	0.31	11.32	
		T2	50.82	260.74	6.66	11.06	103.92	33.71	<DL	8.26	3.05	0.15	600.97	0.41	0.26	0.21	12.35	
Sulfate	B22	T0	76.68	537.19	18.83	18.27	141.13	1014.50	2.13	26.23	0.07	0.34	NA		0.31	0.98	382.19	
		T2	62.46	560.44	19.68	18.57	155.09	1096.53	1.67	24.90	0.07	0.26	2.81	0.25	0.21	0.88	401.56	
	BW205	T0	147.82	597.60	7.93	12.42	105.32	1059.87	NA	10.94	0.19	0.19	0.98		0.44	0.30	355.58	
		T2	133.46	604.15	7.82	12.18	107.96	1104.83	<DL	10.27	0.06	0.19	3.91	3.04	0.38	0.58	359.79	
	60	T0	69.87	563.61	7.06	11.53	101.96	1059.04	<DL	9.51	0.08	0.19	0.75	0.03	0.36	0.31	361.41	
		T2	49.99	534.09	6.62	11.05	104.82	1106.56	<DL	12.19	0.09	0.14	2.49	2.50	0.27	0.56	356.48	
Chlorate	B22	T0	77.79	290.57	18.89	18.54	145.70	5.12	2.08	26.04	0.08	NA	NA		0.31	0.98	8.49	813.25
		T2	269.25	301.09	19.64	18.59	146.46	22.42	<DL	24.61	0.10	<DL	3.10	0.42	0.21	0.87	10.67	827.55
	BW205	T0	148.96	333.80	7.92	12.60	105.32	17.26	NA	10.93	0.32	NA	1.16		0.44	0.30	7.61	806.28
		T2	335.35	337.02	7.61	12.10	107.68	21.23	<DL	9.99	0.10	<DL	4.11	0.20	0.37	0.18	7.87	803.18
	60	T0	76.57	297.01	7.26	11.57	103.54	30.47	<DL	8.36	0.10	<DL	1.02		0.37	0.31	11.72	781.57
		T2	249.38	265.96	6.57	11.17	105.26	34.54	<DL	8.15	0.12	<DL	3.56	0.20	0.26	0.15	12.12	792.72
Ferrihydrite	B22	T0	115.53	60.38	17.86	16.93	114.28	4.53	NA	24.76	0.10	0.32	NA	3.60	1.13	0.25	2.67	
		T2	105.12	64.02	19.39	17.27	113.40	20.18	<DL	23.85	0.08	0.18	2.98		0.48	0.07	7.77	
	BW205	T0	184.79	101.49	7.88	11.47	90.54	13.25	NA	9.91	0.31	0.27	1.02		1.10	0.25	5.07	
		T2	171.74	100.97	7.35	11.20	89.83	16.49	<DL	8.15	1.44	0.21	4.34	0.12	0.98	0.07	5.89	
	60	T0	115.28	38.11	6.83	10.73	89.99	22.95	<DL	7.96	0.09	0.18	0.99		1.00	0.25	7.95	
		T2	93.29	39.18	6.45	10.30	88.30	26.22	<DL	7.78	0.09	0.13	4.54	0.16	0.90	0.08	8.99	
No Additives	B22	T0	78.17	62.70	19.25	18.77	143.22	5.83	1.97	26.96	0.11	0.37	NA		0.32	0.95	56.65	
		T2	94.85	76.80	13.61	15.16	121.73	28.07	0.98	24.81	0.10	0.21	3.13	0.21	0.19	0.76	33.99	
	BW205	T0	145.66	103.19	7.85	12.51	102.49	17.78	<DL	10.54	0.33	0.26	0.81		0.44	0.32	6.95	
		T2	92.75	72.24	7.19	11.82	107.83	21.26	<DL	9.57	0.07	0.19	4.51	2.03	0.38	0.43	7.94	
	60	T0	69.55	38.38	7.17	11.77	100.46	30.70	<DL	8.15	0.09	0.16	0.73		0.37	0.33	11.44	
		T2	32.68	38.75	6.66	11.16	106.56	34.20	<DL	7.78	0.09	0.16	4.03	2.13	0.27	0.49	11.51	

1.3 Mass balances

Table 26: Mass balances of sulfat and sulfur, and ammonium, nitrate and nitrite in the batches. The total concentration of T0 and T2 are calculated in mmol/L.

			SO_4^{-2}	S		NH_4^+	NO_2^-	NO_3^-				
		molar mass	96.06	32.065		18.04	46.01	62.00				
	batch	mmol/L	SO_4^{-2}	S	total	NH_4^+	NO_2^-	NO_3^-	total			
No Additives	B22	T0	0.06	1.77	1.83	1.49	0.00	0.00	1.50			
		T2	0.29	1.06	1.35	1.38	0.00	0.05	1.43			
	BW205	T0	0.19	0.22	0.40	0.58	0.01	0.01	0.60			
		T2	0.22	0.25	0.47	0.53	0.00	0.07	0.61			
	60	T0	0.32	0.36	0.68	0.45	0.00	0.01	0.47			
		T2	0.36	0.36	0.72	0.43	0.00	0.06	0.50			
Oxygen	B22	T0	0.06	1.73	1.79	1.49	0.00	0.00	1.49			
		T2	0.46	0.50	0.97	1.26	0.00	0.02	1.28			
	BW205	T0	0.17	0.25	0.42	0.58	0.00	0.01	0.60			
		T2	0.22	0.26	0.48	0.01	0.29	0.29	0.60			
	60	T0	0.32	0.35	0.67	0.49	0.00	0.01	0.51			
		T2	0.36	0.38	0.74	0.01	0.25	0.23	0.49			
Oxygen+Nutrients	B22	T0	0.40	1.22	1.61	1.87	0.00	0.00	1.87			
		T2	0.53	0.59	1.12	1.73	0.00	0.02	1.75			
	BW205	T0	0.55	0.57	1.12	1.14	0.01	0.02	1.16			
		T2	0.61	0.60	1.21	0.02	1.15	0.04	1.21			
	60	T0	0.68	0.69	1.37	1.06	0.00	0.01	1.08			
		T2	0.74	0.69	1.44	0.02	1.10	0.02	1.14	ClO_3^-	Cl^-	total
Chlorate	B22	T0	0.05	0.26	0.32	1.44	0.00	0.00	1.45	9.75	2.19	11.94
		T2	0.23	0.33	0.57	1.36	0.00	0.05	1.42	9.92	7.60	17.51
	BW205	T0	0.18	0.24	0.42	0.61	0.01	0.02	0.63	9.66	4.20	13.86
		T2	0.22	0.25	0.47	0.55	0.00	0.07	0.62	9.63	9.46	19.08
	60	T0	0.32	0.37	0.68	0.46	0.00	0.02	0.48	9.37	2.16	11.53
		T2	0.36	0.38	0.74	0.45	0.00	0.06	0.51	9.50	7.03	16.53
Nitrate	B22	T0	0.05	1.41	1.46	1.45	0.00	9.31	10.76			
		T2	0.46	0.50	0.96	1.33	0.47	9.76	11.55			
	BW205	T0	0.18	0.23	0.40	0.61	0.01	9.80	10.41			
		T2	0.22	0.23	0.45	0.55	0.03	10.01	10.58			
	60	T0	0.31	0.35	0.67	0.51	0.00	9.42	9.93			
		T2	0.35	0.38	0.74	0.46	0.07	9.69	10.22			
Sulphate	B22	T0	10.56	11.92	22.48	1.45	0.00	0.00	1.46			
		T2	11.42	12.52	23.94	1.38	0.00	0.16	1.54			
	BW205	T0	11.03	11.09	22.12	0.61	0.01	0.05	0.67			
		T2	11.50	11.22	22.72	0.57	0.00	0.22	0.79			
	60	T0	11.02	11.27	22.30	0.53	0.00	0.04	0.57			
		T2	11.52	11.12	22.64	0.68	0.00	0.14	0.82			
Ferrihydrite	B22	T0	0.05	0.08	0.13	1.37	0.00	0.00	1.37			
		T2	0.21	0.24	0.45	1.32	0.00	0.05	1.37			
	BW205	T0	0.14	0.16	0.30	0.55	0.01	0.02	0.57			
		T2	0.17	0.18	0.36	0.45	0.03	0.07	0.55			
	60	T0	0.24	0.25	0.49	0.44	0.00	0.02	0.46			
		T2	0.27	0.28	0.55	0.43	0.00	0.07	0.51			
Sterile	B22	T0	0.11	0.25	0.36	1.43	0.00	0.00	1.43			
		T2	0.16	3.67	3.83	1.32	0.00	0.02	1.34			
	BW205	T0	0.18	5.38	5.56	0.54	0.01	0.02	0.56			
		T2	0.18	5.45	5.63	0.52	0.01	0.05	0.58			
	60	T0	0.31	3.22	3.52	0.76	0.00	0.02	0.78			
		T2	0.32	3.06	3.37	0.42	0.00	0.02	0.45			

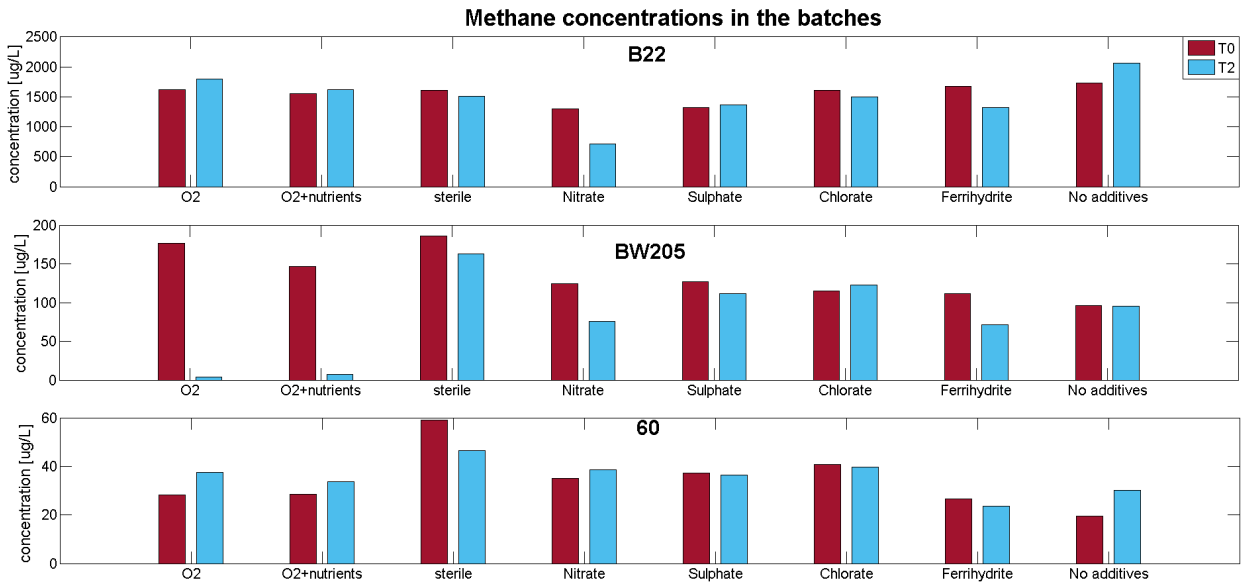

Figure 28: Methane concentrations in the batches at the moment of T0 (red) and T2(blue).

2 Appendix B

2.1 Naphthalene Carboxylase qPCR assay

Naphthalene, 2-methylnaphthalene and monoaromatics have a relatively high solubility and mobility and therefore endanger the quality of drinking water supplies and represent a significant environmental threat (Anderson & Lovley, 1997; Chakraborty & Coates, 2004). Previous studies conducted by Christensen *et al.* (1994); Heider & Fuchs (1997); Boll *et al.* (2002); Gibson & Harwood (2002); Chakraborty & Coates (2004); Meckenstock *et al.* (2004); Carmona *et al.* (2009) on the natural attenuation of naphthalene revealed two different anaerobic degradation pathways for naphthalene. Adding a methyl group to the molecule leads to the formation of 2-methylnaphthalene which can be degraded with by adding fumarate. Naphthalene can also be degraded via the carboxylation pathway. Adding a carboxyl group to the molecule forms 2-naphthoic acid and is further degraded to 2-naphthoyl-CoA (DiDonato Jr *et al.*, 2010). During both pathways, 2-naphtholy-CoA is formed as central metabolite (see figure29). DiDonato Jr *et al.* (2010), however, concluded that the first step of napthalene degradation most likely proceeds via the carboxylation

way. Hence in this study we developed a novel qPCR assay for the detection of the enzyme naphthalene carboxylase

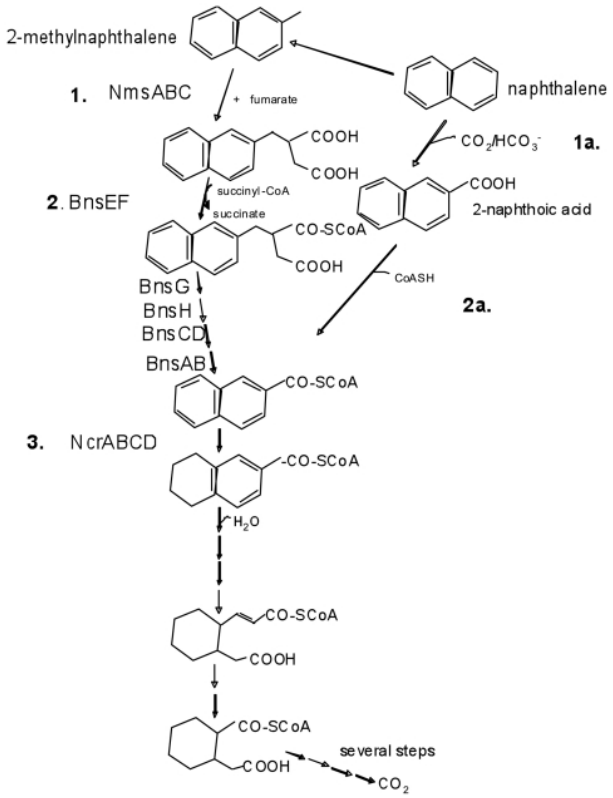

Figure 29: Anaerobic degradation pathways of naphthalene and 2-methylnaphthalene. Figure adapted from DiDonato Jr *et al.* (2010).

Bioinformatics

BLASTn was used to identify the uniqueness of the gene sequence. The Primer3 website suggested several primer pairs to target the gene NC and subsequently amplify it. After evaluating the Primer3 output the most suited primer pairs were selected. after affirming the uniqueness of these primers a qPCR assay was performed to verify the effectiveness of the selected primers using samples from a different project with previously confirmed naphthalene content.

TaKaRa

Thereafter, a standard calibration curve had to be designed. For this purpose, a TaKaRa Ex Taq DNA Polymerase PCR was performed with the same samples. TaKaRa Ex Taq DNA Polymerase combines the performance of Takara Taq polymerase with the proofreading activity of an efficient 3' to 5' exonuclease for high sensitivity and efficiency PCR reactions. In normal PCR applications, using the Ex Taq polymerase and Ex Taq Buffer system results in higher yields of PCR products as compared to standard Taq DNA polymerase. In addition, Ex Taq polymerase has a higher fidelity than standard Taq (mutation rate approximately 4.5X lower, as determined by the Kunkel method). Ex Taq DNA Polymerase also can be used for long range PCR; high yields of long products, up to 20 kb from genomic DNA templates and up to 30 kb from lambda DNA templates, are possible with this enzyme (www.clonetech.com).

Gel electrophosresis

Agarose gel electrophoresis is used to visualize the size of the PCR product. 100ml TAE and 0.5g of agarose were cooked and subsequently mixed with 5 μml ethidium bromide. EtBr is the most common reagent used to stain DNA in agarose gels (Sharp *et al.*, 1973). When exposed to UV light, electrons in the aromatic ring of the ethidium molecule are activated, which leads to the release of energy (light) as the electrons return to the ground state. EtBr works by intercalating itself in the DNA molecule in a concentration-dependent manner. This allows for an estimation of the amount of DNA in any particular DNA band based on its intensity. Because of its positive charge, the use of EtBr reduces the DNA migration rate by 15%. EtBr is a suspect mutagen and carcinogen, therefore, one must be careful when handling agarose gels containing it. In addition, EtBr is considered a hazardous waste and must be disposed of appropriately.

To the undiluted DNA 10 μml of 6x loading dyes were added. This serves three major purposes. First, they add density to the sample, allowing it to sink into the gel. Sec-

ond, the dyes provide color and simplifies the loading process. Finally, the dyes move at standard rates through the gel, allowing for the estimation of the distance that DNA fragments have migrated. Thereafter the gel is examined under UV light visualizing the length of the gene. If the desired length of the gene is confirmed, the bar where the gene is present is cut out and transported in a 1.5ml tube. After adding BE buffer and incubating the tube for 10 min in 36 °C, the gel is dissolved. Thereafter, several steps from the DNA gel extraction kit manual were performed to isolate the gene and elute it in 30 μ l elution buffer.

Cloning in E.coli plasmid vector

The next step was to include the gene in a microorganism. For this purpose, a one-step cloning for the direct insertion of Taq polymerase amplified PCR products into a plasmid vector was performed. The plasmid vector is supplied linearized within single 3' T overhangs for TA Cloning and a Topoisomerase I covalently bound to the vector (activated vector). Taq polymerase has a nontemplate-dependent terminal transferase activity that adds a single deoxyadenosine (A) to the 3' ends of the PCR products. The linearized vector has single, overhanging 3' deoxythymidin(T) residues. This allows PCRS inserts to ligate efficiently with the vector.
Topoisomerase I from Vaccinia virus binds to duplex DNA at specific sites and cleaves the phosphodiester backbone after 5'CCCTT in one strand (Shuman, 1991). The energy from the broken phosphodiester backbone is conserved by a tyrosyl residue (Tyr-274) of topoisomerase T. The phospho-tyrsoyl bind between the DNA and enzyme can subsequently be attacked by the 5' hydroxyl of the original cleaved strand, reversing the reaction and releasing topoisomerase (Shuman, 1994).

Ligating the gene into the vector is done by mixing and incubation for 5 min at room temperature. After pipetting 2 μl of the ligation mix into the vial of the chemically competent E. coli culture the vial is exposed for 30 seconds to a 47°C warm water bath followed by the exposure to ice. During the heat shock, the E.coli cells open which enables

the vectors to enter the cells. Placing the vials on ice induces the cells to close again. The vectors with the gene naphthalene carboxylase are now hopefully inserted in the E. coli cells. After adding 250 μl of S.O.C media the cells are incubated for one hour at 37°C. While incubated the vials have to be placed horizontally and shaken continuously.

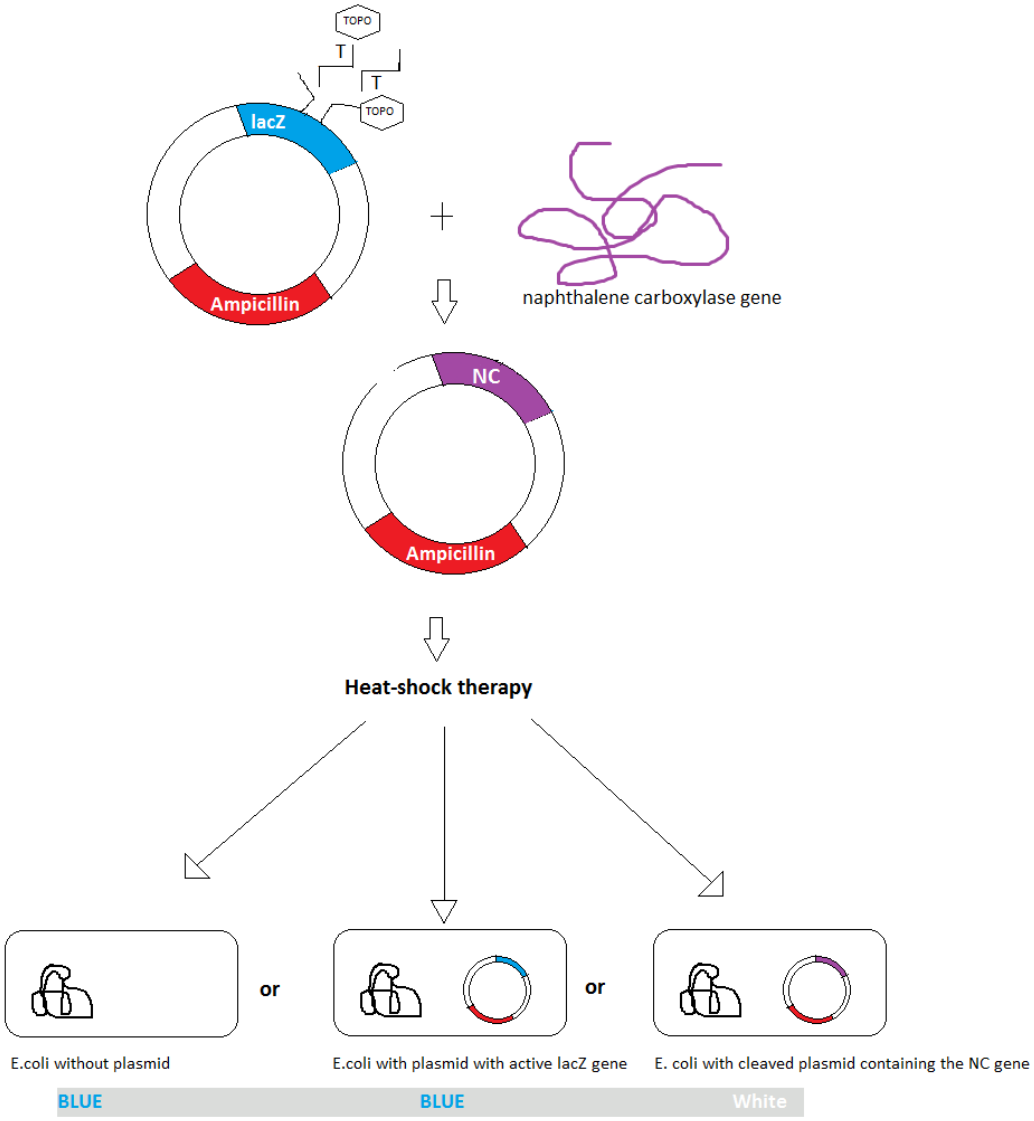

Figure 30: Simplified visualization of the ligation of the naphthalene carboxylase gene in a vector and subsequent cloning in a chemically competent E.coli cell

Cultivation of E.coli with the cleaved vector

To grow and cultivate the E. coli with the gene encoding for naphthalene carboxylase the bacteria has been spread on LB plates with ampicillin and X-gal (5-Bromo-4-Chloro-3-Indolyl β-D-Galactopyranoside). The plates have been prepared previously (Dissolve 1 g tryptone, 0.5 g yeast extract, and 1 g NaCl in 95 mL deionized water, liquid autoclave for 20 min at 15 psi, add 500 μg of ampicillin and pour into the plates). After pouring the LB media in the plates, the ampicillin and X-gal are added to only grow bacteria that have incorporated the plasmid DNA and are, therefore, resistant to ampicillin. The X-gal detects the activity of the lacZ gene in the vector. Due to a dark blue precipitate at the site of the enzymatic activity, some of the colonies are colored blue some white (blue-white screening). The blue colonies have the intact lacZ gene in the vector, hence no cleaved gene. These colonies can be neglected. The white colonies correspond to an inactive lacZ gene which implicates the presence of the cleaved naphthalene carboxylase gene (see figure 30). These colonies are solely extracted and cultured on LB plates and in falcon tubes both enriched with ampicillin.

2.1.1 Plasmid isolation and visualization

Subsequently, the DNA from the cultivated LB tubes was isolated by using the allocated kit. After several steps the 1,5 ml tubes with the isolated plasmid were stored in -20°C and further processed for the qPCR (see figure 31) and for the control Taq PCR provided from the cloning kit. Thereafter, the length of the product was visualized in a gel electrophoresis. Thereafter, the product was cut out and extracted using the QIAquick ®Gel Extraction Kit QIAquick ®PCR & Gel Cleanup Kit. Afterward, it was ready for downstream applications (see figure 31).

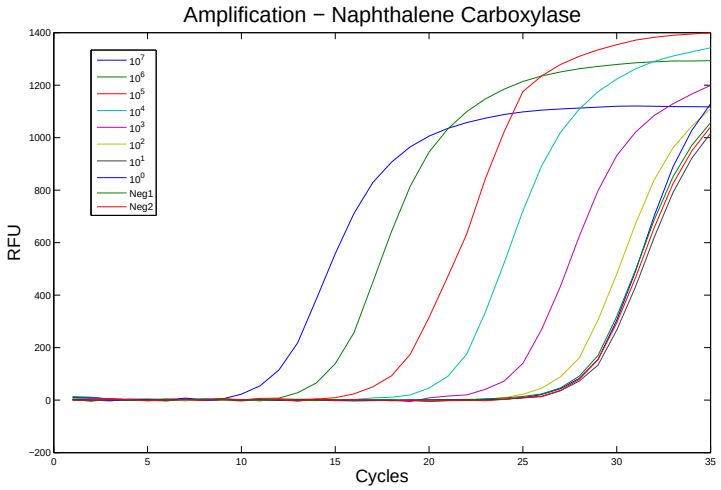

Figure 31: Amplification of the naphthalene carboxylase calibration line